

DAMAGING EFFECTS OF CIGARETTE SMOKE ON
ORGANS AND STEM/PROGENITOR CELLS AND THE
RESTORATIVE POTENTIAL OF CELL THERAPY

Daria Barwinska

Submitted to the faculty of the University Graduate School
in partial fulfillment of the requirements
for the degree
Doctor of Philosophy
in the Department of Cellular and Integrative Physiology,
Indiana University

October 2017

Accepted by the Graduate Faculty of Indiana University, in partial
fulfillment of the requirements for the degree of Doctor of Philosophy.

Doctoral Committee

Keith L. March, MD., PhD, Chair

David P. Basile, PhD

Hal Broxmeyer, PhD

June 23, 2017

Matthias Clauss, PhD

Dmitry O. Traktuev, PhD

DEDICATION

I am dedicating this work to my parents and my mentors.

Mom and Dad, my gratitude for your endless love, support, and sacrifice is immense. You have instilled in me the values of perseverance, integrity, and love for science and learning.

Dr. Keith March, mentor and thesis advisor, you offered to me the chance to join your lab and provided me an enormous opportunity to grow as a scientist and as a person. Thank you for supporting my dreams.

Dr. Dmitry Traktuev, mentor, your office door has always been open and you have without any exception always been available to listen to my questions, success stories, and concerns. Thank you for being my guardian and advocate as I walked the path toward my degree.

ACKNOWLEDGEMENTS

Dr. Keith March, you are the one who encouraged me to join the great scientific environment at Indiana University. You have ignited my love for stem cell research and regenerative medicine. Your expertise in the field, true ability to balance a large number of high-priority tasks, and continuous warm and welcoming smile have and will always be my inspiration. Our meetings at coffee shops, work on grants that often would go late into the night, and your always thoughtful invitation to join you at conferences are the kinds of exceptional experiences that have made me the researcher that I am today. Thank you for all your incredible support.

Dr. Dmitry Traktuev, from designing studies, discussing results, your plentiful words of wisdom shared about the world of science and what it means to be a researcher, to your consistent great advice for life; I cannot express how grateful I am for all of these numerous conversations. You have been my advocate and have had the best intentions in mind both in your role on my Research Committee and as a mentor. Thank you for all you have done for me.

Dr. David Basile, I have an enormous appreciation for all your support. Thank you for your continuous encouragement and the multitude of words of wisdom that you have shared with me over the years. Every piece of advice you gave me as a member of my Research Committee has been very valuable. Thank you for believing in me, motivating me, keeping me on track, and teaching me many kidney related techniques. Thank you for opening your lab to me, and letting me move in with my kidney samples from smoking mice.

Dr. Hal Broxmeyer, rotation in your lab has been wonderful. You have provided me with my first lab experience at the IU School of Medicine, and assisted me as I moved on

to accomplish the next milestones as a graduate student. I truly cherish the memories I have of long hours spent over the microscope counting bone marrow progenitor colonies. Thank you for all the guidance and support you have given to me as a member of my Research Committee.

Dr. Matthias Clauss, thank you for your continuous interest in my research, support with the grant applications, and for our conversations about science. I treasure my memories of working with you to organize seminars and other science-related events. Thank you for the feedback and direction you have given me while on my Research Committee.

Dr. Natalia Bogatcheva, thank you for being an enormous source of information and always having answers for me, both in science and in everyday life. Thank you for all your help along the way with experiments, writing, and grant applications.

Stephanie Merfeld-Clauss, Dr. Hongyan Lu, Dongni Feng, Todd Cook, Alexandria Galloway and everyone who has been part of the March Lab, I am extremely grateful for all the help you have given me over the years. Your company and teamwork was something I always looked forward to each morning.

Dr. Heather O'Leary, Dr. Jason Colette, Dr. Tom Jones, Dr. Jie Xie, Dr. Yameena Jawed, Dr. Ting Wang, I will always cherish the memories of working alongside you. Thank you for teaching me new skills, for making my transition into academia easier, and above all I am thankful for having found great friends in you.

Dr. Jonathan Tune, I appreciate all your help as I navigated through the program requirements and I am grateful for you for watching over me during this wonderful journey.

Dr. Irina Petrache, Dr. Houssam Oueini, Dr. Robert Bacallao, Dr. Troy Markel, Dr. Fred Pavalko, Dr. Mervin Yoder, Seth Winfree, Dr. Joseph Unthank, Dr. Keith Condon,

Dr. Sergio Li Calzi, Dr. Clark T. Barco and all the many great individuals who crossed my path during my time as a graduate student at Indiana University, thank you for all your help and support for you have truly done more than words can explain to make this journey so delightful and memorable.

Friends, you have been an incredible support. Thank you for your understanding of my unusual work schedule and always providing me with kindness.

I want to thank and acknowledge American Heart Association (AHA), Roudebush VA Medical Center Research Office, Indiana Institute for Medical Research (IIMR), and Cryptic Masons Medical Research Foundation (CMMRF). Without your support, studies described in this dissertation would not be possible.

I also would like to thank and acknowledge the International Federation for Adipose Therapeutics and Science (IFATS). From the moment I joined the society I have gained amazing new insight into the field of stem cell research and the impressive ways of translating science into clinical practice. I am extremely grateful to have been able to share my findings within such a knowledgeable and globally recognized group of scientists and clinicians.

DAMAGING EFFECTS OF CIGARETTE SMOKE ON ORGANS AND
STEM/PROGENITOR CELLS AND THE RESTORATIVE POTENTIAL OF CELL
THERAPY.

Cigarette smoking (CS) continues to be a significant modifiable factor contributing to a variety of diseases including cardiovascular, pulmonary and renal pathologies. It was suggested that smoking have detrimental effect of the body's progenitor cells of bone marrow and peripheral organs. Since the concept of cell therapy that utilizes adipose stem/stromal cells (ASC) is gaining momentum it becomes critical to assess the therapeutic activities of the progenitors isolated from smokers. This study has revealed that CS negatively impacts the vasculogenic potential of ASC, *in vitro*, as well as weakening their therapeutic activity *in vivo* when tested in mouse model of hindlimb ischemia. We hypothesized that the decrease in vasculogenic activity of ASC is attributed to a higher level of expression of an angiostatic factor Activin A by ASC from CS donors. These findings clearly suggest that smokers should be evaluated for potential exclusion from early clinical trials of autologous cell therapies, or assessed as a separate cohort. The donor's health status should be considered when choosing between autologous vs allogeneic cell therapies.

We then examined the effect of CS on development of kidney pathology in mice. CS exposure led to decrease in kidney weights, capillary rarefaction, and

cortical blood perfusion, and in parallel led to increase in kidney fibrosis and iron deposition. Interestingly, infusion of healthy ASC to the mice following CS-exposure reversed CS-induced damages. This strongly support the notion that ASC-based therapy may provide rejuvenation effect.

In the other subset of studies, we hypothesized that CS-induced lung emphysematous changes are preceded by suppression of bone marrow (BM) hematopoietic progenitor cells (HPC). We have revealed that intermittent BM mobilization with AMD3100 may mitigate the CS-induced myelo-suppression and deterioration of lung function and morphology. We observed that treatment of mice with AMD3100, while exposed to CS, preserves HPC at the levels of healthy control mice. Furthermore, AMD3100 treatment preserved lung parenchyma from pathological changes. These data suggest that while CS has a myelo-suppressive effect, administration of AMD3100 preserved BM-HPC and ameliorated lung damage.

Keith L. March, MD., PhD, Chair

TABLE OF CONTENTS

LIST OF TABLES	x
LIST OF FIGURES	xi
LIST OF ABBREVIATIONS	xii
Chapter 1. Introduction	
1.1 Cigarette smoking and the implications on human health	1
1.2 Cell therapy offers promise in regenerative medicine	9
1.3 Research focus	15
Chapter 2. Effects of cigarette smoking on angiogenic potential of adipose-derived stem cells	
2.1 Introduction	17
2.2 Materials and Methods	21
2.3 Results	34
2.4 Discussion	70
Chapter 3. Contribution of cigarette smoking to renal pathology and the beneficial effect of adipose-derived stem cell therapy on ameliorating renal damage	
3.1 Introduction	84
3.2 Materials and Methods	89
3.3 Results	94
3.4 Discussion	103
Chapter 4. Smoking-induced myelosuppression and emphysema development in mice are ameliorated by AMD3100 administration	
4.1 Introduction	111
4.2 Materials and Methods	119
4.3 Results	124
4.4 Discussion	130
Chapter 5. Future directions	134
References.....	136
Curriculum Vitae	

LIST OF TABLES

Table 1. Forward and reverse primer sequences	32
Table 2. List of proteins secreted in CM by one smoking and one non-smoking ASC donor	53
Table 3. List of cytokines tested using RayBio Human Cytokine Array (C5)	55
Table 4. Demographics of male and female ASC donors used in the study	69

LIST OF FIGURES

Figure 1. Schematic representation of ASC utilization for clinical use	13
Figure 2. Teague Smoking Chamber	24
Figure 3. Vascular Network Formation Assay: well assessment.....	28
Figure 4. Morphological, differentiation and phenotypical assessment of ASC from smoking and non-smoking donors	36
Figure 5. Analysis of therapeutic effect of ASC from smoking and non-smoking donors	40
Figure 6. Analysis of vasculogenic activity of ASC from smoking and non- smoking donors	44
Figure 7. Vasculogenic activity of ASC conditioned media	46
Figure 8. Semi-quantitative assessment of pro-angiogenic proteins in human ASC CM using RayBio Human Cytokine Assay	54
Figure 9. Analysis of accumulation of selected cytokines in human ASC CM ..	58
Figure 10. Assessment of supplementation of ASC co-culture with conditioned media from non-CS-ASC donor or with growth factors	60
Figure 11. Assessment of SDF-1 inhibitor activity on vascular network formation potential of ASC derived from smoking donors	62
Figure 12. Assessment of DPP4 activity in human ASC CM	64
Figure 13. Assessment of Activin A activity of nonCS-ASC and CS-ASC	66
Figure 14. Assessment of the kidney weights	95
Figure 15. Assessment of fibrosis and capillary density in renal cortical tissue of C57Bl/6 mice exposed to cigarette smoke or ambient air	97
Figure 16. Assessment of M1 and M2 macrophage presence in the renal cortical tissue of C57Bl/6 mice exposed to cigarette smoke or ambient air	98
Figure 17. Assessment of iron presence in the kidney tissue of NSG mice using Pearl's iron stain	100
Figure 18. Assessment of superficial cortical renal blood flow in C57Bl/6 mice using LDI	102
Figure 19. Hematopoiesis model in a human	115
Figure 20. Schematic representation of AMD3100-mediated HSC mobilization into peripheral blood	118

Figure 21. Timeline for AMD3100 injection and analyses	120
Figure 22. AMD3100 limits CS-induced myelosuppression of BM hematopoietic progenitor cells	125
Figure 23. AMD3100 limits CS-induced emphysematous changes in lungs ...	127
Figure 24. Assessment of the inflammatory cells in BAL	129

LIST OF ABBREVIATIONS

ACE	angiotensin converting enzyme
α -SMA	alpha-smooth muscle actin
AKI	acute kidney injury
AMD3100	drug, plerixafor, bone marrow mobilizer
ANOVA	analysis of variance
ASC	adipose stem / stromal cells
BAL	bronchoalveolar lavage
BFU-E	erythroid burst forming unit
BM	bone marrow
BMP-7	bone morphogenic protein-7
BSA	bovine serum albumin
C57Bl/6	mouse strain
CBD	cord blood derived
CFU	colony forming unit
CFU-GEMM	granulocyte, erythroid, monocyte, megakaryocyte colony forming unit
CFU-GM	granulocyte, macrophage colony forming unit
CKD	chronic kidney disease
CM	conditioned medium
COPD	chronic obstructive pulmonary disease
CS	cigarette smoker / cigarette smoking
CSE	cigarette smoke extract
CXCL12	stromal derived factor-1
CXCR4	receptor for stromal derived factor-1
DAB	3,3'-diaminobenzidine
DAPI	4',6-diamidino-2-phenylindole dihydrochloride
DMEM	Dulbecco's Modified Eagle's medium
DPP-4	dipeptidyl peptidase-4

EC	endothelial cell
EDTA	ethylenediaminetetraacetic acid
ELISA	enzyme-linked immunosorbent assay
EMT	epithelial to mesenchymal transition
EndMT	endothelial to mesenchymal transition
EPC	endothelial progenitor cell
EPO	erythropoietin
FBS	fetal bovine serum
FDA	United States Food and Drug Administration
FGF-2	fibroblast growth factor-2
GFR	glomerular filtration rate
GM-CSF	granulocyte macrophage colony stimulating factor
GVHD	graft versus host disease
HGF	hepatocyte growth factor
HPC	hematopoietic progenitor cells
HRP	horseradish peroxidase
HSC	hematopoietic stem cells
IgG	immunoglobulin G
IL- β 1	interleukin β 1
IP	intra peritoneal
IV	intra venous
KIM-1	kidney injury marker-1
LDI	laser Doppler imager
MLI	mean linear intercept
MSC	mesenchymal stem cells
nonCS	non-smoker
NSG	immunodeficient mouse strain
OCT2	organic cation transporter-2

PAI-1	plasminogen activator inhibitor 1
PBS	phosphate buffered saline
PCR	polymerase chain reaction
PFT	pulmonary function test
PMN	polymorphonuclear cell
PSR	picrosirius red
ROS	reactive oxygen species
SCF	stem cell factor
SCM	spleen cell medium
SDF-1	stromal derived factor 1
SEM	standard error of mean
SQ	sub-cutaneous
TGF β	transforming growth factor- β
TNF α	tumor necrosis factor- α
TPV	tissue perfusion value
TSG-6	TNF-induced protein 6
VEGF	vascular endothelial growth factor
VNF	vascular network formation

Chapter 1: Introduction

1.1 Cigarette smoking and the implications on human health

1.1.1 A brief history of cigarette smoking

Tobacco has been part of human civilization for over 7000 years, and its utilization was first described in the South America region [1, 2]. With the arrival of Europeans in the 1500s, tobacco soon spread to other continents to become a popular trading commodity [1, 2] and as the human lifespan extended, the effects of tobacco became more prominent. Along with increasing popularity of cigarette smoking (CS), various opposition groups also emerged that suggested potential negative health outcomes of the habit as early as the 1600s. It was not until 1948, however, that British researcher, Richard Doll, raised a serious concern about CS adverse health effects, publishing a study in 1950 linking CS to development of lung cancer [3].

While the tobacco industry was booming, it took several more years until 1964 when the United States Surgeon General released the Report on Smoking and Health which, pointed out the connection between tobacco use and cancer [4]. This precipitated the birth of numerous anti-tobacco advocacy and awareness groups and also gave rise to multitude of research projects that revealed not only the negative effects of CS on the human body, but also began to shed light on the mechanism through which different components of CS affect the physiology [4]. In 1994, the authors of the Oxford Medical Companion famously stated that

“Tobacco is the only legally available consumer product which kills people when it is entirely used as intended” [5].

As estimated by the World Health Organization, there are approximately 1.1 billion cigarette smokers worldwide, and almost six million people die each year from tobacco-associated diseases. In the United States, the number of smokers continues to be alarming: close to 17% of the population, or roughly forty million people, are active smokers [6]. Most recently a study published in the New England Journal of Medicine revealed that 28% of the 45,971 youth and adult study participants used at least one type of tobacco product between 2013 and 2014, while 40% of tobacco consumers used more than one tobacco product [7]. In addition, a 2015 report by the Centers for Disease Control and Prevention (CDC) estimates that approximately 443,000 people die each year in the U.S. from diseases linked to CS or second-hand smoke exposure [4].

1.1.2 The harmful ingredients

There are an estimated 4000 chemicals in an average cigarette, 70 of which are known to be toxic or carcinogenic to humans [8-10]. Among them are phenols, nitrosamines, carbonyls, tar, and various gases, the most well-known being carbon monoxide [8]. Nicotine, an alkaloid, is one of the most commonly studied chemicals found in cigarettes. Nicotine's effects on the human body have been assessed in numerous studies and are associated with various pathologies [11-14], including promoting angiogenesis in animal models of age-related macular degeneration [15], atherosclerosis [16, 17] and carcinoma development [17-19]. Often the mechanism responsible for these outcomes involves stimulation of nicotinic acetylcholine receptors (nAChR), which are members of family of cholinergic

receptors, present on the endothelium. It has been shown that nAChR promotes endothelial cell migration *in vitro* thus simulating the action of native pro-angiogenic cytokines [15]. In 1996, Carty et al. showed that nicotine, applied at clinically relevant concentrations of 10^{-9} to 10^{-6} mol/L (similar to plasma levels seen in active smokers), stimulates proliferation of smooth muscle cells [20]. It has been proposed that one of the mechanisms of nicotine's mitogenic effect is stimulation of fibroblast growth factor (FGF) production by these cells, which then acts in autocrine manner to promote smooth muscle cell proliferation [20]. Heeschen et al. have shown that nicotine increases progression of plaque formation and tissue neovascularization, in addition to intensifying the progression of pathological angiogenesis associated with tumor formation [17].

In parallel, cotinine, a metabolite of nicotine, also has adverse effects on human health. It acts via stimulation of bFGF secretion and upregulation of collagenase by 29-fold, promoting hyperplasia as well as aneurysm formation [20, 21]. Cotinine is known to be oxidized in the liver by one of the cytochromes p450: CYP2A6 (which plays a role in metabolism and removal of toxins from the body) [22]. It has become a popular biomarker to assess a person's tobacco use and the amount of exposure, since it is easily found in urine, saliva, and blood, and has a long half-life of 15-40 hours [23]. Presence of cotinine in the serum has been linked to higher hemoglobin 1Ac levels [21]. Taken together, nicotine and cotinine lead to or exacerbate numerous pathologies.

Aside from these two molecules, one of the most bioactive compounds found in the gaseous phase of CS is carbon monoxide, an odorless gas. While

carbon monoxide for the most part is considered to be toxic, studies have shown that it is also produced in the body (e.g. during the process of heme breakdown) and plays significant role alongside nitric oxide as a vasodilator [24]. However, it is important to note that upon carbon monoxide inhalation, it binds to hemoglobin, resulting in carboxyhemoglobin. This decreases the availability of oxygen distribution throughout the body with serious negative implications in tissue oxygenation, promoting injury of the central nervous system, specifically white matter, which most often is the first one to be affected [8, 25, 26].

As more and more compounds in CS are being identified as toxic, an increasing number of studies are also revealing additional biochemical pathways that are involved. Several studies have indicated that the aryl hydrocarbon receptor (AhR) signaling pathway is activated by CS exposure, linking CS to increased risk of cancer [27]. AhR is known to play a role in embryonic development and removal of xenobiotic compounds, through cytochrome p450 and induction of enzymes of metabolizing processes [28]. However, in some cases, such as in the case of the toxic compound benzo[a]pyrene (which is found in tobacco smoke) interaction with AhR ultimately leads to generation of metabolites that are toxic and act as mutagens [29]. In a study with AhR null mice, it has been revealed that these mice are resistant to chromosomal damage upon exposure to CS condensate when compared to wild type controls [29].

1.1.3 Types of smoke exposure

The majority of studies are focused on so-called “first-hand smoke” exposure – the effects of tobacco on the user himself/herself. However, during the

past few decades multiple studies have been conducted to evaluate the health effects of passive or second-hand smoke (SHS) exposure, which is defined as inhaling the smoke exhaled by another person smoking a cigarette [30].

Similarly to first-hand smoke, exposure to SHS may lead to multiple respiratory symptoms such as shortness of breath, coughing, asthma attacks, as well as cardiovascular symptoms [31]. Long term exposure to SHS leads to increase in risk of developing cancer, chronic obstructive pulmonary disease (COPD), and other CS associated diseases [32]. Children exposed to SHS are more prone to develop respiratory conditions [33]. Interestingly, a study by Yankelevitz et al., has shown that non-smokers who were exposed to SHS in their lifetime are 48-69% more likely to develop atherosclerosis compared to those with no SHS exposure [34]. A study by Aydogan et al., revealed that passive smokers required more analgesia following a surgery compared to non-smokers [35]. Collectively, these findings indicate that even indirect CS exposure results in significant pathology. SHS, however, is not the only indirect aspect of CS-exposure: “third-hand smoking” (THS) is defined as exposure to films of toxic CS-derived compounds deposited on various surfaces including clothing, furniture, car interiors, and hair [36]. In the case of THS, absorption of such chemicals occurs through skin, inhalation, or ingestion [36]. THS results in increased cellular oxidative stress via superoxide dismutase activity as well as in increase in the hydrogen peroxide level in mouse quadriceps muscle tissue [37]. The same study has also shown that THS decreases levels of glutathione peroxidase in the muscle. This enzyme is responsible for breaking down hydrogen peroxide into water and

oxygen, resulting in increase in peroxidation and DNA damage, leading in turn to hyperglycemia and insulinemia [37]. The toxicity of THS is also conferred via activity of a wide range of volatile organic compounds, including acrolein, an unsaturated aldehyde and a neurotoxin that recently has been recognized as end product of glycerol breakdown following burning of fat [38]. Research by Bahl et al., revealed that acrolein in THS causes blebbing, immotility, vacuolization, cell fragmentation, severing of microfilaments, and de-polymerization of microtubules in mouse neural stem cells [38]. In addition, acrolein alone changed the expression of cell cycle regulatory genes and inhibited cell proliferation [38]. A study by Due et. al. has shown that acrolein accumulates in the spinal cord of mice exposed to CS just for three weeks, and has been linked to increased pain sensitivity [39]. These phenomena have also been observed in people with injury to the spinal cord and multiple sclerosis [39].

1.1.4 Health effects of cigarette smoke

There are numerous studies that establish a link between CS and various pathologies, with cardiovascular diseases showing a particularly strong correlation. A study by Al-Arifi et al., revealed that CS induces expression of cardiac hypertrophic genes like atrial natriuretic peptide, brain natriuretic peptide and β -myosin heavy chain (through alteration in mRNA expression), and cytochrome P450 (CYP) enzymes, therefore increasing the probability of an adverse cardiovascular event [40]. CS has been shown to be one of the primary factors contributing to peripheral arterial disease [41] and abdominal aortic aneurysm [42]. Myocardial infarction and coronary artery disease are more likely

to occur in individuals who have smoked cigarettes in their past or continue to do so [4, 43]. Furthermore, it has also been shown that SHS exposure increases the prevalence of coronary artery disease by 30%, while active CS does so by 80% when compared to non-smokers [43, 44].

Numerous studies have linked CS to pulmonary [45-47] and immune [48-51] pathologies, as well as to increased chances of cancer development [19, 52-54]. Expectant mothers who continue to smoke are at higher risk for giving birth to children with defects [55-58]. Studies assessing the harmful effects of CS and evaluating its mechanism of action have revealed that CS correlates with impaired vasodilation and, in fact, contributes to immediate vasoconstriction via decreased nitric oxide synthesis by endothelial cells [59, 60]. As CS includes various oxidants, it is postulated that these molecules cause damage to endothelial cells. CS increases heart rate and blood pressure (through nicotine signaling pathway) escalating the chances of heart attack and stroke [61, 62]. It also results in delayed myocardial relaxation [13], increased concentration of C-reactive protein, and inflammatory factors in plasma [63, 64]. A study by Maclay JD et. al. has shown that CS exposure is responsible for the stickiness of platelets that may contribute to thrombosis [65]. CS has been demonstrated to correlate with elevated serum cholesterol levels [60]. Corre et al. has found an increase in blood leukocyte concentration (close to 30%) in smokers [66], as well as elevated levels of C-reactive protein, fibrinogen, and homocysteine [67]. In addition to vascular disorders, there is also strong evidence that CS results in impaired wound healing, including tissue necrosis, infections, and skin flap detachment [68] in post-surgical

period [69-72]. Nicotine by itself causes an increase in arterial stiffness, which in turn is associated with arteriosclerosis development [11]. Furthermore CS, as it causes a dysfunction of vascular system, leads to delay in tissue functional recovery after acute ischemic episodes, demonstrated both in animal models [73] and human subjects [74, 75]. Studies have shown that prior exposure to CS has long-lasting effects even after smoking cessation [76, 77].

While a large body of evidence as reviewed briefly above indicates that CS, both directly and indirectly, results in numerous pathologies or exacerbates already existing diseases, little has been done to elucidate the effect of CS on cell types that are considered to offer therapeutic benefit to patients who suffer from a variety of diseases, some of which are caused by CS.

1.2 Cell therapy offers promise in regenerative medicine

1.2.1 Variety of cells with therapeutic potential

During the past several years, multiple pre-clinical and clinical studies have shown that local or systemic administration of various stem/progenitor cells results in beneficial therapeutic effects, in a variety of pathological conditions [78-82]. Cell therapy is based on two major approaches that confer the regenerative activity: post-administration differentiation into particular cell types, and paracrine effects, characterized by secretion of cytokines with anti-inflammatory, pro-angiogenic and anti-apoptotic properties. Such paracrine activity can also increase additional recruitment of endogenous stem cells.

One widely studied cell type is bone marrow derived mesenchymal stem cell (BM-MSC). These cells have been tested in multiple clinical trials involving subjects with myocardial ischemia [78, 79, 83]. In addition to BM-MSC, other cell types have been shown to offer therapeutic benefit in clinical settings. Numerous studies have demonstrated that subtypes of BM-MSC [84] as well as circulating endothelial progenitor cells [85] play important reparative functions after acute injuries, including kidney or limb ischemia.

In recent years, new attention has been placed on the interaction of endothelial cells, which comprise the lining inside blood vessels, and pericytes, which wrap around the endothelial cells. This close interaction with endothelial cells plays a role in vascular remodeling [86], often involving vascular endothelial growth factor (VEGF), transforming growth factor beta (TGFb), platelet derived

growth factor BB, and its beta receptor (PDGF-BB and PDGFRb), all key factors in angiogenesis [87-90]. Studies have also been conducted investigating the regenerative capacity of cord-blood derived stem cells [85, 91] and neural stem cells [92]. In addition to the mentioned cell types considered for use in regenerative medicine, adipose tissue is a repository of cells known for their abundance and reparative capacity: adipose derived stem cells (ASC) [89, 93-96].

1.2.2 Factors affecting stem cells

Several groups have shown that such factors as aging [97-99], Body Mass Index [100, 101], and metabolic syndrome or diabetes [102, 103] affect the regenerative potential of ASC. We postulated that multiple other factors would likely play a role in modulating the therapeutic efficacy of these cells; and that not accounting for these factors might result in unsuccessful outcomes of patient treatment. We felt it important to acknowledge that some diseases that are considered for treatment with ASC may have arisen through a patient's own modifiable lifestyle choices, and that these factors may have a broader negative impact on the overall health and regenerative capacity of the body. Consistent with this concept, a recent clinical trial, POSEIDON, led by Hare et al. revealed that allogeneic BM-MSC are significantly better in restoring heart health after non-ischemic cardiomyopathy, compared to autologous donors [78], thus suggesting that patients whose health is sub-optimal have also decreased regenerative potential of their own stem cells.

One such prominent factor often implicated in a wide array of illnesses is cigarette smoking. Up until now, little has been done to evaluate the effect of CS

on regenerative potency of ASC. Although Wahl et al. initiated evaluation of this question, their study exclusively focused on assessing the impact of CS **extract** on ASC migration, differentiation, and expression of several factors, which was compromised in every instance [104]. Their study also was limited to *in vitro* simulation of CS exposure, and did not fully recapitulate the physiological process. The vast majority of both *in vitro* and *in vivo* prior studies have been done using cells obtained from relatively healthy donors, which do not represent the real case scenario seen in clinical practice. Most patients who require therapies, especially for cardiac and vascular diseases, are of advanced age and suffer from multiple comorbidities including diabetes, high blood pressure, dyslipidemia, and metabolic syndrome. These patients often have a history of CS. The function of stem cells is substantially affected by local and systemic factors including CS and diabetes. A study by Xie et al, has demonstrated that even a short-term exposure of mice to CS was strongly myelosuppressive [105], and Kim et. al. reported that bone marrow-derived mesenchymal stem cells from diabetic donors are ineffective in restoring blood flow in ischemic limbs [106]. In parallel, another study has shown that high glucose levels result in decreased proliferation and increased apoptosis of endothelial progenitors [107].

While allogeneic cell therapy approaches are under evaluation in various settings, many ongoing clinical trials involve autologous cells [108, 109]. There is an urgent need, therefore, to evaluate the therapeutic activity of progenitor cells obtained from donors that closely match the patient with have a smoking history.

1.2.3 ASC as readily available therapeutic agents

Enzymatic digestion of adipose tissue produces stromal vascular fraction (SVF), composed of ASC, endothelial cells (EC), pericytes, lymphocytes, granulocytes, and fibroblasts [110]. Upon *in vitro* expansion, a pure population of ASC can be obtained within days [111]. ASC are multipotent cells that can differentiate *ex vivo* into bone, cartilage, or adipose tissue [110, 112]. Autologous ASC are readily obtained in high numbers via minimally invasive liposuction (Figure 1). In clinical settings, ASC administration may occur either locally or systemically. Damaged tissue is known to secrete various chemo-attractants that aid stem cells in migrating towards the site of injury, which is highly beneficial, especially if the site of injury is not well defined or difficult to access [111, 113].

ASC exhibit robust pro-angiogenic, anti-apoptotic, and anti-inflammatory paracrine properties, and multiple pre-clinical and clinical studies have shown that both local and systemic administration of ASC promotes tissue revascularization and blood flow perfusion in acute or chronic ischemic tissues [80, 89, 90] including brain after stroke [114], infarcted heart [83, 115, 116], emphysema [45], and ischemic muscles in case of peripheral arterial disease (PAD) [117]. ASC also possess immunomodulatory activity, and have been shown to diminish graft versus host disease [118, 119] and arthritis [120] in animal models and humans. In recent years it has become commonly accepted that the primary mechanism of many ASC therapeutic effects is their paracrine activity, which is defined as secretion of biologically active molecules that initiate a response from other cells. This

paracrine mode of action has been proposed because very low, if any, persistent accumulation of ASC in the area of injection or damage is generally observed.

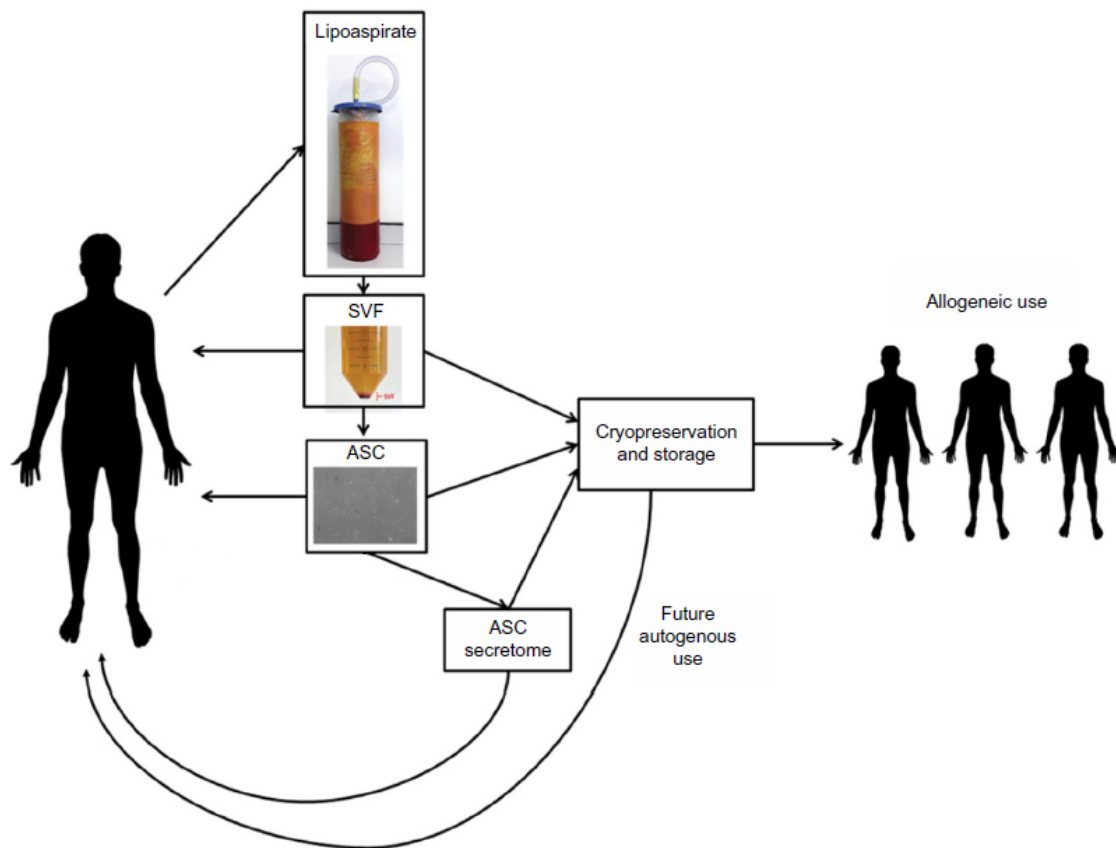


Figure 1. Schematic representation of ASC utilization for clinical use. Upon aspiration of adipose tissue (or pannus excision), material is enzymatically processed to yield stromal vascular fraction (SVF) which can be subsequently infused to the patient (tissue donor), or subject to *in vitro* cultivation, leading to cell expansion, into a homogenous population of ASC, which then can be either infused, enriched with conditioned medium or preserved for allogeneic use. Source image modified from: [111]

1.2.4 ASC in clinical trials

As ASC have been increasingly recognized as having therapeutic potential, numerous clinical trials have been initiated utilizing these cells in the United States and around the world (according to the ClinicalTrials.gov website). Studies have begun to support the efficacy of ASC in treating vascular disorders including limb ischemia [121], fistulas [122], skin ulcers [123], and knee arthritis [120] in human patients. The newly emerging therapies are subjected to high scrutiny from regulatory agencies in order to ensure their safety. In 2016 the Food and Drug Administration (FDA) held a hearing addressing the vision of ASC-based therapies [124]. The FDA guidance document currently under consideration categorized adipose tissue, from which ASC are isolated, as primarily structural tissue that is more than “minimally-manipulated” in order to be used for therapeutic purposes. This current proposal could add significant restrictions on ASC-based therapies that have been shown to present therapeutic potential and act as more than structural tissue, conveying their main regenerative (pro-angiogenic and anti-inflammatory) functions via paracrine activity [125, 126]. Numerous studies in the past several decades have revealed the highly complex role of adipose tissue and ASC in the process of regeneration. As the scientific and medical community awaits the FDA response, studies involving ASC as therapeutic cells are ongoing and will contribute toward our greater understanding of the restorative potential of these cells, as well as shedding light on the mechanisms underlying their therapeutic capacity.

1.3 Research focus

1.3.1 Study background

As indicated above, the evidence of harmful effects of CS on body is overwhelming [16, 40, 48, 68]. Concurrently, as cell therapies slowly begin to move into clinical use, it is increasingly important to evaluate in depth the effect of CS on the therapeutic potential of stem/stromal cells. The innate regenerative mechanisms of the body may be compromised in patients exposed to systemic effects of CS-derived toxins. This habit is known to affect the cardiovascular system [16, 43] and it has been shown that certain molecules present in tobacco smoke enter the blood stream from the lungs and subsequently are distributed to various vital organs.

With the knowledge that CS has negative effects on various organs and subsequently on the individual cells within the body, we felt that it was crucial to assess various effects of CS on stem/stromal cells. While undertaking these studies, which involved the chronic exposure of mice to tobacco smoke we undertook the assessment of several organs for smoking-induced pathology, which led to novel observations concerning renal changes due to smoke exposure, and the effects of ASC on these changes. I also had the opportunity to collaborate on related experiments directed to understanding the interplay between hematopoietic progenitor cells (HPC) and the effect of CS on lung health which had been suggested by prior studies from our laboratory.

1.3.2 Interconnection of cigarette smoking, hematopoietic progenitor cells, adipose-derived stromal cells, and kidney

In the following set of studies, CS is the main damage-causing factor. We focused on assessing the impact that CS has on both organ and cell pathophysiology. We conducted studies involving the effect of CS on lung and kidney tissue, as well as hematopoietic progenitor cells (HPC), and ASC. We were aware of evidence suggesting that CS may exacerbate kidney damage, and desired to explore whether there were chronic renal effects that we might be able to address or ameliorate by ASC administration, much as our laboratory had previously shown for chronic lung pathology. As we were learning that the ASC population in smokers was compromised (Chapter 2), we began to explore whether the CS-induced bone marrow damage we had also previously described might actually contribute to the lung damage, or whether these were two independent CS-induced effects. We reasoned that if HPC from bone marrow played a role in lung repair following smoke exposure, and also could retain this activity despite smoke exposure, then enhancing their mobilization with AMD3100 might be able to limit lung damage. Conversely, if HPC in smoke-exposed animals either were refractory to the mobilizing effect of AMD3100, or were unable to augment lung repair in the context of cigarette smoke exposure, then this would suggest that allogeneic therapies might be preferred or even required to address lung disease in smokers, much as I now hypothesize for vascular disease in smokers.

Chapter 2: Effects of cigarette smoking on angiogenic potential of adipose-derived stem cells

2.1 Introduction

2.1.1 Cigarette smoking and clinical trials

Cigarette smoking is undisputedly associated with numerous negative health effects. While the progress in the area of regenerative medicine and cell therapy continues to move ahead, it is important to recognize that many diseases which have the potential to be treated using stem cells or stem cell derived products may be caused by CS exposure. Interestingly, the majority of current clinical trials listed on the ClinicalTrials.gov website evaluate the therapeutic effects of autologous ASC **do not list tobacco use as an exclusion criterion**. Therefore, there is a great need to determine whether exposure to CS adversely affects the production of various cytokines and growth factors by ASC, and thus alters the overall therapeutic activity of these cells.

2.1.2 Media conditioned by ASC

Since stem cells, including ASC, have been shown to mediate their regenerative effect via secretion of various paracrine factors [80, 90, 126], the use of those very factors while excluding the cells (i.e. utilizing conditioned media) has been proposed. Recently, multiple studies have evaluated mesenchymal and adipose stem cell conditioned media (CM) as a replacement sufficient to provide key activities of these cells in various *in vitro* and *in vivo* models [126-129]. CM is

typically generated in protein-poor media in which a confluent monolayer of stem cells has been cultured for a specified amount of time, typically 24-72 hours. While this media may not favor proliferation, the cells actively secrete therapeutically active factors [88, 130]. Such CM has been shown to be able to deliver a therapeutic effect, comparable to that of stem cells, in diseases like stroke [131, 132], myocardial infarction [133, 134] and limb ischemia [126].

Clinically there is an interest in the possibility of scalable production of CM that could be allogeneic in origin, and has been defined via a series of CM assays to determine the level of beneficial factors and therefore its therapeutic potency. Clinical use of such CM could reduce the practical problems relating to autologous cell procurement as well as allogeneic cell cryopreservation.

Recent studies have shown that the beneficial effect of CM may be importantly conferred through processes involving transport and secretion of vesicular bodies, often referred to as exosomes; these are small vesicles (70-100nm in diameter) surrounded by membrane, thought to be released outside of the cell via exocytosis of an endosome that encapsulates these micro-vesicles. Timmers et al. has demonstrated that systemic administration of exosomes improves cardiac function in a mouse model of ischemia reperfusion [135]. Cantaluppi et al. has shown that administration of isolated exosomes into a rat model of non-ischemic acute kidney injury is able to reverse the damage and improve kidney function. In addition, he has demonstrated that exosomes isolated from EPC and administered systemically localize to peritubular capillaries, presumably aiding in the regenerative process [136].

2.1.3 EC/ASC co-culture-based networks

The interaction of endothelial cells (EC) and pericytes (known to wrap themselves around capillaries and venules) has been shown to have a significant role in vascular network remodeling [137, 138]. As both bone marrow-derived mesenchymal stem cells (MSC) and ASC have been shown to have pericyte-like properties [86], their role in blood vessel maintenance has been increasingly investigated in the context of regeneration of the cardiovascular system. ASC have been shown to play a role in restoration of injured vasculature [80, 89, 93]. Numerous *in vitro* studies have demonstrated that ASC participate in vessel network formation and remodeling via EC/ASC interactions when both cells are co-cultured together in an appropriate ratio [139]. ASC help to establish these networks via secretion of pro-vasculogenic growth factors like hepatocyte growth factor (HGF) and vascular endothelial growth factor (VEGF) [80, 90].

In addition, it has been proposed that for therapeutic purposes, a co-implantation of EC and ASC offers a more robust regenerative effect of vascular network formation due to immediate availability and close proximity of these two types of cells [140]. Traktuev et al. demonstrated that subcutaneous co-implantation of EC and ASC in a collagen plug in mice established robust vascular networks comparing to implantation of EC or ASC alone [141]. These seminal studies have led to ongoing clinical trials of autologous stromal vascular fraction preparations for critical limb ischemia in several countries, including an FDA-approved clinical trial, NCT02234778.

I recognized that subjects enrolled in such trials would likely include a high frequency of prior or current smokers. Accordingly, in order to assess the effect of CS on vasculogenic properties of ASC we performed *in vivo* studies utilizing a mouse model of hindlimb ischemia to compare the effects of subsequent administration of human ASC derived from smoking or non-smoking donors. In order to determine the mechanism of observed differences in the efficacy of ASC obtained from different donors, I subsequently conducted a series of *in vitro* studies assessing vasculogenic potential of these cells as well as the composition of their secretome.

2.2 Materials and Methods

2.2.1 Approvals and patient samples

Procedures for collecting umbilical cord and adipose tissue were approved by the Indiana University School of Medicine IRB. Human cord blood derived endothelial cells (CBD-EC) were isolated and expanded as previously described [142] and used at passages 5-8. Normal human dermal fibroblasts were purchased from Lonza, expanded in EGM-2MV (Lonza), and used at passage 5.

Pools of non-smoking (4 male, 6 female) and smoking (4 male, 3 female) patients for comparison purpose were matched for gender and age (male: 64.1 ± 5.5 years old, female: 39.6 ± 5.5 years old; mean \pm SD) and BMI (male: 33.5 ± 6.8 , female: 22.8 ± 2.2 ; mean \pm SD), detailed donor demographics is presented in Table 4.

2.2.2 Cell culture

Human adipose tissue samples were collected during elective liposuction procedures. Tissue was digested with collagenase Type 1 (1 mg/ml, Worthington Biochemical) for 1 hr at 37°C under gentle agitation and centrifuged at 300g for 10 minutes to facilitate separation of stromal vascular fraction (pellet) from adipocytes. Pellets were then re-suspended in media, passed through 100 μ m filter (Fisher Scientific), and centrifuged at 300g for 5 minutes. Final pellets were re-suspended in EGM-2MV media and plated. The attached cells have been described as enriched in ASC, and were expanded till passages 3-5 and used for experiments. Cells were at equal passages across all the donors for any given experiment.

Mouse ASC were isolated from subcutaneous fat pads of C57Bl/6 female mice (14 weeks old, Jackson Laboratories) following the same protocol used to isolate human ASC. Mouse ASC were expanded in EGM-2MV media and used at passage one. Cord blood-derived endothelial cells were isolated as previously described [139, 142], expanded, and used at passages 5-8.

2.2.3 Adipogenic differentiation of human ASC

Human ASC were plated at full confluency in EBM-2/5%FBS media. On the following day, media on the cells was exchanged to Adipocyte Differentiation Medium (ZenBio) for six days with single media exchanged at day three. Then cells were incubated in Adipocyte Maintenance Medium (ZenBio) for six days with a media exchange at day three. After twelve days, cells were fixed, stained with Nile Red dye (to visualize lipid droplets) and Hoechst 33342 (to visualize nuclei), and imaged using a fluorescent microscope. For quantitative analysis, plates were scanned with a fluorescent plate reader (Acumen Explorer).

2.2.4 Flow cytometry analysis of human ASC

Semi-confluent human ASC cultures were detached with 2 mM Ethylenediaminetetraacetic (EDTA) / PBS and incubated with fluorescently-tagged IgG to cell surface markers: CD13, CD29, CD73, CD90, CD105, CD140a, CD140b, CD31, CD34, CD45, Notch 2, Notch 3 (all purchased from BD) for 20 min on ice. After incubation, cells were washed and fixed with 1% formaldehyde. Labeled cells were evaluated on BD Accuri analyzer and FlowJo software.

2.2.5 Mouse cigarette smoke exposure model

Animal studies were approved by the Institutional Animal Care and Use Committee at Indiana University School of Medicine. C57BL/6 mice (female, 10-week old) were placed into a Teague 10E chamber (Teague Enterprises, Figure 2) and exposed to 11% mainstream and 89% side-stream CS (Cigarette Smoke group) for 5 hrs/day (5 days/week for one month or five months) [105]. CS was generated by reference cigarettes (3R4F; Tobacco Research Institute, University of Kentucky, Kentucky). The total amount of suspended particulates (on average 90 mg/m³) and carbon monoxide (on average 350 ppm) within the chamber were monitored on a daily basis, as previously described [105]. In parallel, another set of mice was maintained in ambient air as Air Control group. After a one month smoking regimen was completed, mice were euthanized, subcutaneous adipose tissue was collected and used to isolate adipose stem cells. In a study that involved 5-month smoke exposure, animals were subjected to hindlimb ischemia inducing surgery after completion of the preconditioning period.

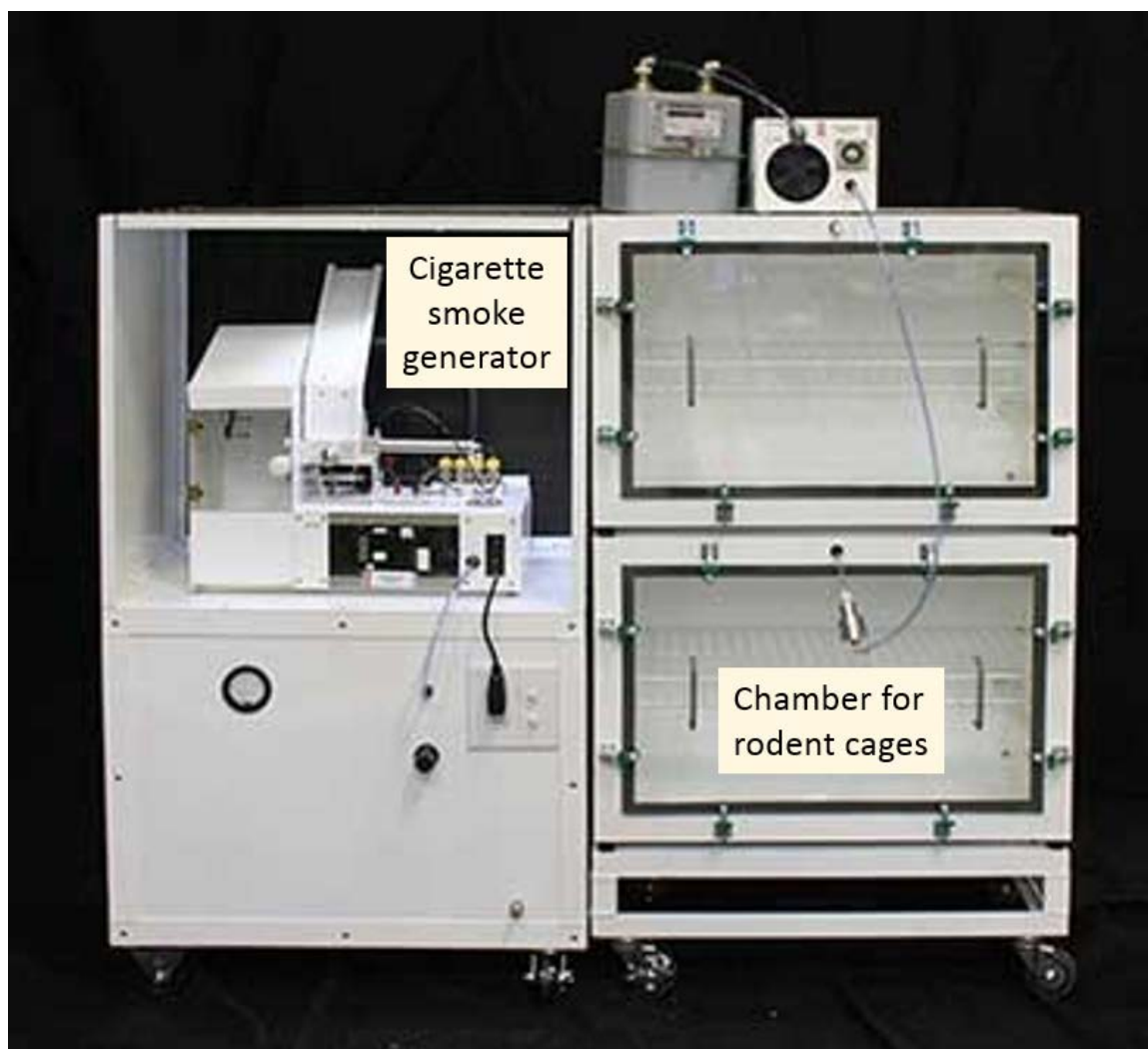


Figure 2. Teague Smoking Chamber (Teague Enterprises). Photo illustrates a smoke machine and two exposure chambers

2.2.6 Mouse hindlimb ischemia model

C57Bl/6 mice (male and female, 10-week old) were anesthetized with 2.5% isofluorane. A small incision was made at the middle section of the left hindlimb, followed by ligation and excision of the femoral artery, vein, and vascular branches along the length from inguinal ligament to bifurcation of saphenous and popliteal arteries. The incision was closed using 6-0 silk sutures. Animals were randomized into two cohorts to test early (two groups A, all female mice, cell or control injection 24-hours post-surgery; n=6-8) and delayed (two groups B, male and female (ratio 1:1), cell or control injection 32 days post-surgery; n=6) therapy approaches. Mice received injections via tail vein in 120 µl of basal medium. In cohort A, mice received either basal medium (EBM2, Lonza) or 5×10^5 human ASC from either smoking or non-smoking donors. The effects of ASC obtained from three non-smoking and three smoking donors were tested individually here. In cohort B, mice received either 5×10^5 human ASC obtained from either one smoking or one non-smoking donor. Blood flow in ischemic and contralateral intact limbs was evaluated using Laser Doppler Imager (Moor Instruments, Wilmington, DE) [143]. For each mouse, three consecutive images were obtained from plantar area, and mean perfusion value was calculated. The tissue perfusion value (TPV) in affected limb is presented as $TPV [\%] = (\text{left limb} \times 100\%) / (\text{right limb})$. Blood flow was assessed before the surgery and then on days 1, 4, 7, 14, 21, 28 post surgery for cohort “A”, and were further expanding to days 39-74 (will scans every 7th day) for cohort “B”.

In addition, we conducted a study during which a subset of mice was placed in an environmental chamber and exposed to CS for 5 hours/day, 5 days/week for

5 months, while the remaining mice were exposed to ambient air for the same time course. Two weeks prior to the completion of the preconditioning period, a small subset of animals was removed from ambient air group and euthanized in order to remove their fat pads to isolate mouse ASC (mASC), following the same protocol used for human ASC isolation. Upon completion of the full conditioning period, all remaining mice were subjected to the standard hindlimb ischemia-inducing surgical procedure. The following day, mice received intravenous administration of mASC from non-smoking donors, at passage 1, or vehicle. Blood flow was assessed prior to surgery and on days 1, 4, 7, 14, 21, 28 post-surgery.

2.2.7 Vascular Network Formation Assay

The EC-ASC co-culture vasculogenesis model was arranged as routine and previously described [139]. Briefly, EC (10^4 cell/cm²) were pre-mixed with either human or mouse ASC (6×10^4 cell/cm²) or normal human dermal fibroblasts (NHDF, 6×10^4 cell/cm²) and incubated in either EBM-2/5%FBS media alone or supplemented with 50% human ASC-CM. The co-cultures were incubated for six days with media exchange at day three. In separate set of experiments, EC-ASC co-culture incubation media was supplemented with either vascular endothelial growth factor (VEGF-A), or hepatocyte growth factor (HGF), or stromal derived growth factor1 (SDF-1), each at 10 ng/ml. To test the role of SDF-1 in network formation, EC-ASC co-cultures were supplemented with AMD3100 (an antagonist of SDF-1 receptor CXCR-4) at 0.1, 1, 5, or 10 µg/ml or with 5mM of Diprotin A (an inhibitor of DPP4), at the time of plating. To test for a role of CD26/DPP4 in modulating vascular network formation. To evaluate the degree of vascular

network formation, co-cultures were fixed in methanol (-20°C, for 5 minutes), stained with biotinylated Lectin (Ulex Europaeus Agglutinin I, Vector labs) for 1 hour, followed by incubation with Streptavidin Alexa 488 (Invitrogen) for 30 min. Fluorescently stained cultures were imaged using a Nikon Eclipse Ti microscope (example of the scanning area is shown in Figure 3). Digital images were acquired using a 4x objective (nine images per well) and processed with MetaMorph software using the “Angiogenesis Tube Assay” algorithm (Molecular Devices, Downingtown, PA).

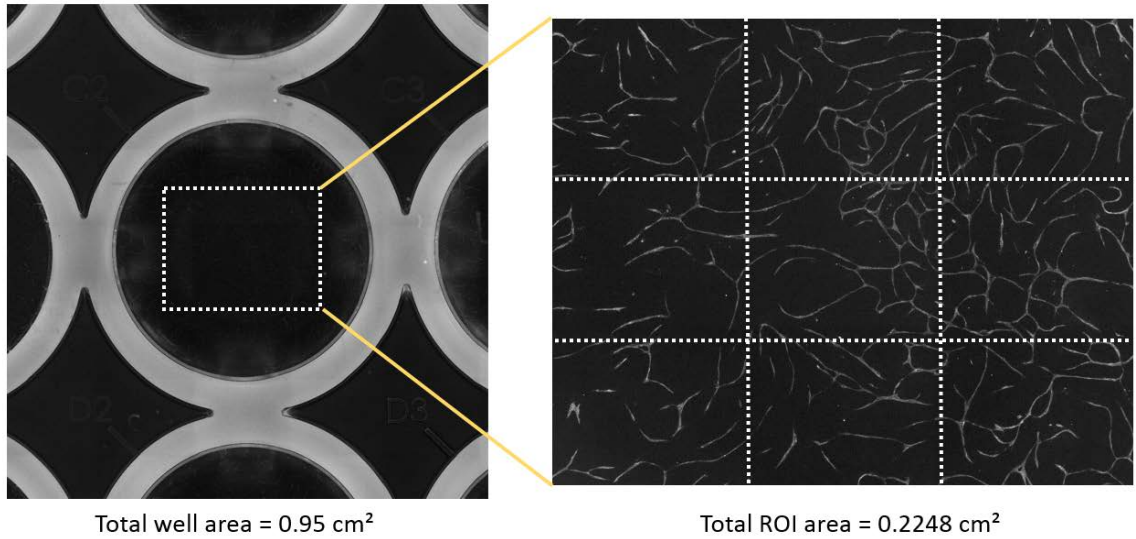


Figure 3. Vascular Network Formation Assay: well assessment. **A**, 8x8 scan of part of 48-well plate. White square inside the well indicates the area of interest that is photographed for VNF analysis purposes. **B**, 3x3, stitched, scanned image from within the well, with 5% overlap between each of the 9 individual images.

2.2.8 Conditioned media generation

To generate ASC conditioned media (ASC CM), human ASC (passage 3-5) confluent monolayers were incubated over EBM-2/5%FBS medium for 48 hours. Conditioned media were collected, centrifuged at 400g for 10 minutes, and supernatants were aliquoted and stored at -80°C. For subsets of experiments, CM were 2.5-fold concentrated using Amicon Ultra-15 Ultracell 10K columns (Millipore). In subset of tests, human ASC we incubated in the presence of 10 ng/ml of tumor necrosis factor-alpha (TNF α) or interleukin-1 β (IL-1 β) for 48 hours. CM from EC/ASC co-cultures was collected on Day 6, after 72 hours of incubation.

2.2.9 EC survival assay

Cord Blood derived (CBD)-EC (passage 5) were seeded at 10⁴ cells/cm² in control EBM-2/5%FBS media. Next day, media on the cells was exchanged to control media alone or premixed with human ASC-CM in ratio 1:1. Cells were incubated for four days, then fixed and stained with 4',6-Diamidine-2'-phenylindole dihydrochloride (DAPI). Series of images were taking using Nikon Eclipse Ti microscope followed by their processing using ImageJ software to calculate the cell numbers.

2.2.10 Proteomic analysis of human ASC conditioned media

Concentrated samples of media conditioned by human ASC as described earlier were transferred to the Indiana University Proteomics Core. Samples from one non-smoker and one smoker were solubilized with equal volumes of 8 M urea/10mM DTT at room temperature, and protein concentration was determined

by the Bradford assay (48). Each sample was processed as previously described (49).

Sample digests were analyzed using a Thermo Scientific Orbitrap Velos Pro hybrid ion trap-Orbitrap mass spectrometer coupled with a Surveyor autosampler and MS HPLC system (Thermo Scientific). Mass spectral data were collected in the “Data dependent MS/MS” mode of Fourier transform-ion trap (MS-MS/MS) with the electrospray ionization interface using normalized collision energy of 35% (collision induced dissociation).

The acquired data were searched against the UniProt protein sequence database of HUMAN (released on 02/04/2015) using X!Tandem algorithms in the Trans-Proteomic Pipeline (<http://tools.proteomecenter.org/software.php>) (TPP, v. 4.6.3). The identifications of peptide and protein made by X!Tandem were validated by PeptideProphet (50) and ProteinProphet (51) in the Trans-Proteomic Pipeline (<http://tools.proteomecenter.org>). Only validated proteins and peptides with protein probability ≥ 0.9000 and peptide probability ≥ 0.8000 of being correct, were reported. Protein quantity was determined using a label-free quantification software package, IdentiQuantXL (53).

2.2.11 RayBiotech

Semi-quantitative assessment of relative protein expression was determined using Human Cytokine Antibody Array (C5) (RayBiotech). In principle, the capture antibodies from the angiogenic panel were embedded in a “dot-manner” on a nitrocellulose membrane. The assessment process involved bathing

the membranes in the tested ASC CM, application of biotinylated detection antibody and subsequent chemiluminescent signal assessment. The membranes were photographed and the intensity of each dot was determined using ImageJ software.

2.2.12 ELISA analysis of human ASC conditioned media

The presence and concentration of hepatocyte growth factor (HGF), vascular endothelial growth factor (VEGF), stromal cell-derived factor 1 (SDF-1), Angiopoietin-1, Angiopoietin-2, and Activin A in ASC-CM was assessed by ELISA using the reagents purchased from RnD Systems and following manufacturer's protocols. Additionally, ASC-CM were analyzed for expression of selected cytokines and growth factors using RayBiotech C-Series Human Cytokine Antibody Array C5 (RayBiotech Inc.) according to the manufacturer's instructions.

2.2.13 Analysis of mRNA expression in human ASC

ASC semi-confluent monolayers were lysed and total RNA was isolated using NucleoSpin RNA II kit (Clontech, Mountain View, CA). cDNA was generated using iScript RT kit and polymerase chain reactions were performed using iTaq SYBR Green PCR Supermix (Bio-Rad, Hercules, CA) on StepOnePlus machine (Applied Biosystems). Primers were used, as listed in Table 1.

Primer	Forward	Reverse
βActin	caccattggcaatgagcgggtc	aggctcttgcggtatgccacgt
HGF	gagagttgggttcttactgcacg	ctcatctcctcttccgtggaca
SDF1	gcccgtcagcctgagctaca	ttcttcagccgggctacaatct
VEGF	ttgccttgctgctctacctcca	atggcagtagctgcgctgata
Pai1	ctcatcagccactggaaaggca	gactcgtgaagtcagcctgaaac
TSG-6	cggggtaccatgatcatcttaatttactt	ggatgatcagtggtctaaatctcca
CD140a	ttcccttggtggcaccc	ggtagccactcttgatcttattgtagaa
CD140b	gccttaccacatccgctc	tcacactcttccgtcacattgc

Table 1. Forward and reverse primer sequences.

2.2.14 Analysis of DPP4 activity in human ASC CM

The Dipeptidylpeptidase (DPP) 4, protein known as CD26 and expressed on the surface of many cell types, has been shown to act as protease by cleaving various cytokines and chemokines containing proline or alanine, hence modifying their function [144]. Since SDF-1, which was observed to be expressed and secreted to a lesser degree in ASC from CS donors, can potentially be cleaved by DPP4, therefore rendering it non-functional, the DPP4 activity in ASC CM derived from smokers and non-smokers was assessed using DPPIV-Glo Protease Assay (Promega, Madison, WI) according to the manufacturer's instructions. Colorimetric change was assessed using a luminometer machine.

2.2.15 Statistical analysis

Quantitative data is expressed as mean \pm SEM. Statistical analysis of the data that include only two experimental groups was performed with an unpaired t-test. Analysis of data with at least three groups was performed with ANOVA with Tukey's multiple comparisons test. Statistical analysis was performed using Prism 4 (Graphpad, San Diego, CA).

2.3 Results

2.3.1 Morphological and phenotypic assessment of human ASC from smoking and non-smoking donors

To determine whether CS exposure affects ASC morphology and proliferation rate, isolated cells were plated in EGM-2MV media and expanded for several passages. Evaluation of ASC at passage 3 using phase contrast microscopy revealed no visual differences of CS-ASC (ASC from smoking donors, n=3) when compared to non-CS-ASC (ASC from non-smoking donors, n=4) (Figure 4A). Furthermore, proliferative rates (doubling time) of ASC of both cell types were similar (Figure 4B). To test the effect of CS exposure on cell differentiation potential, ASC were subjected to adipogenic differentiation protocol. Quantitative analysis performed by staining of differentiated cell monolayers with Nile Red to reveal lipid droplets and counterstained with Hoechst 33342 to reveal nuclei showed that both CS and non-CS ASC undergo adipogenic differentiation to the same degree (Figure 4C, D). Flow cytometric analysis of surface markers known to be expressed by ASC revealed that both non-CS-ASC and CS-ASC at passage 4 are positive for CD13, CD29, CD73, CD90 and CD105. At the same time, cell populations were free of endothelial cells (CD31) and leukocytes (CD45). As also expected, samples were negative for CD34, which we previously described as expressed only in freshly isolated ASC. These findings are consistent with previous observations by many groups [145] in regards to expanded ASC. However, we did observe a difference in expression of CD140a (PDGFR α) and 140b (PDGFR β , a pericyte marker). Both receptors were expressed to a lower

extent in CS-ASC by comparison with non-CS-ASC. The assessment of Notch 2 and 3 expression revealed a dramatically higher expression of Notch 2 and slightly higher expression of Notch 3 in CS-ASC (Figure 4E).

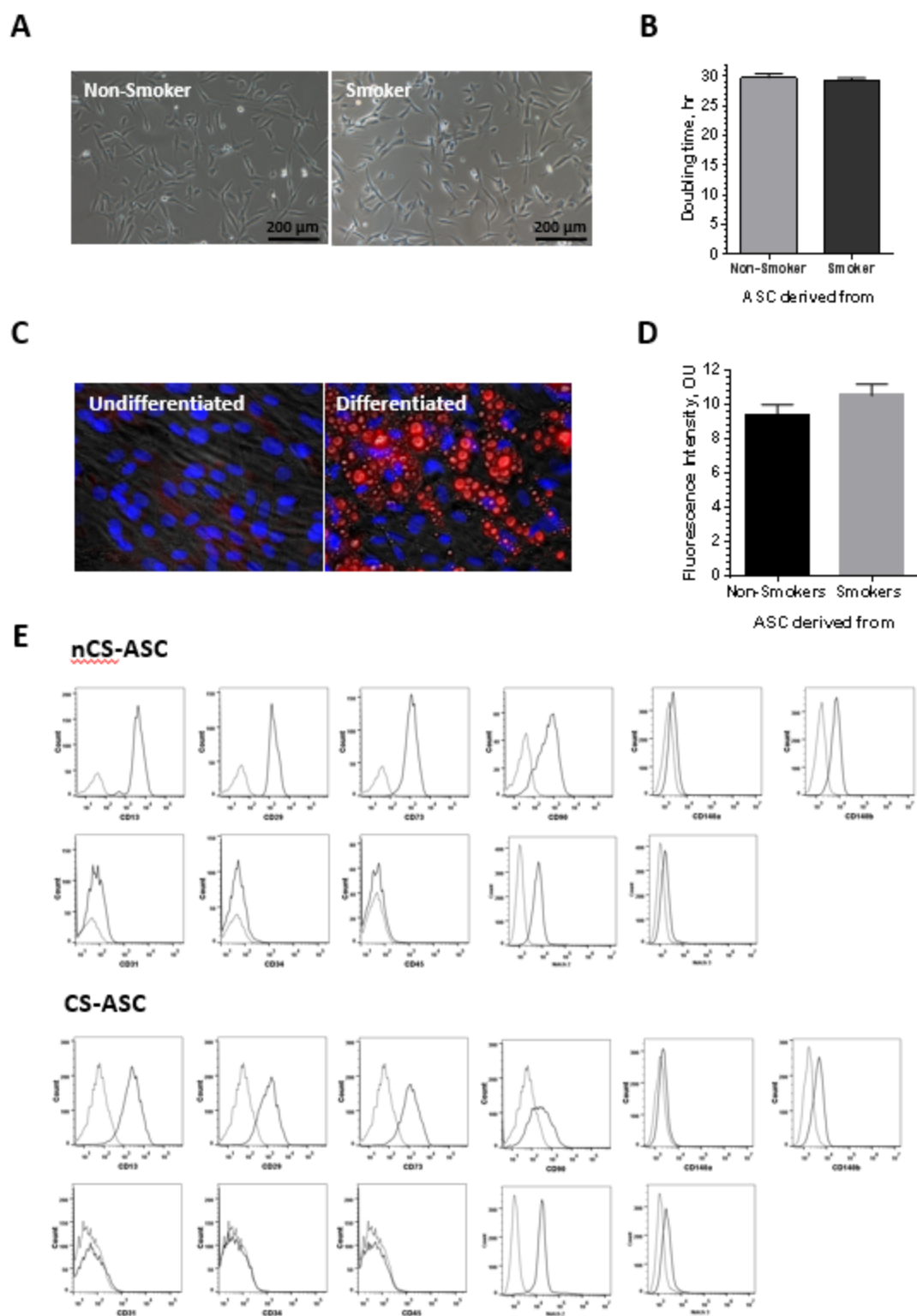


Figure 4. Morphological, differentiation and phenotypic assessment of ASC from smoking and non-smoking donors. A, Representative images of

ASC from nonsmoking and smoking donors at passage 3. **B**, Analysis of proliferative rate of ASC. Cell were plated at semi-confluency and incubated in EGM-2MV media for one or four days. Difference in cell counts at these time-points was used to calculate cell doubling time. **C**, Representative images of undifferentiated and differentiated ASC at day 12 of adipogenic differentiation protocol. Cells were fixed and stained with Nile Red (red) to reveal lipids and Hoechst 33342 (blue) to reveal nuclei. **D**, Quantitative analysis of lipid accumulation (intensity of fluorescent signal of Nile red) in ASC, from nonsmoking and smoking donors, subjected to adipogenesis differentiation protocol. **E**, Flow cytometric analysis of surface marker expression by ASC at passage 4, from non-smoking and smoking donors.

2.3.2 Analysis of therapeutic effect of ASC from smoking and non-smoking donors

To evaluate whether chronic smoke exposure affects the therapeutic potency of *in vitro* expanded ASC, mice with hindlimb ischemia induced as described above received systemic injections of ASC obtained from one of three non-CS or one of three CS female human donors (six mice per each donor) next day post-surgery. As expected, non-CS-ASC routinely and significantly improved blood flow in the ischemic limbs by day seven ($p < 0.001$), whereas CS-ASC were ineffective regardless of the CS donor (Figure 5A, B). In the subsequent study I evaluated whether ASC would be able to improve the blood flow in chronically ischemic limbs. After induction of limb ischemia, mice were allowed to recover for one month and then received intravenous infusion of ASC from one non-CS and one CS female donors. Similar to the first study, non-CS-ASC significantly improved perfusion in affected limbs, whereas CS-ASC were entirely ineffective ($p < 0.001$) (Figure 5C).

In addition we conducted a study during which mice were exposed to CS or ambient air for 5 hours/day, 5 days/week for 5 months, followed by immediate induction of hindlimb ischemia. Next day after surgery seven mice in each group (AC and CS) have received intravenously either AC-mASC, obtained from eight months old ambient air-exposed animals, or vehicle. Analysis of blood flow restoration in the ischemic limbs revealed that mASC administration was ineffective when provided to either AC or CS mice, when compared to vehicle treatment. However, in the secondary analysis, where data with blood flow

recovery in CS mice, independent of the treatment (ASC+Veh), was evaluated against the flow recovery in all AC mice, the statistically significant reduction in the rate of recovery in CS mice was detected ($p=0.02$, Figure 5D).

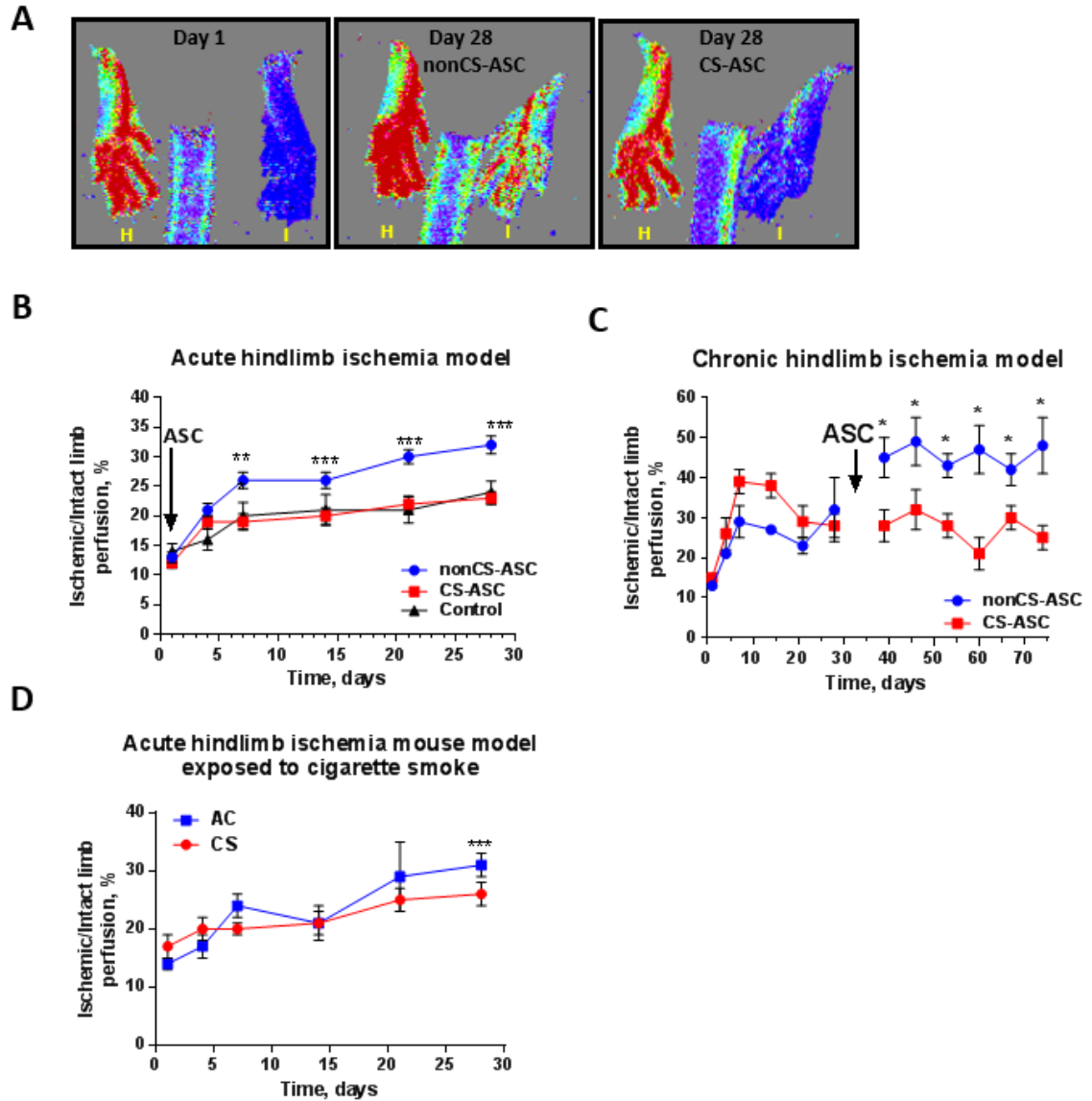


Figure 5. Analysis of therapeutic effect of ASC from smoking and non-smoking donors. **A**, Representative Laser Doppler Imager-generated flux images from planter area of healthy (H) and injured (I) limbs of mice at day 1 and day 28 after surgery. Mice were treated with human ASC from nonsmoking (non-CS-ASC) and smoking (CS-ASC) female donors. **B**, Quantitative analysis of blood flow restoration in hindlimb in model of acute ischemia. 5×10^5 ASC were systemically administered through tail vein one day after ischemia induction. Graph represents

data from three non-CS-ACS donors and three CS-ASC. Each sample of ASC was provided to six animals. Control group was composed of seven mice. **C**, Quantitative analysis of blood flow restoration in hindlimb in model of chronic ischemia. 5×10^5 ASC were systemically administered through the tail vein 32 days after ischemia induction. Graph represents data from one non-CS-ACS donors and one CS-ASC (n=6/group). **D**, Quantitative analysis of blood flow restoration in hindlimb in model of acute ischemia conducted in a CS-pre-exposed mice. Mice were pre-exposed to AC or CS for five months, followed by surgical procedure to induce limb ischemia. Next day, 5×10^5 mASC, obtained from 8-month old AC-exposed mice, or Vehicle were administered through the tail vein. Graph represents the combined data (mASC-treated and Vehicle-treated) for AC and CS mice (n=14). For all graphs: * $p < 0.05$, ** $p < 0.01$, *** $p < 0.001$.

2.3.3 Analysis of vasculogenic activity of ASC from smoking and non-smoking donors

To determine whether the marked abnormality found in the ability of ASC to influence recovery from hindlimb ischemia was recapitulated *in vitro*, we employed a co-culture model of ASC with EC established by our laboratory. In this model, cells are incubated in growth factor-poor media (EBM2/5%FBS), and ASC support EC reorganization into vascular structures in a manner which is highly dependent on direct as well as paracrine interactions between ASC and EC. In assessing the vasculogenic activities of ASC from three non-CS and three CS female donors we determined that while EC cultured on monolayers of non-CS-ASC established dense vascular cords as expected (Figure 6A), EC cultured on CS-ASC established less dense vascular networks. Quantitative analysis revealed a 33% decrease in vessel density when formed on CS-ASC (Figure 6B). To evaluate whether this detrimental effect of smoking on ASC vasculogenic activity was influenced by donor sex, we also conducted this analysis with ASC from male donors. In parallel with our findings for female ASC, EC incubated on CS-ASC from male donors produced vascular networks 35% lower in density than EC cultured on non-CS-ASC male donors ($p < 0.01$) (Figure 6B). To further extend these results from human donors, we conducted an additional set of experiments in which human EC were co-cultured with mouse ASC isolated either from healthy (Air Control) female mice or from mice which had been exposed to CS for one month. We found that human EC were able to establish vascular cords when cultured on mouse ASC, but the density of vessels was 23% lower in co-cultures containing

ASC from CS-exposed mice compared with co-cultures with healthy ASC (Figure 6C), confirming that the adverse effect of CS on the ability of ASC to support vascular network formation was also conserved across species.

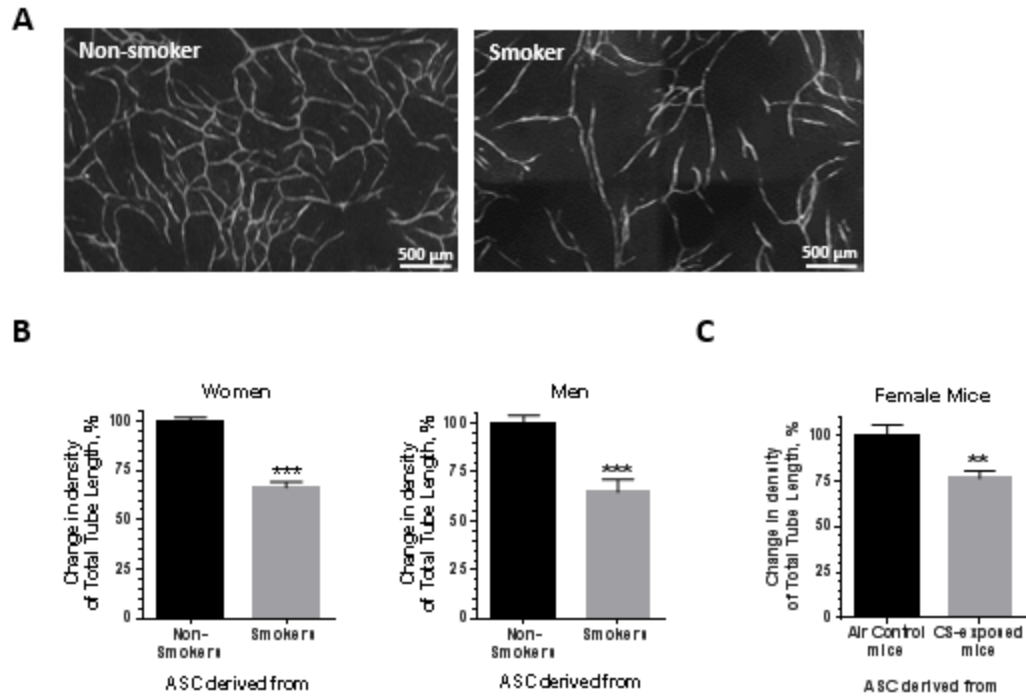


Figure 6. Analysis of vasculogenic activity of ASC from smoking and non-smoking donors. **A**, Representative images of vascular networks formed by EC co-cultured with ASC derived from non-smoking or smoking human female donors. EC-ASC co-cultures were incubated for six days, then fixed and stained with Ulex Europaeus Agglutinin I (white) to reveal vascular cords. **B** and **C**, Quantitative analysis of vascular network formation (expressed as density of total tube length) by EC co-cultured with ASC derived from non-smoking or smoking human female and male donors (**B**) or with ASC obtained from female C57Bl/6 mice after one month exposure to either ambient air (Air Control) or CS (**C**). For all graphs: ** $p < 0.01$, *** $p < 0.001$.

2.3.4 Vasculogenic activity of ASC conditioned media

To specifically investigate the role of paracrine activity of ASC on vasculogenesis, we evaluated the ability of ASC conditioned media (CM) to augment vascular network formation by EC when cultured on fibroblast monolayers. Fibroblasts, as previously reported [139], are inherently relatively weak in the ability to support EC vasculogenesis, rendering the EC-fibroblast co-culture model suitable as a system in which to test the effects of pro-vasculogenic factors, including ASC CM [139]. Exposure of EC-fibroblast co-cultures to 50% non-CS-ASC CM increased the density of vascular networks by 74% compared to co-cultures incubated in control media, however exposure of the similar co-cultures to CS-ASC CM produced a lesser degree (25%) of improvement in network density(Figure 7A).

To address potential mechanisms of this finding, ASC CM was tested for ability to promote EC survival. Semi-confluent EC cultures were incubated in EBM-2/5%FBS media alone or supplemented with 50% of female donor ASC-CM (non-CS and CS) for four days. non-CS-ASC CM improved EC survival/proliferation by 150%, whereas CS-ASC CM produced only 94% improvement (Figure 7B).

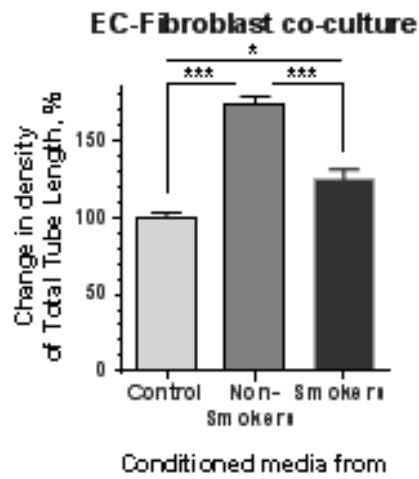
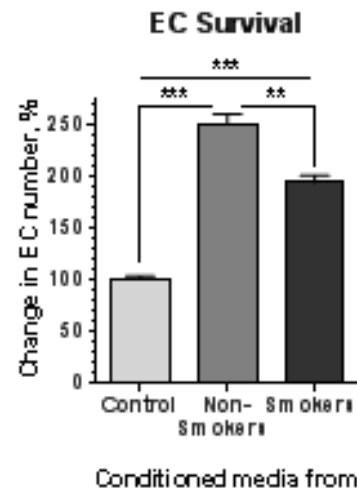
A**B**

Figure 7. Vasculogenic activity of ASC conditioned media. **A**, Quantitative analysis of vasculogenic activity of 48-hour ASC conditioned media in EC-Fibroblast co-culture model. EC-Fibroblast co-cultures were incubated in control media alone or supplemented with ASC-CM from non-smoking or smoking female donors (in ratio 1:1). Co-cultures were incubated for six days with media exchange at day 3. **B**, Analysis of the effect of ASC-CM from non-smoking and smoking donors on EC proliferation/survival. Semi-confluent monolayers of EC were exposed to control media alone or supplemented with ASC CM (in ratio 1:1) for four days, then fixed, stained with DAPI to reveal nuclei, and counted. For all graphs: * $p < 0.05$, ** $p < 0.01$, *** $p < 0.001$.

2.3.5 Proteomic analysis of human ASC CM

Proteomic assessment of CM derived from one non-CS (healthy non-smoker) and one CS (most severe smoker) human ASC donor, using MS/MS technique, revealed 714 unique proteins. This method allows for quantitative identification of proteins in the tested sample. MS/MS, also known as Tandem Mass Spectrometry, relies on a generation of ions that are separated by mass-to-charge ratio to be further photo-dissociated and detected. The detected ions are then matched with corresponding peptides via the use of one or more databases. Among the identified proteins, 12 were decreased in CS sample, while 13 were increased in the CS sample by 3-fold or more. The analysis revealed a decrease in SDF-1 in the CS-ASC CM. Notably, presence of pro-angiogenic factor, VEGF, was not detected in either of the samples. In addition, certain proteins that are associated with smoking history of the donor and can be detected in the patient's serum, were also present in the CS-ASC CM. These include ASAH1, a biomarker for emphysema, CTSB, a protein induced by CS and implicated in tumor metastasis, LTBP1, a protein correlated with COPD development, SIX3, a protein which when downregulated is associated with lung adenocarcinoma, APOE, a protein which decreases with aging and is a free radical scavenger. All proteins with 2 or more fold difference between the CS and non-CS donors are listed in Table 2. Parallel protein analysis of CM media sample from the same donors using a semi-quantitative Human Cytokine Antibody Array (C5) has revealed a marked decrease of the relative expression level of 10 out of 80 different cytokines in the sample derived from CS donors including IL6, IL8,

MCP1, CCL5, Angiogenin, VEGF-A, CXCL6, HGF, MIP-3a, TIMP1 (Figure 8, Table 3).

Gene Name	Protein Name	Protein Probability	non-CS-ASC CM [Relative abundance]	CS-ASC CM [relative abundance]	Fold Difference
GAS6	Isoform 4 of Growth arrest-specific protein 6	1.00	934220	5731400	6.1
TARS	Isoform 2 of Threonine--tRNA ligase, cytoplasmic	1.00	1378078	7264500	5.3
ASAH1	Isoform 3 of Acid ceramidase	1.00	659363	3435175	5.2
AP2M1	AP-2 complex subunit mu	1.00	2607551	10643975	4.1
CTSB	Cathepsin B	1.00	382262770	1444213400	3.8
ABI3BP	Target of Nesh-SH3	1.00	47295678	175541025	3.7
CDC37	Hsp90 co-chaperone Cdc37	0.94	688975	2499225	3.6
CXCL1	Growth-regulated alpha protein	1.00	13973951	47150933	3.4
COMP	Cartilage oligomeric matrix protein	1.00	8492298	26807117	3.2
RPL8	60S ribosomal protein L8	1.00	726116	2171784	3
DKK3	Dickkopf-related protein 3	0.94	304992	922000	3
SERPINE2	Glia-derived nexin	1.00	37743733	114677733	3
PAPPA	Pappalysin-1	1.00	2640993	7950100	3
COL16A1	Collagen alpha-1(XVI) chain	1.00	4167375	12061634	2.9
LTBP1	Latent-transforming growth factor beta-binding protein 1	1.00	7456508	20867643	2.8
CXCL6	C-X-C motif chemokine	1.00	25652450	71316000	2.8
ASAH1	Acid ceramidase	1.00	1618546	4519825	2.8
CLEC11A	C-type lectin domain family 11 member A	1.00	16081542	42856800	2.7
ALDOC	Fructose-bisphosphate aldolase	1.00	637942	1698375	2.7

LTBP1	Isoform 4 of Latent-transforming growth factor beta-binding protein 1	1.00	15385147	41546988	2.7
LTBP1	Isoform 3 of Latent-transforming growth factor beta-binding protein 1	1.00	13546688	36285298	2.7
AEBP1	Adipocyte enhancer-binding protein 1 (Fragment)	1.00	682938	1743725	2.6
HIST1H1C	Histone H1.2	1.00	1095634	2855117	2.6
RCN1	Isoform 2 of Reticulocalbin-1	1.00	2599323	6753800	2.6
FAT2	Protocadherin Fat 2	0.97	1487189	3927500	2.6
PSMA4	Proteasome subunit alpha type	0.97	236484	595261	2.5
ACTN4	Alpha-actinin-4	1.00	188291467	465277880	2.5
RPL30	60S ribosomal protein L30	1.00	6212300	14876975	2.4
STC2	Stanniocalcin-2	1.00	2600795	6123636	2.4
ARPC1B	Actin-related protein 2/3 complex subunit 1B	1.00	3648439	8706650	2.4
GAS6	Isoform 2 of Growth arrest-specific protein 6	1.00	35761020	85913700	2.4
SH3BGR13	SH3 domain-binding glutamic acid-rich-like protein 3	1.00	1679634	3793134	2.3
AGRN	Agrin	1.00	404157	915088	2.3
ARPC4	Actin-related protein 2/3 complex subunit 4	1.00	882865	2055367	2.3
RPS19	40S ribosomal protein S19 (Fragment)	1.00	3389170	7933850	2.3
LAMA1	Laminin subunit alpha-1	1.00	5562100	12702450	2.3
ARPC4	Actin-related protein 2/3 complex subunit 4 (Fragment)	1.00	293882	688151	2.3
ADAMTSL1	ADAMTS-like protein 1	1.00	1182025	2755550	2.3
RPL23A	60S ribosomal protein L23a	1.00	1301075	2822467	2.2
CD59	CD59 glycoprotein	1.00	2655434	5715133	2.2

RPL11	60S ribosomal protein L11	0.97	753763	1652988	2.2
WDR1	WD repeat-containing protein 1 (Fragment)	1.00	1163981	2458975	2.1
RPLP0	60S acidic ribosomal protein P0	1.00	1698298	3553386	2.1
COL1A1	Collagen alpha-1(I) chain	1.00	1279345230	2682566450	2.1
RDX	Isoform 5 of Radixin	1.00	1349525	2882750	2.1
CAND1	Cullin-associated NEDD8-dissociated protein 1	0.94	383421	813950	2.1
SIAE	Isoform 2 of Sialate O-acetyltransferase	1.00	9120400	18722125	2.1
FBN2	Fibrillin-2	1.00	35581622	71356611	2
OLFML3	Isoform 2 of Olfactomedin-like protein 3	1.00	16586451	33384918	2
ACTR3	Actin-related protein 3	1.00	6342950	12438050	2
ARPC3	Actin-related protein 2/3 complex subunit 3	0.96	871483	1701384	2
ANXA6	Annexin	1.00	2890500	5848275	2
NEU1	Sialidase-1	0.96	470940	965375	2
RPL3	60S ribosomal protein L3	1.00	1363825	2726900	2
RCN3	Reticulocalbin-3 (Fragment)	1.00	3653517	7129884	2
RCN3	Reticulocalbin-3	1.00	8529491	17095659	2
IPO7	Importin-7	1.00	589658	1161600	2
TIMP1	Metalloproteinase inhibitor 1	1.00	1056989900	2079538450	2
SERPINE1	Plasminogen activator inhibitor 1	1.00	527223650	1060162950	2
HSPA8	Heat shock cognate 71 kDa protein	1.00	154396703	301719550	2
ACTN1	Isoform 4 of Alpha-actinin-1	1.00	22156883	45079863	2
RPS12	40S ribosomal protein S12	1.00	11789600	24042800	2
LOX	Protein-lysine 6-oxidase	1.00	44983450	88717200	2
CXCL5	C-X-C motif chemokine 5	1.00	52634872	106439400	2
FKBP1A	Peptidyl-prolyl cis-trans isomerase FKBP1A	1.00	11113550	22647750	2

GSTO1	Glutathione S-transferase omega-1	1.00	14799064	29595583	2
GAS6	Growth arrest-specific protein 6	1.00	31038985	63498100	2
PSAT1	Isoform 2 of Phosphoserine aminotransferase	0.91	580350	1139075	2
PLAU	Isoform 2 of Urokinase-type plasminogen activator	1.00	1207834	591780	-2
RPS15A	40S ribosomal protein S15a	1.00	6781375	3242625	-2.1
FLNB	Filamin-B	1.00	247657	119933	-2.1
WISP2	WNT1-inducible-signaling pathway protein 2	1.00	125547550	59272450	-2.1
MARCKS	Myristoylated alanine-rich C-kinase substrate	0.97	6174750	2745675	-2.2
IGF2	Insulin-like growth factor II	1.00	5333783	2407483	-2.2
CAP1	Adenylyl cyclase-associated protein (Fragment)	1.00	574775	255490	-2.2
RARRES2	Retinoic acid receptor responder protein 2 (Fragment)	1.00	7131550	3070400	-2.3
CAPNS1	Calpain small subunit 1 (Fragment)	1.00	4313650	1896975	-2.3
PYGB	Glycogen phosphorylase, brain form	1.00	7677900	3372050	-2.3
PTGDS	Prostaglandin-H2 D-isomerase	1.00	242410500	101110866	-2.4
KNG1	Isoform 3 of Kininogen-1	1.00	9457467	3754500	-2.5
RARRES2	Retinoic acid receptor responder protein 2	1.00	8157315	3277984	-2.5
HIST1H2BB	Histone H2B type 1-B	1.00	2080666	801451	-2.6
HIST2H2AA3	Histone H2A type 2-A	1.00	98988400	37442717	-2.6
PDGFRL	Platelet-derived growth factor receptor-like protein	1.00	98878912	37245100	-2.7
C7	Complement component C7	1.00	8682100	2720100	-3.2
CHI3L1	Chitinase-3-like protein 1	1.00	442732900	139619450	-3.2

FN1	Isoform 7 of Fibronectin	1.00	4519341	1375900	-3.3
AHSG	Alpha-2-HS-glycoprotein	1.00	137093000	40643000	-3.4
ANKRD31	Putative ankyrin repeat domain-containing protein 31	0.98	30940750	8863750	-3.5
CSE1L	Exportin-2	1.00	47798617	13531001	-3.5
SFRP2	Secreted frizzled-related protein 2	1.00	7235300	1951672	-3.7
AP2A1	AP-2 complex subunit alpha-1	1.00	4798470	1279435	-3.8
APOE	Apolipoprotein E	1.00	796471700	210545800	-3.8
GPX3	Glutathione peroxidase	1.00	13578250	2924893	-4.6
CXCL12	Isoform Alpha of Stromal cell-derived factor 1	1.00	6112650	1302851	-4.7
SIX3	Homeobox protein SIX3	0.95	15090500	650732	-23.2

Table 2. Comparative MS/MS analysis of protein composition in media conditioned by ASC from one smoking and one non-smoking donor.

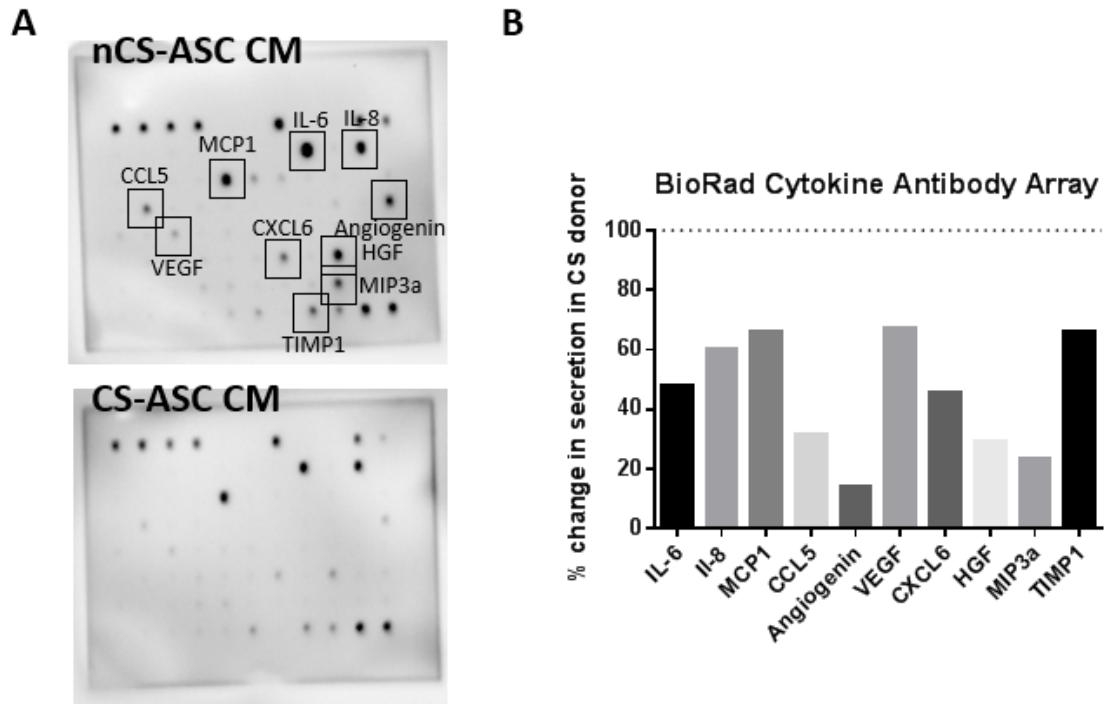


Figure 8. Semi-quantitative assessment of pro-angiogenic proteins in human ASC CM using RayBio Human Cytokine Assay. A, Semi-quantitative membrane-based analysis of angiogenesis relevant cytokines. **B,** Relative change in protein accumulation in CS-ASC CM compared to non-CS-ASC CM. Level of specific protein intensity on the membrane for non-CS-ASC CM was considered as 100%.

Name	Change	No Change	Not Detected	Name	Change	No Change	Not Detected
CXCL5		X		VEGF-A	X		
G-CSF			X	PDGFbb		X	
GM-CSF			X	Leptin		X	
GRO		X		BDNF		X	
CXCL1		X		CXCL13		X	
CCL1			X	CCL23		X	
IL1 F1			X	CCL11		X	
IL1 F2			X	CCL24		X	
IL2			X	CCL26		X	
IL3			X	FGF4		X	
IL4			X	FGF6		X	
IL5			X	FGF7		X	
IL6	X			FGF9		X	
IL7		X		FLT3-ligand		X	
IL8	X			CX3CL1		X	
IL10			X	CXCL6	X		
IL12			X	GDNF		X	
IL13			X	HGF	X		
IL15			X	IGFBP1		X	
IFN-g		X		IGFBP2		X	
MCP1	X			IGFBP3		X	
MCP2		X		IGFBP4		X	
MCP3		X		IL16		X	
M-CSF		X		IP10		X	
MDC		X		LIF		X	
MIG			X	LIGHT		X	
MIP-1b		X		MCP4		X	
MIP-1d			X	MIF		X	
CCL5	X			MIP-3a	X		
SCF			X	NAP2		X	
SDF1a			X	NT3		X	
CCL17		X		NT4			X
TGFb1			X	OPN		X	
TNFa			X	OPG			X
TNFB			X	PARC		X	
EGF		X		PLGF		X	
IGF1		X		TGFb2		X	
Angiogenin	X			TGFb3			X
OSM		X		TIMP1	X		
TPO		X		TIMP2		X	

Table 3. List of cytokines tested using RayBio Human Cytokine Array (C5).

CM was tested from one non-CS-ASC and one CS-ASC donor.

2.3.6 Analysis of accumulation of selected cytokines in human ASC CM

Analysis of accumulation of selected cytokines in ASC CM revealed that concentrations of SDF-1 and HGF were lower in CS-ASC CM by 4.6-fold and 19-fold respectively compared to their levels in non-CS-ASC CM, whereas secretion of VEGF was not affected by prior CS exposure. In addition, secretion of Angiopoietin-1 and Angiopoietin-2 was also lower in case of the CS-ASC CM, however it did not reach statistical significance (Figure 9A). Parallel analysis of expression of mRNA for selected factors revealed that levels of mRNA for SDF1, HGF, TSG-6, CD140a and CD140b were lower in CS-ASC vs non-CS-ASC, though only the decrease in the SDF-1 level reached statistical significance. Surprisingly, the level of VEGF mRNA actually trended higher in CS-ASC, though not statistically significant. Similarly we found that level of plasminogen activator inhibitor-1 (PAI-1) was also trending higher in CS-ASC CM, compared to CM from non-CS donors (Figure 9B).

To assess whether the reduction in vasculogenic potency of CS-ASC could be complemented, co-culture media were supplemented with either complete non-CS-ASC CM or individual recombinant vasculogenic factors. Introduction of non-CS-ASC CM to co-cultures with non-CS-ASC led to a 39% increase in vessel density, whereas non-CS-ASC CM was ineffective in co-cultures with CS-ASC (Figure 10A). Furthermore, neither of the tested recombinant factors (VEGF, HGF, SDF-1) provided at 10 ng/ml, concentrations that are higher than expected to be present in non-CS-ASC CM, was able to improve vasculogenesis when compared

to co-cultures exposed to control media alone (Figure 10B), suggesting that CS-ASC are compromised in their vasculogenic activity in a manner which cannot be effectively ameliorated with growth factor supplementation. One explanation of this would be a requirement for several factors, particularly in the context that multiple factors appear to be reduced in the crippled CS-ASC secretome. However, the inability to rescue the CS-ASC vasculogenesis suggested the notion that the cells might either have intrinsic inability to facilitate normal vascular network assembly, were breaking down necessary factors for assembly, or that they were secreting some factor or factors that were inhibitory to the assembly process. The next lines of experimentation were directed to address selected factors and some of these possibilities.

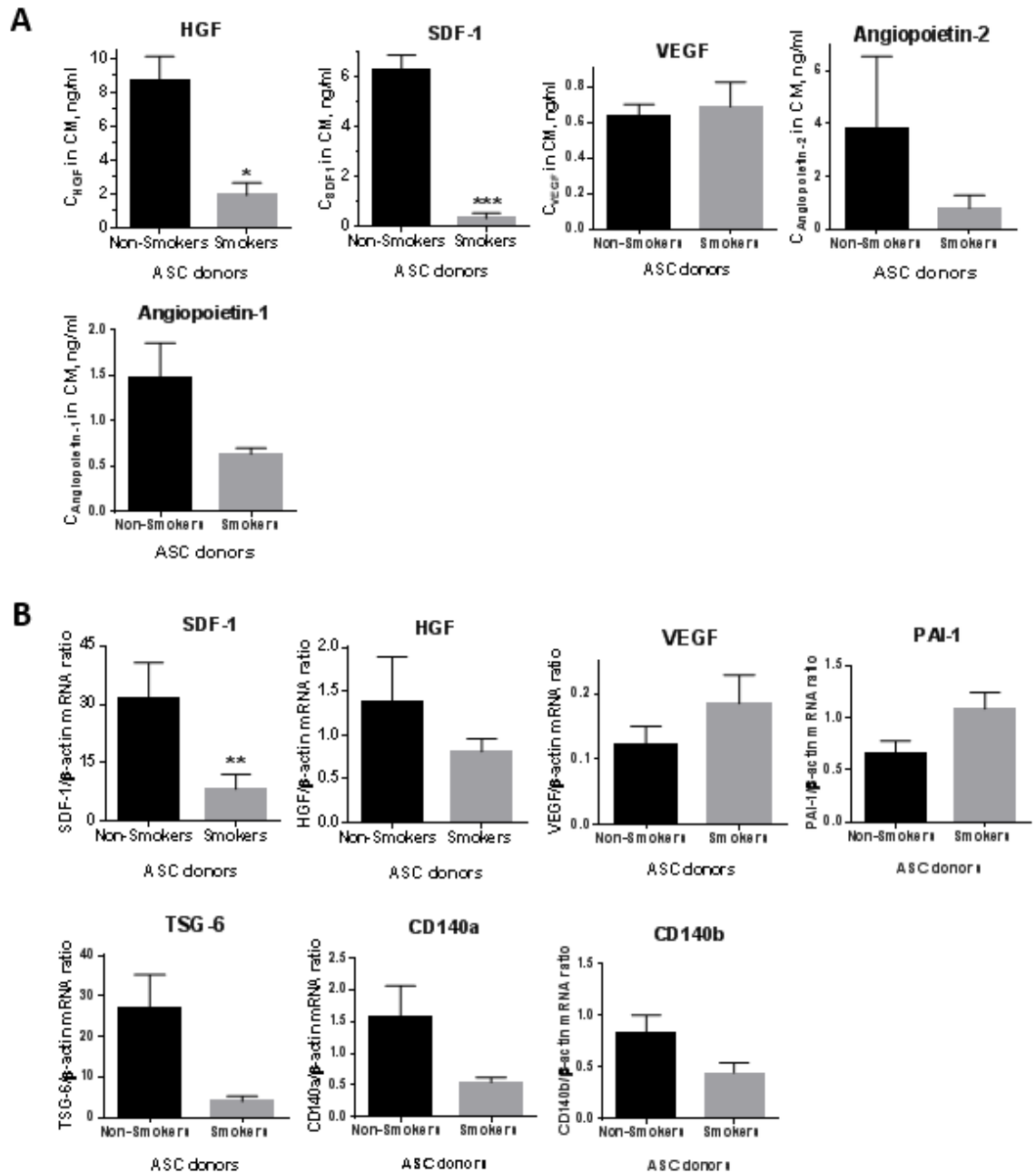


Figure 9. Analysis of accumulation of selected cytokines in human ASC CM.

A, Analysis of HGF, SDF1, VEGF, Angiopoietin-1 and Angiopoietin-2 accumulation in media conditioned for 48-hour by ASC from non-smoking (n=3) and smoking (n=4-5) female donors. **B**, Analysis of HGF, SDF1, VEGF, PAI-1,

TSG-6, CD140a and CD140b mRNA expression in ASC from non-smoking (n=3) and smoking (n=4-7) female donors done by quantitative PCR. For all graphs: *p<0.05, **p<0.01, ***p<0.001.

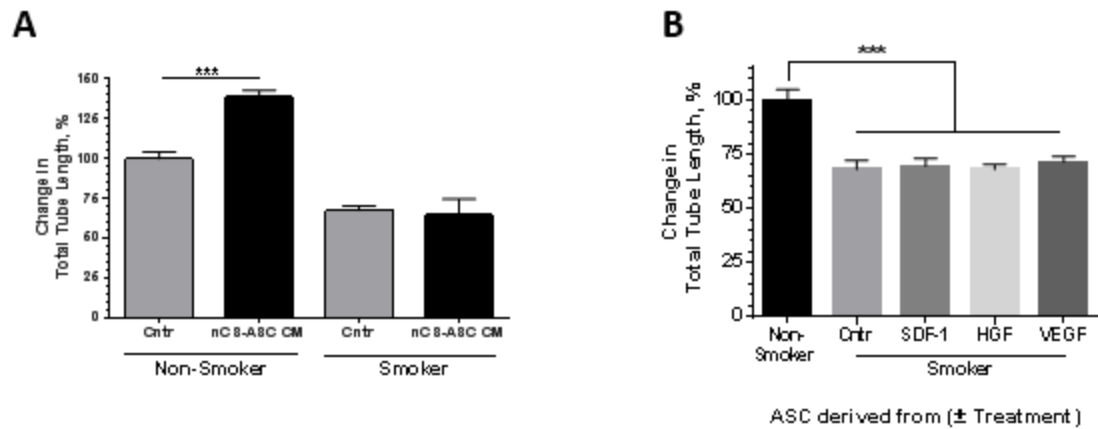


Figure 10. Assessment of supplementation of ASC co-culture with conditioned media from nonCS-ASC donor or with growth factors. A, Quantitative assessment of the effect of 2.5-fold concentrated non-CS-ASC CM on vascular network formation by EC/non-CS-ASC and EC/CS-ASC co-culture. **B,** Assessment of the effect of recombinant SDF-1, HGF, and VEGF (all at 10ng/ml) on vasculogenesis in EC/CS-ASC co-cultures. The degree of vasculogenesis in EC/non-CS-ASC co-cultures was used as 100%. For all graphs: ***p<0.001.

2.3.7 Assessment of the effect of modulating SDF-1 receptor binding on vascular network formation potential of ASC derived from smoking donors

SDF-1 provides its activity through binding to CXCR-4 receptor. Analysis of the effect of CXCR-4 inhibitor, AMD3100, which blocks receptor binding of SDF-1 revealed that supplementation of AMD3100 on Day 1 of EC/non-CS-ASC co-culture resulted in decrease of total tube length and therefore network density. To further determine whether SDF-1 is important not only for network formation but also network maintenance, we supplemented AMD3100 on Day 4 of EC/non-CS-ASC co-culture. As predicted, addition of the drug resulted in deterioration of the established networks in a dose dependent manner (Figure 11).

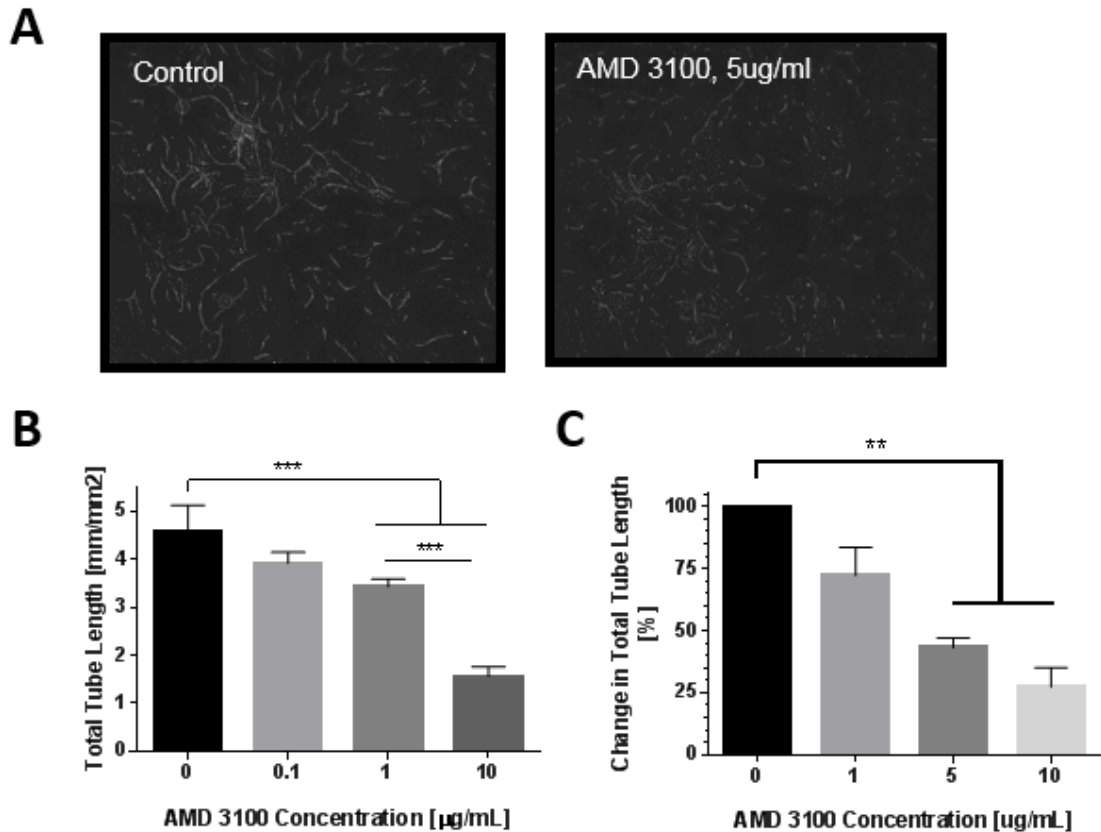


Figure 11. Assessment of SDF-1 inhibitor activity on vascular network formation potential of ASC derived from smoking donors. A, Representative images of the vascular network formed by EC/non-CS-ASC with and without AMD3100 supplementation at 5 $\mu\text{g/mL}$. **B,** Quantitative assessment of the effect of SDF-1 inhibition on Day 1, on vascular network formation by EC/non-CS-ASC co-culture. AMD3100 was administered at dose 0.1, 1, 10 $\mu\text{g/mL}$. **C,** Assessment of the effect of SDF-1 inhibition on Day 4 of EC/non-CS-ASC co-culture. AMD3100 was administered at dose 1, 5, 10 $\mu\text{g/mL}$. For all graphs: ** $p < 0.01$, *** $p < 0.001$.

2.3.8 Assessment of DPP-4 activity in human ASC CM

Dipeptidyl peptidase-4 (DPP-4) is known to cleave SDF-1 to a non-functional form, therefore inhibiting the regenerative function of SDF-1 [146]. It also performs activating cleavage on other factors. It has been shown to be expressed on the surface of various cells and also released in plasma. Luminescent assessment of DPP-4 activity (based on luciferase reaction) in CM from human non-CS and CS ASC donors revealed no significant difference in its activity between both types of donors. There was a measurable drop in the DPP-4 activity on EBM2 media (without FBS), as well as EBM2/5%FBS, supplemented with Diprotin A, which is a known DPP-4 inhibitor (Figure 12A), confirming the activity as not artifactual. Supplementation of non-CS-ASC/EC or CS-ASC/EC co-cultures with 5mM Diprotin A (an inhibitor of DPP4 activity) did not lead to a significant increase of vascular network density (Figure 12B).

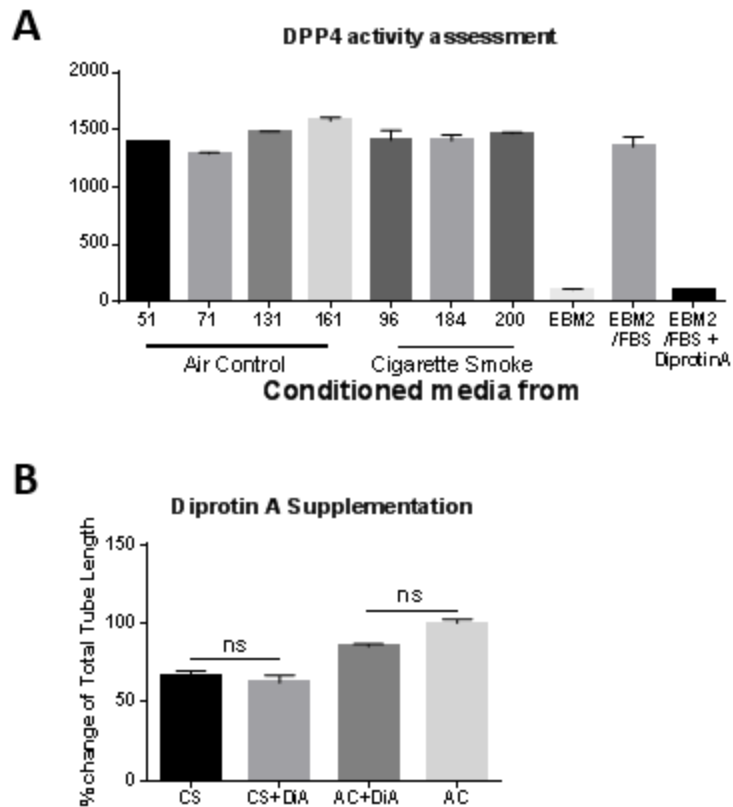


Figure 12. Assessment of DPP4 activity in human ASC CM. **A**, Luminescent assessment of DPP4 activity in non-CS-ASC and CS-ASC CM. Diprotin A is an inhibitor of DPP4 **B**, Assessment of the effect of 5mM Diprotein A on vasculogenesis in EC/non-CS-ASC or EC/CS-ASC co-culture.

2.3.9 Assessment of Activin A activity of CS-ASC

It has been previously reported by our laboratory that Activin A, expressed by ASC in response to direct contact interaction with EC, exhibits significant angiostatic properties [147]. To test whether diminished vasculogenic activity of CS-ASC could be due to increased Activin A expression, CM were collected after 72 hours from co-cultures of both kinds and evaluated for accumulation of Activin A. Analysis revealed a 65% higher concentration of Activin A in CM of co-cultures with CS-ASC compared to its level in CM from co-cultures with non-CS-ASC (Figure 13A). Further testing revealed that neutralizing antibody blockade Activin A signaling in co-cultures led to rescue of the impaired efficiency of vessel network formation by CS-ASC to the level observed in non-CS-ASC co-cultures (Figure 13B).

Local ischemia is associated with systemic and local increase in levels of inflammatory factors. Here we assessed whether exposure of ASC to inflammatory factors such as TNF α and IL-1 β modulates Activin A secretion by ASC. As was expected based on our prior work [148], non-CS-ASC do not secrete Activin A when incubated in control media. Challenging non-CS-ASC with TNF α did not modulate Activin A secretion, while non-CS-ASC treated with IL-1 β showed low level of Activin A secretion. However, CS-ASC incubated in control media show measurable expression of Activin A; and its secretion was further increased by more than 5-fold with TNF α or IL-1 β challenge (Figure 13C).

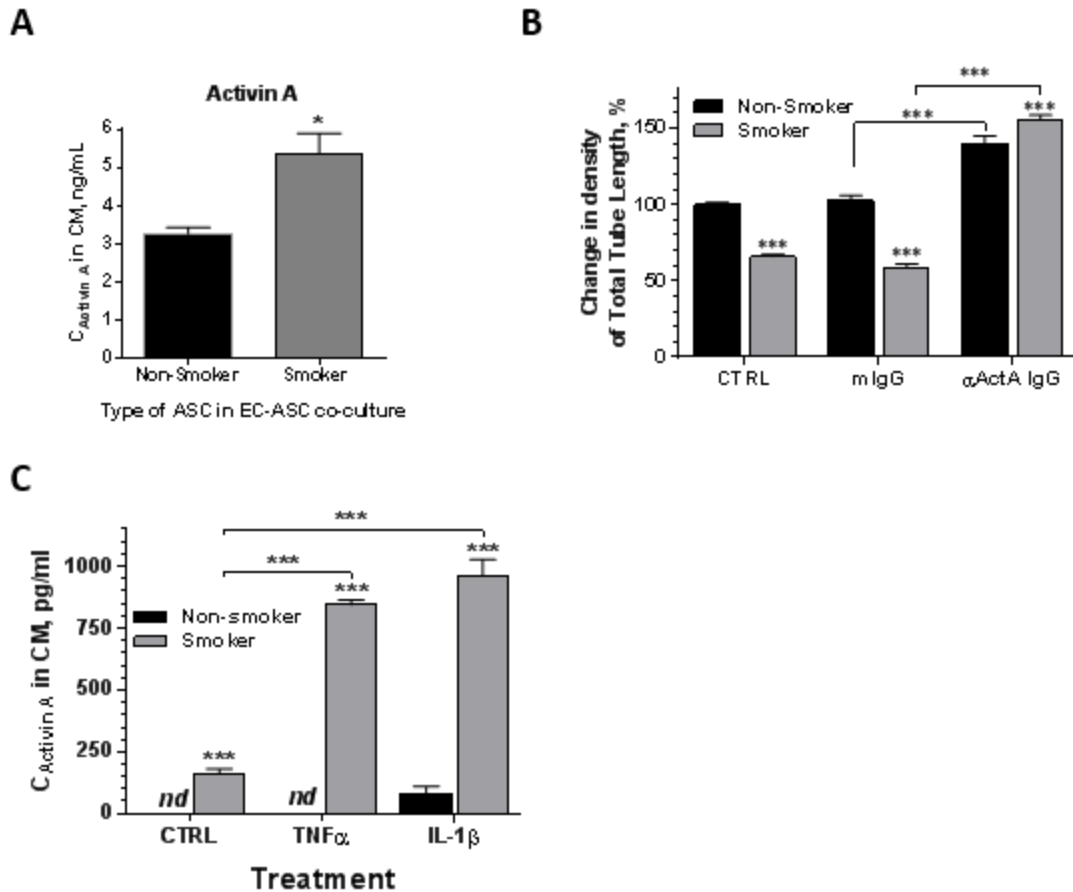


Figure 13. Assessment of Activin A activity of nonCS-ASC and CS-ASC. A, Analysis of Activin A accumulation in media conditioned by EC-ASC co-cultures, composed of healthy EC and ASC derived from human non-smoking or smoking female donors. Media was conditioned for the last 72 hours of day six of incubation. **B,** Assessment of Activin A effect on vasculogenesis (change in density of total tube length of vascular network). Co-cultures composed on healthy EC and ASC from either non-smoking or smoking female donors were incubated in control media alone or in the presence of anti-Activin A or isotype control mIgG (both at 10 μ g/ml) for the last five days of a six day incubation. **C,** Analysis of Activin A accumulation in media conditioned for 48 hours by ASC from non-smoking or

smoking female donors while incubated in control media alone or supplemented with either TNF α or IL-1 β (both at 10 ng/ml); For all graphs: *p<0.05, ***p<0.001.

2.3.9 Choice of individual donors

Throughout the studies described above, we used either a combination of several non-CS and CS donors or the “best” and the “worst” donor. To determine which donor should be considered the “best” or the “worst” from the pool of available ASC specimens, I opted to determine this based on observation of the density of vascular networks that each of the tested donors was able to generate. When assessing the three female CS-ASC donors we noted that each of them reported smoking a different number of cigarettes per day: quarter of a pack, half a pack, or a full pack. Interestingly we observed that the patient who was subsequently considered “the worst” female donor (greatest degree of ASC impairment) was also the heaviest smoker among the group of three females. This donor had the most decreased Angiopoietin-1 concentration based on ELISA as well as the the least dense networks as assayed for both the ASC and the ASC CM (Table 5).

Donor	Gender	CS Note	Age	BMI	Collection Area
F-CS 1	Female	¼ pack	35	22	Lipo-thighs
F-CS 2	Female	½ pack	47	19	Lipo-flanks
F-CS 3	Female	1 pack	36	22	Lipo-flanks
F-non-CS1	Female	0	36	22	Lipo-abdomen
F-non-CS2	Female	0	37	22	Fat excision-abd
F-non-CS3	Female	0	34	26	Lipo-flanks/abd
F-non-CS4	Female	0	38	23	Lipo-thighs
F-non-CS5	Female	0	46	23	Lipo
F-non-CS6	Female	0	47	26	Lipo-hips
M-CS1	Male	2 packs (40 “pack years”)	64	40	Fat excision-groin
M-CS2	Male	1.5 packs (55 “pack years”)	66	24	Fat excision-groin
M-CS3	Male	2 packs (60 “pack years”)	70	34	Fat excision-groin
M-CS4	Male	1.5 packs (40 “pack years”)	63	31	Fat excision-groin
M-non-CS1	Male	0	82	32	Fat excision-abd
M-non-CS2	Male	0	53	NA	Fat excision-abd
M-non-CS3	Male	0	66	42	Fat excision-abd
M-non-CS4	Male	0	70	30	Fat excision-abd

Table 4. Demographics of male and female ASC donors used in the study.

Definitions: “pack year” = 20 cigarettes smoked every day for one year; abd = abdomen

2.4 Discussion

An increasing number of clinical trials have shown that cell therapy offers potential new treatment options and hope for patients suffering from a variety of pathological conditions [149, 150]. Many trials have been conducted using bone marrow mesenchymal stem/stromal cells (BM-MSC), endothelial progenitor cells, or ASC [149]. It is important to recognize that many factors, including aging [97-99] and diabetes [103] negatively affect therapeutic potential of progenitors. Some pathologies that can be corrected with cell therapy are results of unhealthy aspects of lifestyle, including smoking, alcohol abuse, and a Western diet. It should be recognized that these factors may also potentially lower the therapeutic efficacy of progenitor cells, leading to suboptimal or no therapeutic effect of the cells when used in autologous applications. Thus, it is important to assess the effect of each of these factors on therapeutic potential of the ASC.

One such prominent factor implicated in a wide array of illnesses is cigarette smoking [19, 40, 42, 45-58, 69-72, 151-153]. The World Health Organization estimates that approximately 1.1 billion people smoke. While the efficacy of “healthy” ASC as a therapeutic agent has been shown in multiple animal models of human pathologies [80, 93, 96] and in number of clinical trials [83, 114, 117, 121], little has been done to evaluate the effect of smoking on the regenerative potency of these cells. Wahl et al. have conducted studies to address this question; they exclusively assessed the impact of CS extract on ASC migration, differentiation, and secretion of IL-6 and IL-8, all of which were compromised/reduced [104]. Their study was limited to *in vitro* simulation of CS

exposure and did not fully recapitulate processes associated with actual CS inhaling. Our study provides a much more clinically-relevant assessment of the effects of systemic CS exposure on ASC bioactivity.

Basic analysis of non-CS and CS ASC donors, including assessment of cell morphology, growth rate, and adipogenic potential revealed no significant difference in either of the categories. These cells were also, as expected, positive for markers ascribed to ASC and negative for endothelial cell and leukocyte marker. CD34 was also not expressed as the evaluated cells were at passage 4, and CD34 has been shown to be only present freshly isolated ASC. Interestingly CS-ASC exhibited lower expression of CD140a and CD140b, also known as platelet derived growth factor receptor (PDGFR) α and β . PDGFs and PDGFR have been shown to play a significant role in angio/vasculogenesis [81]. While PDGF-BB is secreted by EC, PDGFR is expressed on the surface of pericytes as well as ASC. This finding suggests a possible receptor-based impairment to the angiogenic potential of CS-ASC. In addition, flow cytometric analysis revealed an increased expression of Notch 2 and Notch 3 which also play a significant role in angiogenesis; specifically inhibition of Notch pathways has been linked to increased angiogenesis, as Notch expression has been demonstrated to not only lower the number of circulating endothelial progenitors, but also lower VEGF expression [154]. The association of Notch pathway and angiogenesis continues to be investigated by various groups, however our finding intuitively appears to correlate with the findings of others in respect to vasculature formation.

In order to assess the usefulness of the non-CS-ASC vs CS-ASC as a therapeutic option we chose to first conduct an *in vivo* study. We, and others, have previously shown that systemic or local administration of ASC promotes blood flow restoration in mouse ischemic limbs [80, 155]. Similar to the previous findings, in the current study we observed that non-CS-ASC efficiently improved blood flow in the ischemic limbs, whereas ASC from age and gender matched smoking human donors were ineffective (Figure 5A, B). Most of the prior studies tested the effect of ASC therapy in models where cells were delivered immediately or 24-hours after ischemia induction, the stage of recovery associated with active inflammatory processes. To assess whether ASC therapeutic applicability can be broadened to chronic conditions, the effect of ASC therapy on blood flow improvement was tested in the model where cells were delivered to the mice 32 days after femoral artery removal. This study demonstrated, for the first time, that non-CS-ASC produce therapeutic effect in a model of chronic ischemia (Figure 5C). We speculate that inflammation is no longer a prominent factor in this model, therefore the beneficial effect of ASC is more particularly attributed to cell's angiogenic, rather than anti-inflammatory activities. However, same as in the acute scenario, CS-ASC were ineffective in this model (Figure 5C).

In addition to the studies involving administration of human ASC, we have also conducted a study in which mice were exposed to CS for a period of 5 months (5 hours/day, 5 days/week), and then received mouse ASC (isolated from control group consisting of mice exposed to ambient air for 5 months) to treat subsequently induced hindlimb ischemia. Interestingly, no benefit was observed in

the group treated with ambient air-exposed mouse ASC, compared to vehicle. Most of the mouse studies utilize animals that are 8-12 weeks old. However, in the case of this particular study, both the donors of mouse ASC as well as recipients were over 8 months old. This created a confounding factor whether such advanced age could have played an overriding role in the process, negating the beneficial effect of mouse ASC administration that would have otherwise been seen in younger animals. Studies have shown that ASC and MSC from aged donors exhibit decreased therapeutic potential [97]. Furthermore, several investigators have demonstrated before that mouse ASC do have therapeutic potential in mice [156]. However, since the regenerative capacity of mouse ASC was not the primary goal of the study, we have chosen to not pursue this avenue in search of the answer for the observed effect. Also noted, not surprisingly, is that mice exposed to CS showed lesser recovery from hindlimb ischemia overall, compared to animals exposed to ambient air, indicating the damaging effect of CS (Figure 5D).

Due to the complexity of *in vivo* models, to assess angio-/vasculogenic activities of the tested ASC, an *in vitro* model of vasculogenesis was then used, to further assess the cell potency. This model, based on co-cultivation of EC with ASC, primarily relies on paracrine cross-talk between EC and ASC, leading to EC reorganization into stable luminal cords. Using this model, marked impairment in CS-ASC ability to support EC-cord formation was observed in both male and female donors (Figure 6B). The finding with human ASC was strengthened by observations that mouse ASC, isolated from animals pre-exposed to CS for one month, also provided diminished support to EC in cord formation (Figure 6C). Use

of mouse ASC eliminated variables in lifestyles which are hard to fully account for when studying samples from human donors.

We hypothesized that decreased vasculogenic activity of CS-ASC was attributed to compromised secretion of vasculogenic cytokines. Media conditioned by CS-ASC promoted EC-tubulogenesis in EC-fibroblast co-cultures and augmented survival of EC incubated in growth factor-reduced media to a lesser degree than media conditioned by non-CS-ASC, suggesting that perhaps CS-ASC CM is not only less abundant in pro-angiogenic factors, but also contains factors that inhibit angiogenesis.

It has been shown before that ASC secretome has therapeutic potential. We have confirmed the beneficial activity of non-CS-ASC; however, there was a significant drop in the activity of CS-ASC CM. As a result, we decided to conduct a comprehensive evaluation of the proteome found in the CM from one CS (most severe smoker, female) and one non-CS (non-smoking, female) donor. The MS/MS assessment detected 714 unique proteins present in the CM. This technique, which allows both: for identification of the proteins present in the tested sample and for quantitative analysis, revealed a particularly interesting decrease in the abundance of SDF-1, which plays a role in angiogenesis and therefore is critical for the regenerative capacity of ASC (Table 2). Notably, presence of pro-angiogenic factor VEGF, which has been shown on many occasions to be secreted by ASC, was not detected. Lack of VEGF detection, does not however signify that this protein was not present in the CM; the MS/MS technique assesses a multitude of ions and short peptides which are subsequently matched with various

databases. The accuracy of the final comprehensive list of proteins is dependent on the sensitivity of the assay, as well as the robustness of the database. Interestingly, proteins which were 3-fold or more up or down regulated in smokers often correlated with what would typically be observed in a smoker. For example, ASC CM demonstrated increases in lung adenocarcinoma-associated proteins, biomarkers for emphysema, and proteins that are correlated with autoimmune disease.

In order to conduct a more angiogenesis-focused analysis of proteins present in the CM, and further confirm and strengthen the MS/MS results, we employed a human cytokine array tool, a much more cost-efficient and faster method for detecting a wide range of proteins of special interest even at low abundance. Out of 80 factors assessed, 10 were present at evidently different levels in the two CM tested (one non-CS and one CS donor). Furthermore all 10 of the proteins were less abundant in the CM from CS-ASC; at the same time cross-validating the proteomic findings and further supporting the observation that ASC CM from smokers is lower in levels of pro-angiogenic and therapeutically relevant factors. Levels of some proteins which were revealed to be present via MS/MS proteomic assessment and ELISA were not detected with this technique (Figure 8, Table 3). It is, however, important to mention that the proteomic assessment relied on only one CM sample from smoker and non-smoker-derived ASC. This limits the findings to only those two specific donors, and their particular physiology and health history. Including more donors would help establish a more robust representation of smoking vs non-smoking donor population and the

respective CM, however the large expense that associated with assessing the complete protein composition of CM from more donors was limiting factor.

Equipped with this information about the compromised pro-angiogenic secretome, we decided to narrow down the number of cytokines to a few key options and assess those via ELISA and mRNA analysis. A substantial drop in secretion of HGF, SDF-1, Angiopoietin-1 and Angiopoietin-2 was observed in CS-ASC CM. We have previously reported that blocking HGF activity decreases EC vasculogenesis, whereas Mirshahi et. al. has shown that SDF1 stimulates EC tubulogenesis *in vitro* [157]. Angiopoietin-1 and Angiopoietin-2 has been shown to protect endothelial cells and help promote and stabilize vessel formation [158, 159]. Hence a drop in the secretion of both proteins signifies a limited pro-angiogenic profile of CS-ASC. Interestingly, secretion of VEGF was similar between the groups, indicating that VEGF was not affected by CS exposure (Figure 9A). It is worth noting, however, that there have been studies that reported the levels of VEGF to increase, decrease, or remain unchanged when exposed to CS, indicating that there is no clear consensus within the scientific community regarding VEGF secretion. In addition to elevated VEGF, PAI-1 level of expression was also revealed to be higher in CS-ASC comparing to non-CS-ASC. PAI-1, an inhibitor of urokinase (activator of plasminogen) is an inhibitor of angiogenesis, hence increased levels of this protein may further indicate a decreased pro-angiogenic potential of the system [160]. Moreover, with respect to *in vivo* observations, we previously reported that silencing expression of HGF in ASC abolishes cell therapeutic effects in limb ischemia model [80]. Kondo et. al.

demonstrated that intraperitoneal injection of SDF-1 neutralizing antibodies prevented beneficial effect of ASC, which was associated with decrease in circulating progenitor cell homing to the site of injury [156]. In recent years, it has been demonstrated that administration of SDF-1 to treat myocardial infarction results in recruitment of stem/stromal cells to the site of injury [161]. As SDF-1 is known to be expressed by EC and stromal cells residing in various organs, an injury to those organs has been shown to result in upregulation of SDF-1 expression and subsequent influx of bone marrow stem cells to repair the injury [162-164]. We have shown in this study as well that expression levels of SDF-1, HGF, TSG-6, CD140a and CD140b, were decreased in CS-ASC donors, with SDF-1 showing the only statistically significant difference. Xie et al, has shown that TSG-6, an anti-inflammatory factor secreted by ASC, is able to rescue BM cells from CS-induced myelosuppression [105]. Decrease in TSG-6 expression, however, appears to be linked with CS exposure, and furthermore it may explain the decreased therapeutic potential of the CS-ASC. In addition, we have shown via flow cytometric assessment a reduced level of expression of CD140a and CD140b. Here we additionally confirmed these findings through mRNA analysis, further solidifying the observation that the expression and secretion of pro-angiogenic factors is limited in CS-ASC.

Since CS-ASC exhibited a decreased expression of HGF and SDF-1, we anticipated that enrichment of the incubation media with recombinant forms of these factors would improve the density of vascular network in EC/CS-ASC co-cultures. However, no beneficial effect was observed with either of these factors

nor with non-CS-ASC CM that contains a wide spectrum of pro-angiogenic factors and alone is able to confer the regenerative effect (Figure 10). Interestingly, supplementation of CS-ASC CM, which has been shown to contain less therapeutic factors, was also able to slightly increase the total tube length comparing to incubation media alone in EC/non-CS-ASC co-cultures, however not surprisingly it was not able to provide the same effect in EC/CS-ASC co-cultures. Since both types of CM (non-CS and CS) resulted in an increasing vasculogenic trend, compared with the control group, in the EC/non-CS-ASC, yet no effect was observed in the EC/CS-ASC group, it may be that supplementation of single factor will not be able to improve the network density established with CS-ASC. Furthermore we postulate that the negative effect of CS goes beyond the proangiogenic cytokine poor CM generated by the CS-ASC, but it also affects the cells and the intracellular signaling as well.

In order to further elucidate the mechanism via which CS might affect ASC and since the assessment of the composition of CS-ASC CM revealed that SDF-1 expression and secretion is significantly reduced, we hypothesized that this observation is at least in part responsible for the decrease in vasculogenic potential of CS-ASC. In order to confirm this concept, we have conducted two studies using an SDF-1 inhibitor, AMD3100, also known as a bone marrow hematopoietic stem and progenitor cell mobilizing agent [165]. First we administered AMD3100 to the EC/non-CS-ASC co culture on Day 1, while in the second study we administered the drug on Day 4 of co-culture, after majority of the networks were already established. Data revealed that SDF-1 is important for establishing as well as

maintenance of dense networks. Administration of AMD3100 at the initiation of network formation resulted in inhibited network development, while providing the drug once the networks were established resulted in disintegration of the vascular structures. Furthermore, this effect was concentration dependent (Figure 11). This is a significant finding as SDF-1 is known to facilitate EC incorporation into the vascular structures, and supports prior observations by Newey et al. [166].

To test whether a change in surface enzymatic activity of ASC might play a role in modulating the activity of CS-ASC we conducted two studies aiming to determine whether DPP-4 may be overexpressed on the surface of CS-ASC, therefore contributing to the decrease in active SDF-1, through cleavage of the protein [167, 168]. In non-pathological conditions, DPP-4 is responsible for degradation of various chemokines [167]. We hypothesized that if overexpression of this protein (also known as CD26) was observed in CS-ASC, the decrease in SDF-1 presence in CM and therefore drop in network density could potentially be ameliorated via inhibition of DPP-4. Interestingly, luminescent assessment of DPP-4 activity in non-CS-ASC CM and CS-ASC CM revealed no significant difference between the non-CS and CS donors. The CMs were generated in the presence of 5% FBS; when assessing the DPP-4 activity in EBM2 media alone (no FBS), the activity was markedly reduced, suggesting that most of the detected DPP-4 activity comes from the FBS. Importantly, adding DPP-4 inhibitor, Diprotin A, resulted in reduction of DPP-4 activity to very similar level as seen in the EBM2 media group alone, validating the system. It may be that there is an abundance of DPP-4 in the FBS, which then masks the relatively slight presence of the protein in the CM, or

truly the level of DPP-4 expression is very similar between all donors. Interestingly, supplementing Diprotin A inhibitor to the non-CS-ASC/EC and CS-ASC/EC co-cultures resulted in no significant improvement in network formation.

In order to further elucidate the mechanism of compromised CS-ASC therapeutic activity, we sought to assess the role of Activin A, which has been shown in our laboratory, to exhibit induction in ASC when in an EC/ASC co-culture [148]. Activin A plays a central role in vasculogenesis by affecting bioactivity of both EC and ASC: it induces a smooth muscle cell phenotype in ASC [148] and shifts ASC secretome net activity from pro-angiogenic to angiostatic [147]. Activin A inhibits HGF and SDF-1 expression, stimulates VEGF expression, and in parallel upregulates expression of VEGF scavenger receptor Flt-1 [147]. In the current study, we observed that media conditioned by EC/CS-ASC co-cultures had 65% more Activin A than EC/non-CS-ASC co-culture media (Figure 13A). We thus hypothesized that the decrease in CS-ASC vasculogenic activity might be partially attributed to increase in Activin A secretion, and tested the concept by blocking Activin A activity in EC/CS-ASC co-cultures. Remarkably, this was sufficient to rescue the efficiency of vasculogenesis to that recorded for EC/non-CS-ASC co-cultures (Figure 13B).

Acute ischemia is associated with systemic and local increase in inflammatory cells and cytokines. One of the prominent mechanisms underlying ASC therapeutic effect is anti-inflammatory/immunomodulatory paracrine activity [119, 169]. To further explore the cause of CS-ASC failure to produce beneficial effect in the models of limb ischemia, the effect of inflammatory factors TNF α and

IL-1 β on Activin A expression was tested. Unlike non-CS-ASC, CS-ASC secrete detectable Activin A at baseline; and its expression markedly increased in response to inflammatory factors (Figure 12C). Activin A plays an important role in inflammatory processes, by inducing expression of several inflammatory cytokines in LPS-induced acute respiratory distress syndrome model [170] and CS-induced lung inflammation [171]. Furthermore, it promotes macrophage polarization towards pro-inflammatory M1 phenotype [172]. We speculate that non-CS-ASC, after systemic injection, produce an anti-inflammatory effect, whereas CS-ASC, through an increase in Activin A secretion, may actually have the opposite effect.

Lastly, it is important to note that the observations of these studies are based on a limited number of donors. Each *in vitro* assessment of co-cultures relied on several (5-8) technical replicates per each donor in order to strengthen the validity of the data. The limitation was based on the availability of only three female smoking donors (all within close age and BMI proximity). The non-smoking female donors were age and BMI matched. The female smokers self-reported a range of cigarette packs smoked per day: from $\frac{1}{4}$ through $\frac{1}{2}$ to 1 pack. Interestingly, throughout the studies we have observed a trend of the heaviest smoker exhibiting characteristics of the least pro-angiogenic potential, while the lightest smoker performed the best from the group of three. This implies that the smoking status alone is not sufficient to determine donor's ASC regenerative potential. The degree of influence on cellular reparative activity is highly dependent on the number of cigarettes smoked per day, as well as the number of years that one has been a smoker. A recurring question is one that asks whether quitting

smoking may be able to restore, at least in part, the beneficial activity of ASC. We predict that such restoration, would depend on the time elapsed since quitting. Perhaps importantly, since the ASC used in my studies were passaged cells (between passages 3-5), the observation of compromised cell activity once the cells have gone through several population doublings indicates that they retain a “memory” of being exposed to the smoke-exposed *in vivo* environment, perhaps implicating epigenetic modifications that may have taken place. A robust and reliable assessment of the therapeutic potential of a specific donor’s autologous ASC relies on an interplay between the number of cigarettes smoked, time of exposure, subsequent time of no exposure, as well as potential second and third hand smoke exposure. We also recognize that our findings underscore an important goal for the field of autologous cellular therapeutics: identifying donor characteristics including age, presence of comorbidities and specific lifestyle choices; and evaluating for interaction of these variables with activities manifested by outcomes of pre-clinical and clinical trials. While studies have been conducted to determine the effect of age and co-existing diseases like diabetes on ASC/MSC, more studies need to be carried out to determine the effect of other factors, using a large number of donors, or alternatively a reasonably sensitive and feasible high-throughput assay is needed to aid clinicians in concluding which patient would benefit from autologous cell therapy.

Cigarette smoking continues to be a serious problem globally, but since 2009 a solid drop in this activity in the U.S has been observed from 20.6% to 15.2% in 2015, which translates to approximately 37 million Americans [173]. Regardless

of these great initiatives, CS remains a serious health hazard and those exposed to tobacco will need medical attention.

In conclusion, our study has revealed that CS exposure in humans leaves many facets of the ASC phenotype apparently unaltered, yet has a profound detrimental effect on ASC therapeutic activity *in vivo* and vasculogenic activities *in vitro*. This effect coincides with higher level of Activin A secretion at baseline and in response to inflammatory factors and direct interaction with EC, and is at least partly reversible by blockade of this increase in Activin A. These findings should be considered when designing clinical trials: I suggest that smokers should be excluded from the initial clinical trials with autologous cell therapies or be evaluated as a separate population. Furthermore, smokers may benefit to a greater degree from allogeneic cell therapies.

Chapter 3: Contribution of cigarette smoking to renal pathology and the beneficial effect of adipose-derived stem cell therapy on ameliorating renal damage

3.1 Introduction

3.1.1 Effect of cigarette smoking on kidney damage

The continuous prevalence of smoking within the American society and especially within certain populations, like veterans, provides relevance for additional studies assessing the effects of cigarette smoking (CS) on various organ systems and the interplay between smoking and the efficacy of the currently used and prospective treatments. CS is known to lead to emphysema [174, 175], cancer [176, 177], myelosuppression [105], and cardiovascular diseases [178, 179]. Several studies have recently indicated a link between CS and kidney pathology [180-182]. Smokers are at a higher risk to develop kidney disease or worsen pre-existing symptoms of renal pathology [183], oftentimes resulting in progression to end-stage renal failure, for which the only effective treatments are kidney transplant or dialysis [184]. CS is associated with development of proteinuria [185] progression of nephropathy in patients with diabetes [186], chronic kidney disease (CKD) [187] as well as with higher risk of renal transplant graft failure [188, 189].

Few studies have reported correlations between CS and nicotine and kidney damage [190-193]. Since nicotine is a substrate of the cation transporter OCT2, expressed on the basolateral membrane of the cells comprising the renal

proximal tubules, this transporter is responsible for allowing nicotine to access the renal epithelial cells, leading to injury in the form of oxidative stress [194]. Oxidative stress in the kidney also results in compromised vascular stability [195]. Chin et al. has demonstrated that patients who smoke manifest impaired creatinine clearance [196]. They also observed a correlation between the number of cigarettes smoked and decreased creatinine clearance [196]. Arany et al. has indicated that CS predisposes kidneys to ischemia and may facilitate progression of acute kidney injury (AKI) into CKD [197]. Therefore, prior studies suggest that it is important to further assess the effects of smoking on progression of renal pathology, as well as to develop treatments that will protect the kidneys in patients who may be at higher risk for renal pathology development. Additionally, patient's history of CS should be taken into consideration when proposing the most optimal therapy regimen [192, 198].

3.1.2 Chronic kidney disease overview

The number of patients with kidney disease, especially with end stage renal failure, has increased in the recent decades. Due to increasing costs associated with treatment of the patients with renal damage, focus has been placed on both methods to prevent kidney disease, and treatment options to address the already existing injury [199].

Deterioration of renal function is associated with a decrease in the glomerular filtration rate (GFR), increased serum creatinine levels, and severity of albuminuria [199]. Each progressive stage of renal damage is associated with complications that further intensify the damage, like cardiovascular disease

(arterial calcification) [200]. Advancement of kidney damage together with other complications can result in death of the patient [199].

Chronic kidney disease (CKD) has been predominantly associated with interstitial fibrosis, as well as capillary rarefaction which has been noted to occur even several weeks post initial ischemic event. Acute kidney injury (AKI), defined as a loss of kidney function that develops over just a few days has been shown to lead to CKD [201]. AKI has been demonstrated in rodent models to be associated with microvascular alterations like endothelial cell damage and apoptosis, and changes in endothelial cell-cell contact, leading to generalized disruption of the endothelial monolayer [202, 203].

3.1.3 Mechanism of renal fibrosis development

Fibrosis development is often associated with pre-existing local inflammation and influx of macrophages and lymphocytes [204]. These cells secrete pro-fibrotic cytokines, including TGF β and FGF-2, which convert resident fibroblasts into myofibroblasts [205]. As the kidney is subjected to ischemic events, some renal epithelial cells undergo apoptosis [204]. Affected tissue will attempt to rebuild the structures by increasing cell proliferation that may alternatively lead to new and functional epithelium or may result in upregulation of TGF- β secretion by macrophages which will stimulate proliferation of resident myofibroblasts [204], defined as alpha-SMA positive cells, as well as fibrosis development, characterized by collagen type I and III deposition in the interstitium [204]. It has been proposed that such collagen production is carried out by renal fibroblasts, as well as by renal pericytes [204, 206]. While collagen type I production is a critical

step in wound healing, the presence of tubulointerstitial fibrosis leads to compromised kidney function and therefore increased likelihood of progression to end-stage renal disease [184, 204].

Renal pericytes and resident fibroblasts have been shown to transform into myofibroblasts during AKI [207]. Another set of studies has explored the role of epithelial and endothelial cells' participation in fibrosis formation. Epithelial-to-Mesenchymal Transition (EMT) contributes to fibrosis formation via loss of cell-cell adhesion as well as production of extracellular matrix by tubular epithelial cells [208]. Interestingly, recently several studies have indicated that epithelium may not be a major contributor to myofibroblasts, and only 5% (or less) of kidney myofibroblasts come from epithelial cells [204, 209-212]. At the same time, Endothelial-to-Mesenchymal Transition (EndMT), has been shown to play a major role in fibrosis development [213, 214]. EndMT is characterized by loss of cell-specific markers by endothelial cells (e.g. VE-Cadherin and CD31+) and acquisition of mesenchymal cell markers (e.g. alpha-SMA, FSP-1) [215], along with endothelial cell detachment, transformation into spindle-shaped cells, migration into parenchyma and contributing to matrix deposition [213]. Studies conducted by Basile et al., have shown that AKI leads to capillary rarefaction and precedes EndMT, which can be inhibited by VEGF therapy [214].

Remarkably, in recent years it has been shown in various animal models that reversal of fibrosis is possible, contrary to previous notions that fibrotic lesions are permanent [216-220]. New studies have demonstrated that fibrosis of kidney, liver and heart can be reversed with the use of cell therapy or growth factor rich

media [221-225], yet data about prevention or reversal of CS-induced fibrotic changes in the kidney is lacking. Similarly, no studies have been done to assess the effect of CS exposure on kidney pathology and subsequently no optimal treatments are proposed to mitigate CS-induced kidney damage.

Therefore, I decided to assess the effect of CS on formation of kidney pathology, specifically fibrosis and capillary rarefaction, by conducting histological assessment of kidney tissue as well as renal blood perfusion using Laser Doppler Imager. These animals were available during several of the ischemia and pulmonary experiments with which I was engaged; and it was of interest to pursue parallel experimental outcomes in these readily available groups. We were then poised to evaluate the potential beneficial effect of ASC to ameliorate CS-induced kidney damage.

3.2 Materials and Methods

3.2.1 Mouse model of cigarette smoke-induced kidney damage (kidney harvest and weight assessment)

Animal studies were approved by the Institutional Animal Care and Use Committee at Indiana University School of Medicine. Three separate animal studies were conducted using 8-10 weeks old NSG or C57Bl/6 female mice that were subjected to cigarette smoking (CS) or ambient air (AC) regimen. Mice were placed into Teague 10E chamber (Teague Enterprises) and exposed to 11% mainstream and 89% side-stream CS (CS group) for 5 hrs/day (5 days/week for five or six months) as previously described [105]. CS was generated by reference cigarettes (3R4F; Tobacco Research Institute, University of Kentucky, Kentucky, USA). The total amount of suspended particulates (on average 90 mg/m³) and carbon monoxide (on average 350 ppm) within the chamber were monitored on daily basis. In parallel, another set of mice was kept at ambient air (Air Control group).

Study subsets:

Study 1: NSG mice were exposed to CS for six months, followed by a two-month recovery period during which a subset of mice received weekly intraperitoneal (IP) injection of human ASC at dose of 1×10^5 cells. At the completion of the treatment regimen mice were euthanized and organs were collected.

Study 2: C57Bl/6 mice were exposed to 5 months of CS, followed by immediate euthanasia and organ harvest. The weights of the mice and their kidneys were recorded.

Study 3: C57Bl/6 mice were exposed to 5 months of CS, followed by a weekly intraperitoneal infusion of 3×10^5 human ASC for 4 weeks. One week after the final treatment, left kidney blood flow was measured using Laser Doppler Imager, followed by animal euthanasia and organ harvest. Mouse body and kidney weights were recorded.

3.2.2 Histological and immune-histochemical assessment of kidney damage

Kidneys were preserved in 10% buffered neutral formalin overnight and then processed for paraffin embedding, sectioned at 5 μ m thickness, and processed using histochemistry or immuno-histochemistry technique.

Detection of collagen deposition using PicroSirius Red staining

PicroSirius Red (PSR) staining was used to detect collagen type I and III, which appears red in the bright-field microscopy. Tissue was deparaffinized and rehydrated, followed by immersion into PSR solution (0.5g Sirius red F3B in 500 ml aqueous solution of picric acid) for 60 minutes. The slides were then quickly dipped in two changes of acidified water (0.5% acetic acid), dehydrated and mounted with resinous medium. Collagen presence (appearing red on a yellow background) was evaluated under unpolarized light (bright field).

Detection of renal capillaries using Cablin staining

Cablin antibody detects the capillary basal lamina and has been previously used to reveal renal capillaries [226]. Following deparaffinization and hydration of the tissue, antigen retrieval was performed using Tris-EDTA Buffer (10mM Tris base, 1mM EDTA, 0.05% Tween 20). Slides were immersed in the buffer and boiled for 20 minutes, follow by 10-minute cool-down period. Blocking solution (10% goat serum, 1% BSA in PBS) was applied for 2 hours. Primary rabbit anti-Cablin antibody (provided by Robert Bacallao, MD, Indiana University) was applied for 30 minutes, followed by secondary goat anti-rabbit antibodies application for 10 minutes. 3,3'-diaminobenzidine (DAB) solution (Sigma) was applied on each section to reveal the antigen.

*Detection of renal vessels using *Lycopersicon Esculentum* (Tomato) Lectin*

Thin sections of kidney tissue were rehydrated and incubated with Carbo-Free solution (Vector Labs), to block non-specific binding, for 30 minutes. Biotinylated *Lycopersicon Esculentum* lectin (Vector Labs) was applied for 30 minutes, followed by incubation of the sections with peroxidase H-Avidin DH complex (Vector Labs) for 30 min. DAB was used to reveal antigen-lectin complexes.

Detection of myofibroblast using Alpha-Smooth Muscle Actin

Thin sections of kidney tissue were treated with 2% hydrogen-peroxide for 10 minutes to inhibit endogenous peroxidase activity and then with M.O.M.[™] Mouse IgG Blocking Reagent (Vector Labs) for 1 hour, to block endogenous mouse IgG, followed by incubation with M.O.M. protein solution for 5 minutes, to blocking

nonspecific binding sites. Mouse anti- α SMA IgG were applied for 1 hour, followed by incubation of the sections with biotinylated anti-mouse IgG for 10 minutes, and then with peroxidase H-Avidin DH complex. Antigen-antibody complexes were revealed with DAB and nuclei were detected with hematoxylin counterstain.

Detection of M1 and M2 macrophages

M1 and M2 macrophage staining was done to assess macrophage polarization (CD68 for M1 macrophage and CD206 for M2 macrophage). Tissue sections were rehydrated and treated with antigen retrieval buffer (pH 9.0) at 90°C for 30 minutes. To block nonspecific binding sites, sections were incubated with 2.5% normal horse blocking serum (Vector Labs) for 20 minutes. Then, sections were incubated with either rabbit anti-CD68 (Abcam, ab125212 1 μ g/ml) or rabbit anti-CD206 (Abcam, ab64693, 0.1 μ g/ml) for 1 hour, followed by incubation with ImmPRESS HRP anti-rabbit IgG (Vector Labs) for 20 minutes and then with peroxidase H-Avidin DH complex. Antigen-antibody complexes were revealed with DAB. Nuclei were detected with hematoxylin counterstain.

Detection of iron deposition in renal tissue using Perl's Iron Stain

Tissue was deparaffinized, rehydrated, and immersed in working solution of 10% Potassium Ferrocyanide/ 20% HCl for 30 minutes, then rinsed in distilled water. Slides were counterstained with Nuclear Fast Red solution for 5 minutes, washed in tap water, dehydrated and coverslipped. The ferric iron appears bright blue.

All histology sections were viewed under the microscope and several, randomly selected images at 100x magnification were taken (6-10) from each section, within

renal cortex. The analysis of the staining was performed using ImageJ software to determine the relative color intensity within each photograph.

3.2.3 Laser Doppler Imager (LDI) assessment of superficial renal blood flow

LDI assessment of left kidney perfusion was performed in C57Bl/6 female mice in Study 3. Mice were anesthetized with 4% isoflurane and then maintained at 2%. A small incision was made on the left side of the abdomen and left kidney was exposed.

The tissue perfusion of the left kidney was analyzed using infrared (830nm wavelength) Class 3B Laser Doppler Imager (MOOR Inc, UK) at 4ms/pixel scan speed with image acquisition rate of 15KHz (for the upper cut-off frequency). The camera and laser source was positioned 30cm directly above the tissue of interest. The penetration depth of LDI is 2mm and corresponds to measuring the perfusion within cortical region of the mouse kidney. Three consecutive images were obtained in approximately 2.5 minutes each. Acquired data was analyzed using mLDIMainV53 Software and the mean of the three measurements was calculated.

3.3 Results

3.3.1 Kidney weight assessment

Study 1: NSG mice were exposed to CS for 6 months, followed by a two-month recovery period during which a subset of mice received weekly intraperitoneal (IP) injection of human ASC at dose of 1×10^5 cells.

Study 2: C57Bl/6 mice were exposed to 5 months of CS, followed by immediate euthanasia and organ harvest.

Study 3: C57Bl/6 mice were exposed to 5 months of CS, followed by a weekly IP injection of human ASC at dose of 3×10^5 for each of 4 weeks.

The weights of the kidneys from C57Bl/6 mice in Studies 2 and 3 were analyzed. The weight of kidneys in Study 1 was omitted. The combined weight of both kidneys (left and right) from animals in Study 2 revealed a significant 20% drop ($p < 0.01$) from the CS cohort compared to that of the AC group (Figure 14B). The analysis of the combined kidney weight in Study 3 demonstrated a 12% decrease in the kidney weight in CS animals, and a slight increase in the weight in the group treated with ASC (compared to CS group), though it did not reach statistical significance (Figure 14C). Assessment of kidney-to-body ratio did not yield a significant difference between the groups in Study 2 and 3 (data not shown). Mice exposed to CS have lost weight, as determined based on weight measurement immediately post CS regimen, but gain weight after CS cessation. The drop in weight immediately post CS (Pre-ASC Treatment) and despite of ASC treatment remained significant. (Figure 14D).

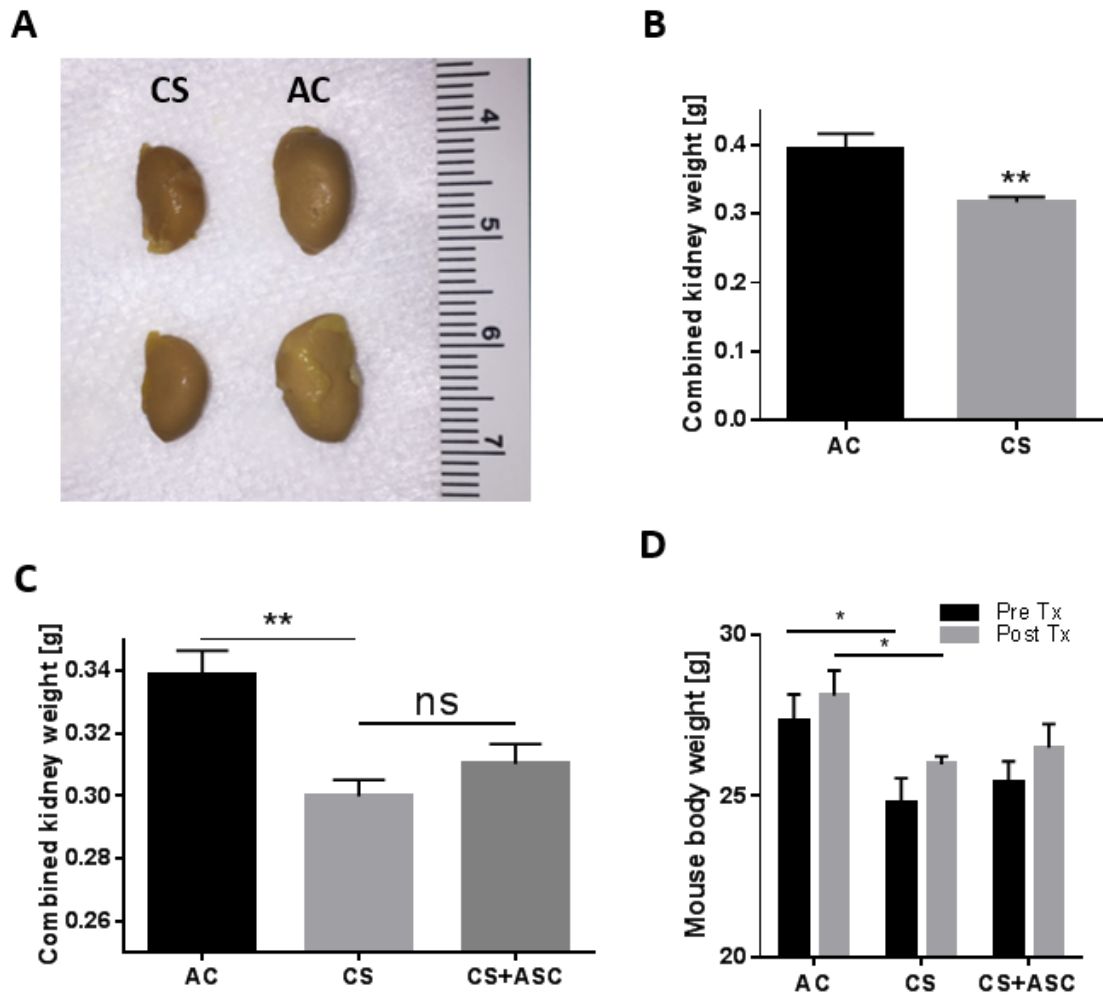


Figure 14. Assessment of the kidney weights. **A.** Image of kidneys from NSG mice in Study 1. **B.** Combined weight of both kidneys from C57Bl/6 female mice in Study 2. **C.** Combined weight of both kidneys from C57Bl/6 female mice in Study 3. **D.** C57Bl/6 mouse body weight (Study 3) assessment immediately before and after ASC treatment period. For all graphs: * $p < 0.05$, ** $p < 0.01$

3.3.2 Assessment of fibrosis and capillary rarefaction

Study 2: C57Bl/6 mice were exposed to 5 months of CS, followed by immediate euthanasia and organ harvest.

Kidney tissue of mice from Study 2 was used for histological assessment. Analysis of renal fibrosis, using PicroSirius Red stain, revealed a 53% increased deposition of Collagen Type I and III in cortical region ($p<0.02$), in mice exposed to CS, compared to AC group (Figure 15A-C). Assessment of renal capillary density, using of Cablin antibodies, demonstrated a remarkable decrease in capillary number (by 86%) in the cortex in that same group of CS-exposed mice ($p<0.0001$) (Figure 15D-F). These findings were further supported by staining with Tomato Lectin, which also revealed a major decrease (by 45%) in endothelial cell density in CS mice ($p<0.05$) (Figure 15G-I).

Histological analysis of the presence of myofibroblasts, assessed via detection of alpha-SMA, revealed no alpha-SMA positive cells in either CS or AC groups. (Data not shown). M1/M2 macrophage polarization analysis, carried out by staining for CD68 (M1) and CD206 (M2) markers demonstrated absence of macrophages in the renal tissue in both mouse cohorts (Figure 16).

Assessment of pathological changes within medullary area of the kidney revealed no statistically significant difference for any of the stain outcomes.

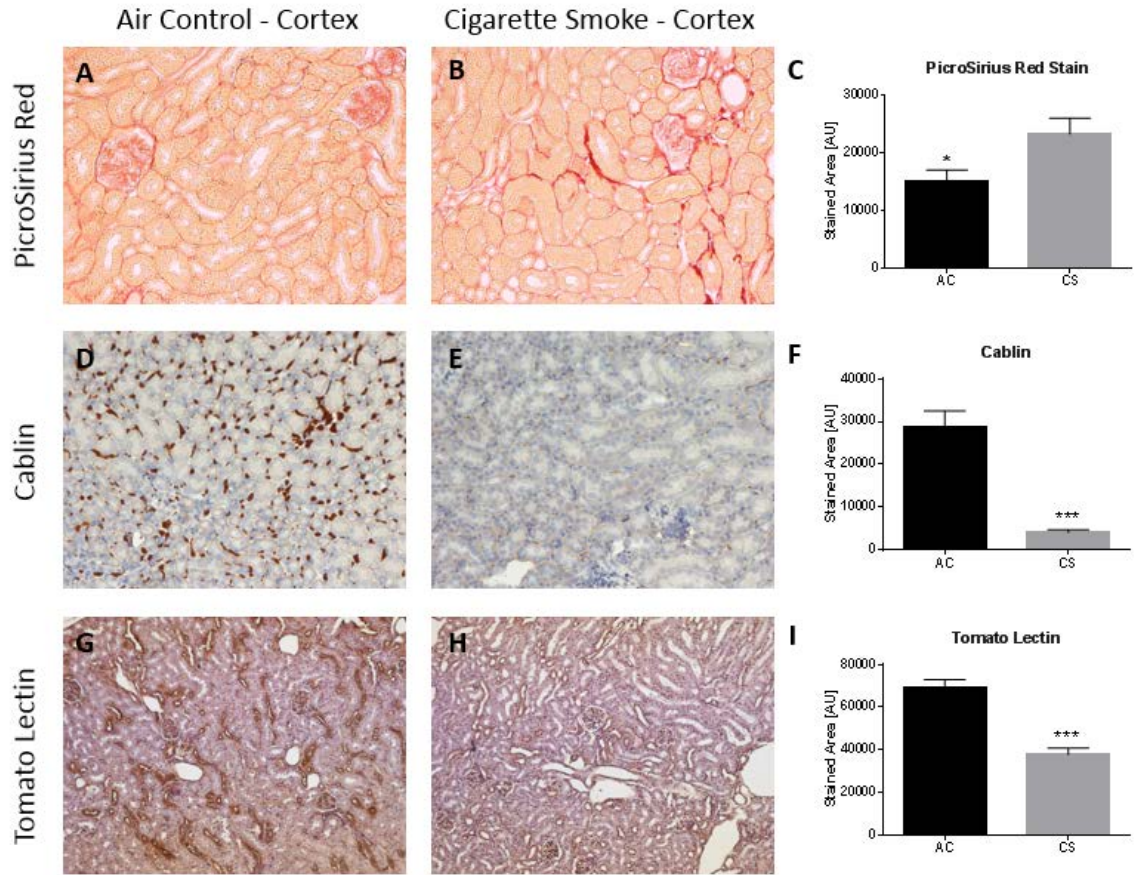


Figure 15. Assessment of fibrosis and capillary density in renal cortical tissue of C57Bl/6 mice exposed to cigarette smoke or ambient air (from Study 2). **A-C**, Representative images of collagen deposition in renal parenchyma revealed by PicroSirius Red stain. **D-F**, Assessment of cortical capillary density using Cablin antibodies. **G-I**, Assessment of cortical capillary density revealed by Tomato lectin. CS group: n=6 mice, AC group n=5 mice. 6-10 images were taken at random from the cortex region of each kidney. For all graphs: *p<0.05, ***p<0.001

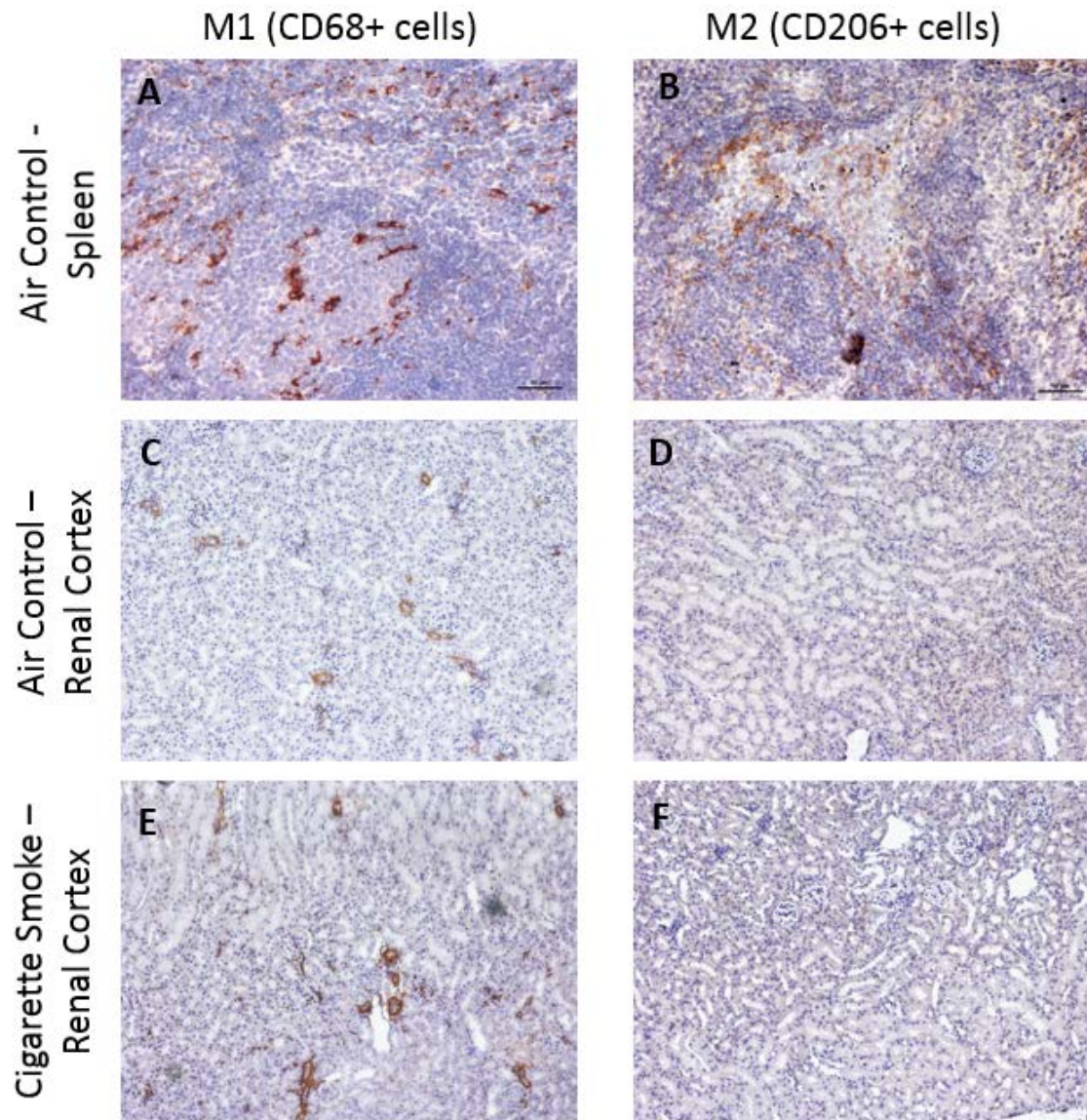


Figure 16. Assessment of M1 and M2 macrophage presence in the renal cortical tissue of C57Bl/6 mice exposed to cigarette smoke or ambient air (Study 3). A-B, Representative images of spleen as positive control for M1 and M2 macrophages. **C-F,** Representative images of renal cortex stained for CD68 and CD206 positive cells.

3.3.3 Assessment of the iron deposition in the kidney tissue and iron clearance following ASC administration

Study 1: NSG mice were exposed to CS for six months, followed by two-month recovery period during which a subset of mice received weekly IP infusion of 1×10^5 human ASC.

Free iron molecules have been shown to be cytotoxic and are thought to assist in Reactive Oxygen Species (ROS) production [227]. Presence of free iron, stored as hemosiderin, in the kidney could indicate hemolysis of red blood cells [228, 229]. Increased iron accumulation has been correlated with increased urinary protein excretion and can lead to acute kidney failure [227].

Assessment of the presence of iron in the form of hemosiderin, conducted via Perl's Iron staining in NSG mice from Study 1 showed nearly a 9-fold increase in the group of animals exposed to CS, compared to mice breathing ambient air. Interestingly and remarkably, the NSG mice treated with intraperitoneal administration of 1×10^5 human ASC showed clearing of the iron deposits in the kidney tissue, with 3.4-fold decrease comparing to the control group (Figure 17).

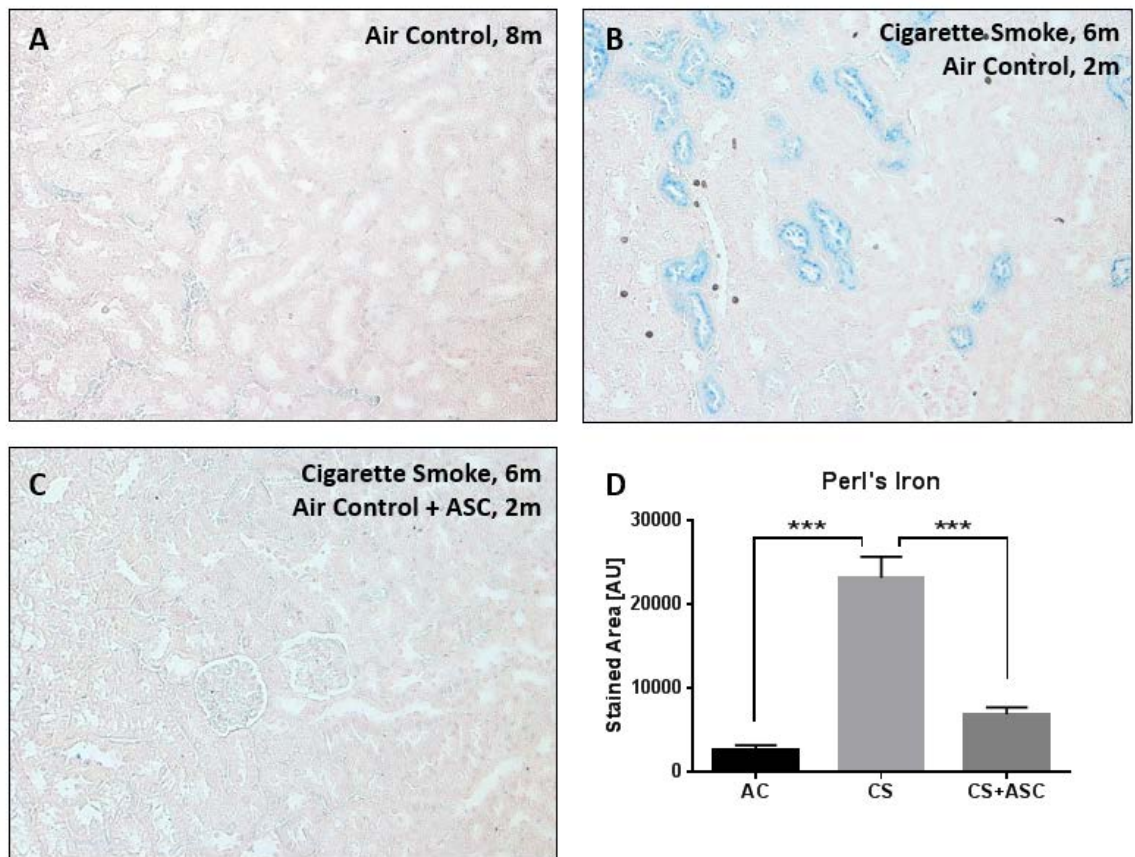


Figure 17. Assessment of iron presence in the kidney tissue of NSG mice using Perl's Iron stain (Study 1). A-C, Histological assessment of iron deposition in mice exposed to ambient air, CS, and CS + ASC treatment. Human ASC treatment was administered intraperitoneally with cell concentration of 1×10^5 . D, Quantitative assessment of histological findings (using arbitrary units) was done using an average score value for each of the kidneys assessed (n=6 images per kidney). ***p<0.001.

3.3.4 Assessment of the effects of cigarette smoke exposure on renal blood flow and therapeutic effect of ASC

Study 3: C57Bl/6 mice were exposed to 5 months of CS, followed by a weekly infusion of IP human ASC at dose of 3×10^5 for 4 weeks.

C57Bl/6 female mice (Study 3) were exposed to CS for a period of 5 months (5 hours a day for 5 days a week). Upon completion of this exposure, mice received intraperitoneal administrations of basal media or human ASC (3×10^5 cells), once a week for four weeks. Effect of cell therapy on tissue perfusion was evaluated by LDI in left kidney (due to ease of access). Analysis revealed a significant drop of 37% in the cortical blood flow in the kidneys of mice exposed to CS, compared to air control cohort. However, mice that were exposed to CS, and received ASC treatment, showed substantial recovery of blood flow (32% increase), when compared to the flow rate in CS-exposed mice that received vehicle as a treatment ($p < 0.01$). Furthermore, no statistically significant difference between the control mice and the ones receiving the ASC treatment was observed (Figure 18), importantly indicating the restoration of normal blood flow even after several months of smoke exposure.

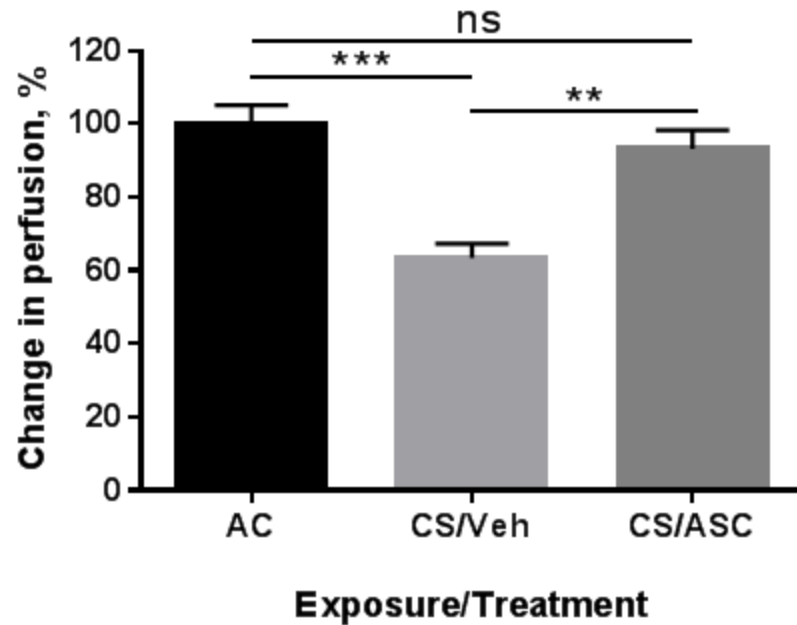


Figure 18. Assessment of superficial cortical renal blood flow in C57Bl/6 mice using LDI. Mice were exposed to ambient air or CS for 5 months (5 hours/day, 5 days/week). Upon completion of CS conditioning, subset of mice exposed to CS, received human ASC treatment (3×10^5 , IP) or vehicle, once a week for 4 weeks. (** $p < 0.01$, *** $p < 0.0001$)

3.4 Discussion

Cigarette smoking is a preventable, but significant, factor contributing to increased morbidity and mortality. The association between smoking and decline in the cardiovascular and pulmonary health is well known [4, 43, 46, 67], as is the increased risk of cancer development [4, 17]. The correlation between smoking and decline in renal function, however, has not received much attention. It has been demonstrated that smoking negatively impacts endothelial cells, homeostasis (due to oxidative stress) leading to decrease in tissue perfusion and impairment in vascular dilation [59, 61], eventually resulting in deterioration of renal function over time [192]. However, the exact mechanisms of detrimental effect of CS on kidney physiology remain to be elucidated.

Our study revealed a significant decrease in the kidney weight in C57Bl/6 mice exposed to CS (Figure 14). However, kidney-to-body ratio did not appear to be significantly different between the groups. This may be a result of the proportional decrease of body weight of the animals exposed to CS. Indeed, our laboratory previously found that chronic CS exposure results in marked decrease in the total body weight [45], perhaps because it decreases appetite [230]. Taking this observation into consideration, the kidney-to-body ratio may be masking the effect of CS on the renal tissue and therefore may not be applicable in the mouse model of CS. We postulate that despite organ-to-body ratio being considered a common way to assess potential organ damage, assessment of kidney weight alone in our animal model should be taken into consideration as indicator of injury. Furthermore, we have previously demonstrated that CS results in decreased fat

tissue (measured as subcutaneous fat area) [45]; it is possible that skeletal muscle weight is also lost due to CS-exposure, as has been shown in the past [231, 232].

While the analysis of the kidney weight does not allow for full understanding of the underlying pathology, the evaluation of presence of fibrotic tissue in the kidneys sheds light on the renal changes due to CS exposure. Fibrosis formation is typically considered to be a response to injury [233]. It is characterized by deposition of large amounts of extracellular matrix (ECM) proteins, however excess deposition results in a pathological state, altering the tissue architecture and function of the affected organ [233]. Renal fibrosis, resulting from activation of renal fibroblasts has been shown to lead to functional impairment [233]. It is also associated with CKD [233]. Studies revealed that the greater the extent of kidney fibrosis, the smaller the likelihood of recovery from CKD [234, 235]. One of the commonly studied pro-fibrotic factors, TGF- β , aids in fibroblast transition into myofibroblasts [234, 236, 237]. In our study, PicroSirius Red stain, commonly used for renal fibrosis analysis, revealed a striking increase in Collagen I and III deposition, a hallmark of fibrosis. Quantification of the stained area can indicate the severity of the renal damage; with a higher score (larger area stained with RSR) corresponding to greater pathology. Two approaches to fibrosis assessment are common: percent of fibrotic tissue and percent of tissue affected by pathology [238]; we have focused on assessment of the extent (percent) of the fibrosis within the organ. While Epithelial and Endothelial-to-Mesenchymal Transition (EMT and EndMT) have been increasingly elucidated as the main driving force behind fibrogenesis, other cells have also been proposed to act as fibroblast precursors,

e.g., pericytes [212] and leukocytes [209], especially in cases where CKD is immune-mediated. Surprisingly, while extensive collagen deposition has been observed in the CS mouse cohort, no myofibroblasts were detected in the kidneys, when probed for α -SMA.

In addition to pathological fibrosis as a result of specific insults, ECM deposition is also observed in the context of aging, which is associated with progressively impaired cell turnover and less effective resorption of the ECM. Aging is a critical factor to consider in light of the pathological findings in the kidneys of mice used in this study, as the path to the observed fibrosis relies on 5 or 6-month long CS-exposure. Such prolonged pre-conditioning resulted in animals that were not only affected by the exposure to toxic environment, but also characterized by advanced age (8 months old) compared to mice commonly used in research (2.5 months old). Therefore, we recognize that aging may play a confounding role and that at least part of the observed renal changes may be attributed to this process.

Aside from fibrosis, a different, yet critical injury of the kidney is associated with endothelial cell apoptosis and subsequent decrease in renal capillary density. We have shown that CS-exposure results in significant loss of renal endothelial cells, as assessed via staining with Cablin and Tomato Lectin. Such phenomenon could be ascribed to either endothelial cell apoptosis or impaired proliferation or both. Basile et al. have demonstrated that renal endothelial cells have a minimal proliferative potential in kidneys subjected to ischemic insult, and administration of

VEGF-121 aids tissue recovery, which has been shown to be an effective treatment option immediately post-injury [239].

While, ASC treatment of kidney injury has been shown to be effective [93], multiple studies have been unable to find these cells in the kidney following the infusion [240], suggesting that the therapeutic benefit is conferred via paracrine activity. Recently, bone morphogenic protein-7 (BMP-7) has emerged as a promising candidate for fibrosis amelioration [240]. BMP-7 has been shown to be secreted by ASC and has been shown to be a strong inhibitor of EndMT-mediated fibrogenesis [240-242].

Assessment of M1 and M2 macrophage polarization revealed their absence from the renal tissue. While M1 macrophages are known as pro-inflammatory and are typically present in a greater amount than M2 during the initial stages of injury, M2 type is characterized by the opposite, anti-inflammatory properties and take part in the regenerative processes [243]. Interestingly, when an insult persists for an extended period of time, M2 macrophages have been shown to activate resident fibroblasts which leads to increased fibrosis [243]. Absence of these cells can be attributed to a chronic model of CS-exposure in which the inflammatory milieu is differs markedly between the start and end of the CS regimen.

Interestingly, none of the histological or immune-histochemical stainings revealed any significant changes in the renal medulla, suggesting that cortex, with the glomeruli, proximal and distal convoluted tubules is more sensitive to CS-induced damage, fibrosis and capillary rarefaction.

Maintenance of sufficient tissue perfusion is critical for maintaining healthy tissue. Studies in recent years have increasingly shown association between ischemic damage to the kidney, as observed in the AKI case and subsequent decline in the function of cardiovascular system [244]. AKI predisposes to future development of chronic kidney disease (CKD) [245]. Furthermore, it has been postulated that the effect of CS may further exacerbate such decline. Interestingly, a recently published abstract titled “Cigarette smoking partially negates the kidney protective effect of angiotensin converting enzyme (ACE) inhibition in stage 2 non-diabetic hypertension-associated CKD” revealed that CS-exposure at least in part, negates the benefits conferred by ACE inhibitors, in patients exhibiting CKD. Therefore it is important to investigate the interplay between CS, decline in the renal vascular health and decline in overall kidney function. Taking into consideration our new data revealing decrease in endothelial cell density within cortical region, we hypothesized that with drop in viable renal vasculature, a drop in the blood flow within kidney may be observed as well. Our assessment of renal tissue perfusion in the cortical region indeed indicated decrease in blood flow in mice exposed to CS; however, that effect was ameliorated (and in fact reversed) in the cohort treated with intraperitoneal (IP) injection of human ASC, indicating that cell therapy may be a very important and viable tool to improve kidney health. Importantly administration of cell treatment in the group of mice exposed to CS, after they finished preconditioning, did not merely show a protective effect, but also appeared to reverse damage caused by smoking. Collett et al., has recently shown that endothelial colony forming cells (ECFC) as well as ASC are able to ameliorate

renal vascular dysfunction in an AKI rodent model [246]. The therapeutic effect of ASC in ischemia/reperfusion injury models was also supported by the studies of several other groups [247, 248]. These studies suggest that ASC may represent a promising therapeutic option to a growing number of patients with kidney damage, at the same time offering a solution to the growing costs associated with the large population with renal pathologies [249].

It is notable that intravenous infusion is a common method of cell delivery at least in part based on the desire to deliver cells directly via vascular supply to the site of injury. However, studies are being conducted to determine the most effective route of cell administration for maximum therapeutic efficacy. In conjunction of growing evidence that IP injections are at least just as effective as intravascular ones, indicating that the regenerative effect of stem cells is conferred via paracrine mechanism. Considering the technical difficulty to access mouse vasculature in the tail following repeated weekly injections, we attempted to use the IP route. Additionally, an advantage of IP route could be the avoidance of pulmonary trapping for the cells (occasionally associated with increased chances of mouse death due to pulmonary embolism).

Interestingly, the assessment of intrarenal iron deposition revealed a significant increase in cytoplasmic iron and hence a potential mechanism for marked damage to the kidneys of mice exposed to CS. Free iron molecules are cytotoxic and are thought to aid in generation of Reactive Oxygen Species (ROS) [227]. Iron can be delivered to kidney via hemoglobin, myoglobin or transferrin. Presence of free iron detected in the kidney could be indicative of hemolysis of red

blood cells; released hemoglobin then deposits into the cytoplasm of renal proximal tubular cells [228, 229]. Degradation of hemoglobin releases iron molecules which are then stored as hemosiderin in the lysosomes [250, 251]. Significant accumulation of iron as hemosiderin can lead to acute kidney failure, associated with hemoglobinuria or hemolytic anemia [227-229, 251]. It has been observed that increased iron accumulation correlates with increased urinary protein excretion [227]. Our study has revealed that CS exposure facilitates hemosiderin deposition and therefore increases renal pathology.

It is important to mention that this study relied on data from two mouse strains: NSG and C57Bl/6. It has been shown before that induction of emphysema as well as the native response to the CS-induced changes, including the response of the immune system, differs between the strains. [252] The inflammatory response, involving macrophages and T-cells, may play a significant role in the severity of pathology caused by CS. Similar observations were made by the same group regarding expression of pro-inflammatory cytokines and the observed weight loss following CS exposure [252]. Despite certain discrepancies related to strain variability in response to CS, these mouse models of emphysema and CS-induced damage continue to help shed light on important biological processes that are involved in CS-induced organ damage.

Our study included two different mouse strains with and without ASC administration. The histological assessments that were conducted for Study 2 (C57Bl/6) will need to be also carried out in the remaining two groups, while iron deposition analysis will need to be evaluated in C57Bl/6 mice, with additional KIM-

1 (kidney injury molecule-1) assessment and serum creatinine analysis for mice in Study 3. This will allow to compare the data across different species and treatment options.

The data on the link between CS and kidney damage has started to accumulate in the past few years, however more studies are needed to determine the mechanisms through which smoking affects kidney. Taking into account some of those emerging data, it is becoming clear that CS contributes to decline in renal health and patients who smoke, may experience an increased severity of the symptoms associated with kidney damage. In addition to studies assessing the effect of CS on kidneys, analysis of the effects of smoking cessation on improvement of renal function are needed.

Chapter 4: Smoking-induced myelosuppression and emphysema development in mice are ameliorated by AMD3100 administration

4.1 Introduction

4.1.1 Pathogenesis of chronic obstructive pulmonary disease (COPD) and the role of cigarette smoke

Chronic obstructive pulmonary disease (COPD) is a progressive, irreversible, and devastating condition characterized by obstruction of airflow to the lungs and injury to the microvasculature [253]. It results in shortness of breath, coughing, chest tightness, exhaustion, and sometimes cyanosis (blue lips). These symptoms, which tend to worsen with time, severely decrease the quality of life of COPD patients. Each year, 174 million cases of COPD are being diagnosed globally, and 3.4 million in the United States alone. One of the major factors implicated in COPD pathogenesis is cigarette smoking (CS) [253], which is also associated with increased chances of developing lung cancer [52, 53] and cardiovascular diseases, like atherosclerosis and impairment of vasodilation [43, 67]. These CS-induced pathologies contribute to increased mortality of COPD patients and, to date, there is no known cure for this condition [253].

One of the diseases associated with COPD is emphysema, the development of which is correlated with increased morbidity and mortality [254]. COPD/Emphysema is classified as the third most common cause of death globally directly behind ischemic heart disease and cerebrovascular disease [253], all of

which can be exacerbated by CS [253]. Important goals of COPD management include reducing disease progression, preventing exacerbations, and decreasing the mortality rate. Patients who continue to smoke are enrolled in smoking cessation programs. These patients mostly rely on treatments targeting their individual symptoms and provide support in breathing, like non-invasive ventilator support (oxygen therapy), bronchodilators (associated with adverse cardiovascular events (e.g. prolonged QT interval) in patients with heart disease), and corticosteroids (shown to increase the risk of pneumonia in patients with compromised lung function) [253]. Another often practiced treatment option is gradual introduction of physical activity, which has been shown to reduce COPD-related complications and decrease the risk of hospital admission as well as treating other existing comorbidities like cardiovascular disease or diabetes. Although recent medical advances were shown to help alleviate the symptoms and improve the quality of life, current therapies fail to substantially improve patient survival [255, 256]. While it has been shown that quitting smoking can slow the progression of the disease and ease some of the symptoms, this continues to be insufficient in restoring the quality of life.

There is a currently unmet medical need for a therapy which will stop the progression of COPD by improving lung regeneration. Pre-clinical studies using rodent models of CS-induced emphysema have shown that the use of mesenchymal stem cells is able to ameliorate the lung pathology and improve its function [257-259]. Our group has demonstrated that a 3-day CS exposure is sufficient to induce myelosuppression [105] which is defined as a decrease in the

number of hematopoietic progenitor cells (HPC: BFU-E, CFU-GM, CFU-GEMM). While CS-induced emphysematous changes require a longer period of time to manifest, we postulated that there may be cross-talk between bone marrow (BM) and lung; and pathology associated with one of the organs affects the other.

4.1.2 The role of bone marrow (BM) in the regenerative process

Hematopoietic stem cells (HSC, CD34+ cells) reside in the bone marrow (BM) and give rise to hematopoietic progenitor cells (HPC) that ultimately differentiate into all of the functional cells of the immune system. Lymphoid progenitors give rise to B- and T-lymphocytes. Myeloid cells, which are the focus of this study, include burst-forming unit erythroid (BFU-E), colony forming unit-granulocyte and macrophage (CFU-GM), and colony forming unit-granulocyte, erythroid, macrophage and megakaryocyte (CFU-GEMM). A more detailed lineage tracking of the HSC is presented in Figure 19.

An increasing body of evidence suggests that there is an interplay between BM and lung: several reports have proposed that some populations of bone marrow cells engraft in lung and support tissue repair [260]. Adachi et al. has shown that transplanting healthy BM cells into the mouse model of emphysema is able to reverse the disease progression [261]. They postulate that emphysema development is associated with damage of BM. Huertas et al. demonstrated a reduced number of BM progenitor cells in severe COPD [262]. Interestingly, it has been revealed that patients with COPD who take steroids for their condition (eg. glucocorticoids) are likely to experience a decrease in bone mass and number of osteoblasts as well as colony forming units contributing to increased incidence of

osteoporosis [263, 264]. In addition, Xie et al., recently documented that exposure of mice to CS, for as short as 3 days, results in significant myelosuppression [105]. This finding is important as it has been shown that a decrease in BM HPC is associated with increased morbidity and mortality in patients with COPD and cardiovascular disease [265-267]. Based on the findings presented above that show a correlation between decrease in circulating HPC and severity of COPD in patients [268-270], we hypothesized that circulating HPC play a role in maintenance and repair of lung function, and that HPC reduction is linked to lung inability to counteract CS-induced damage.

Since it has been shown that CS is damaging to BM, new methods to boost BM repair are necessary in light of repairing lungs and protection from additional damage. Currently, in order to ameliorate BM pathologies like leukemia and aplastic or Fanconi anemia, patients are subject to BM transplants. This procedure, however, is highly invasive and associated with a set of potential complications like graft versus host disease (GVHD), infections, graft failure, and slow recovery, as well as relapse of the disease [271]. In recent years it has been shown that infusion of mesenchymal stem cells accompanying BM transplant can help reduce the risk of GVHD, speed up recovery, and minimize graft failure [271]. However the ideal treatment option would be to enhance or rejuvenate the patient's own BM without the need for transplant.

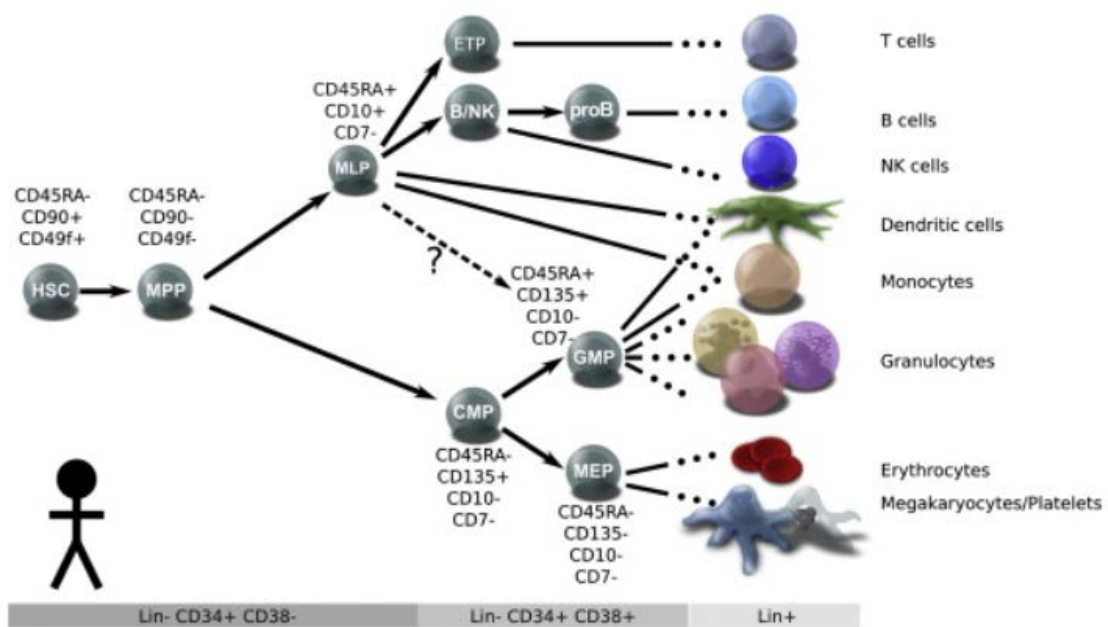


Figure 19. Hematopoiesis model in a human [272]. Cartoon representing development of various blood cells from single hematopoietic stem cell. This process is taking place in the bone marrow. Differentiated cells are represented on the right.

4.1.4 AMD3100 as a therapeutic agent

The bicyclam AMD3100, known as plerixafor or mozobil, is an FDA-approved mobilizer of HPC and HSC to peripheral blood for collection and subsequent transplantation in patients with non-Hodgkin lymphoma and multiple myeloma [165, 273]. AMD3100, which has been proposed to serve as a BM mobilizing alternative to granulocyte colony stimulating factor (G-CSF), is capable of releasing BM cells into peripheral blood within hours of administration, compared to a much longer process involving G-CSF [274].

AMD3100 has been identified as an antagonist of the CXCR4 receptor therefore affecting the CXCR4/SDF-1 (CXCL12, stromal derived factor-1) axis that is known to play an important role in homing and survival of HSC/HPC, as well as preventing the release of these cells from BM niche (Figure 20). The SDF-1 chemokine is abundantly expressed within mouse and human BM environment, predominantly by the endothelial cells, osteoblasts, and reticular cells (type of fibroblasts) [275]. Its receptor, CXCR4, is found on the HSC surface, and upon binding of SDF-1, HSC retention within the BM niche is achieved. Since HSC is sensitive to high SDF-1 gradient present in BM, homing of BM stem and progenitor cells is observed [275]. As AMD3100 is able to modulate this CXCR4/SDF-1 interaction (via antagonizing of SDF-1 binding to CXCR4), it is considered to be a great approach in BM mobilization and transplant studies. While it is known that CXCR4/SDF-1 interaction is crucial to retain BM HSC and HPC within BM niche, interruption of such interactions with AMD3100 results in BM HSC and HPC release, and as shown in mouse studies, the drug mobilizes immature progenitor

cells rather than mature leukocytes (white blood cells) during the fast acting mobilization process, as shown by Dar et al [274]. In addition to the BM HSC and HPC mobilizing properties of AMD3100, Kim et al., has shown that the drug mobilized endothelial progenitor cells (EPC) and helped ameliorate diabetic peripheral neuropathy [276]. Interestingly, Matthys et al. demonstrated that daily administration of AMD3100 for one week prior to the observation of initial symptoms resulted in improvement of indicators of collagen-induced arthritis in mice. He postulated that presence of SDF-1 at the site of injury results in attraction of leukocytes and further propagation of the inflammatory process resulting in joint inflammation and autoimmunity [277]; therefore suggesting that AMD3100 may be useful in targeting diseases mediated by inflammation.

Taken together, these studies demonstrate that AMD3100 shows potential as a therapeutic capable of fostering tissue and organ regeneration. Therefore, we hypothesized that CS-induced myelosuppression as well as emphysema development in mice (as determined by bone marrow colony formation and pulmonary function test) can be ameliorated via AMD3100 administration.

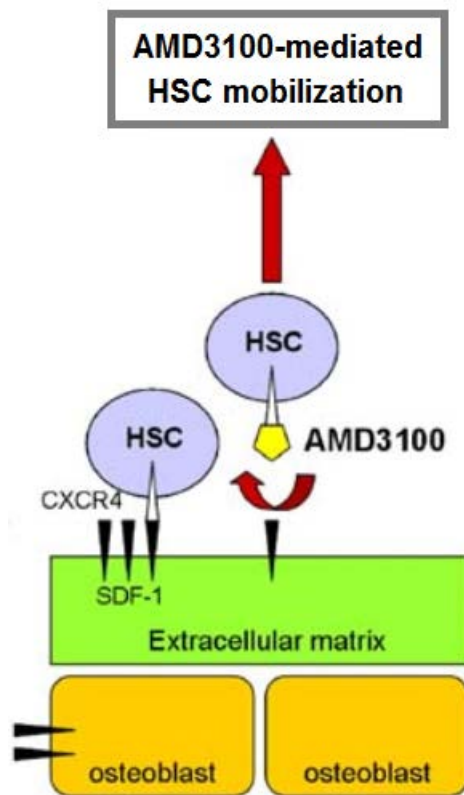


Figure 20. Schematic representation of AMD3100-mediated HSC mobilization into peripheral blood. Modified figure from [278].

4.2 Methods and Materials

4.2.1 Animal model of emphysema and treatment groups

Animal studies were approved by the Indiana University Animal Care and Use Committee. Female C57Bl/6 mice (8-10 weeks, Jackson Laboratories, Bar Harbor, Maine) were exposed to 11% mainstream and 89% side-stream smoke using Teague 10E whole body exposure apparatus (Teague Enterprises, Woodland, CA) for 3 weeks, or 24 weeks for 5 hours/day, 5 days a week, as described previously [45]. CS was generated using 3R4F reference cigarettes (Tobacco Research Institute from Lexington, KY). Control mice were exposed to ambient air for the same duration. Groups of CS-exposed mice received daily subcutaneous injections of 5 mg/kg AMD3100 (Sigma) or PBS (5 consecutive days during week 1, week 12, and week 22 of CS exposure (Figure 21)). Following completion of the treatment, mice were anesthetized and pulmonary function test was conducted, then euthanized prior to BM and lung harvest.

Bone marrow analyses were performed at week 3 and 24 to assess CS-induced effects on HPC. Lung function and MLI were analyzed at week 24 to assess CS-induced lung damage. Inflammatory cells in lung were analyzed at week 3.

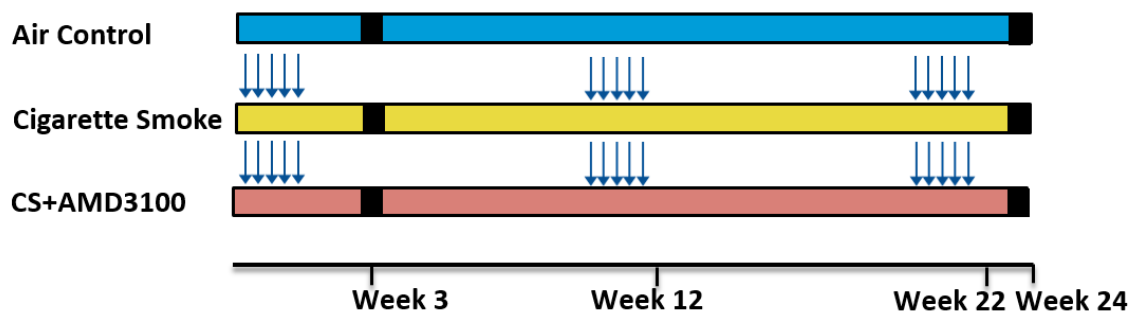


Figure 21. Timeline for AMD3100 injection and analyses. AMD3100 (5 mg/kg/day, subcutaneous) or vehicle were administered daily for 5 consecutive days, Arrows indicate AMD3100 administration. Black squares indicate time of sacrifice and analysis.

4.2.2 Clonogenic progenitor cell assay

Absolute numbers of HPC, as well as individual numbers of granulocyte-macrophage colony-forming units (CFU-GM), erythroid burst-forming units (BFU-E), and multipotential progenitors (CFU-GEMM) were determined, as previously described [165, 279]. To obtain BM cells, left and right femurs were flushed with DMEM. Number of mononuclear cells were assessed using Hemavet 950FS device (Drew Scientific, Dallas, TX). Cells were plated at 4.5×10^4 cell/mL per 35mm dish in 0.9% methylcellulose culture medium, supplemented with 30% FBS (HyClone), 2 mM Glutamine (Gibco), 50ng/ml recombinant mouse stem cell factor (rmSCF; R&D Systems), 1 U/ml recombinant human erythropoietin (EPO, Amgen Corp), 100 μ M 2-mercaptoethanol (Fisher Scientific), 0.1mM hemin (Sigma-Aldrich) and 5% vol./vol. pokeweed mitogen mouse spleen cell conditioned medium (mSCM). mSCM was prepared as previously described [165, 279]. Cells were incubated at 37°C in 5% O₂ and 5% CO₂ for one week and analyzed.

4.2.3 Assessment of lung pathology using Pulmonary Function Test (PFT)

To perform PFT, mice were anesthetized, intubated, and mechanically ventilated with the FlexiVent system (Scireq, Montreal, PQ, Canada) as previously described [280, 281]. An incision was made along the throat area to expose the trachea in order to intubate. A suture was passed under the trachea; the trachea was incised close to larynx. A cannula was inserted into the trachea and secured with the suture. The mouse was then connected to the ventilator. A baseline reading of 30cm H₂O over a period of 3 seconds was performed to confirm the

system setup. Following baseline measurement, the lung performance was assessed.

4.2.4 Assessment of lung pathology using histology

At the completion of PFT, mice were euthanized and their BM, and lungs were collected. For histological analysis, lungs were inflated with 0.25% (v/v) agarose in 10% (v/v) formalin/PBS. Tissues were embedded in paraffin and five micron sections were stained with hematoxylin and eosin. To perform mean linear intercept (MLI) scoring, images of the lungs were generated and then superimposed over a grid and subsequently the number of times that alveolar wall crossed the grid line was counted [282].

4.2.5 Assessment of lung pathology using Bronchoalveolar Lavage (BAL).

For BAL analysis, lungs were flushed 3 times with ice-cold PBS. Obtained BAL was spun down at 600g for 5 min. Supernatant was transferred to fresh tubes and snap-frozen. Pelleted cells were treated with 1 ml of red blood cell lysing buffer (NH_4Cl 8 g/l, KHCO_3 1 g/l, EDTA 0.1mM) for 10 min to remove erythrocytes. After incubation, 10 ml of PBS was added and the content was centrifuged at 600g for 5 min. Cells were re-suspended in PBS. Aliquots of 28,000 cells were loaded into cytospin slides, stained with Three-Step Stain Set (Thermo Scientific), and number of inflammatory cells (macrophages, lymphocytes and polymorphonuclear cells/granulocytes) was determined by counting 300 cells per slide.

4.2.6 Statistical analysis

All results are shown as mean \pm SEM. The analyses were performed with Prism software using one way ANOVA with Tukey Post-hoc. $p < 0.05$ was considered statistically significant.

4.3 Results

4.3.1 AMD3100 ameliorates CS-induced myelosuppression

In patients, AMD3100 induces temporary release of HPC/HSC to peripheral blood followed by a return to baseline after four hours when cells are likely to home to their BM niche [283]. Based on this information, we assessed whether daily mobilization is able to deplete BM pool of HPC. In order to address this question, we assessed the number of HPC in BM of mice subject to CS for three weeks, receiving daily delivery of AMD3100 over a period of 5 days, during the first week.

The data revealed, consistent with prior findings [105], that short term CS exposure results in 60% decrease in mouse BM HPC (Figure 22A). Administration of AMD3100 to a subset of CS-exposed mice restored CS-induced reduction of total HPC (combined numbers for CFU-GM, CFU-GEMM, BFU-E) by 103% (Figure 22A). This treatment effect was noted following two weeks of treatment withdrawal period.

To assess the effect of extended AMD3100 administration on BM HPC, mice were exposed to 24 weeks of CS, three five-day long administrations of AMD3100 were conducted during week 1, 11, 21. The data revealed that CS-induced reduction of total HPC (by 65%), CFU-GM (by 65%), BFU-E (by 58%), and GEMM (by 61%) levels was significantly suppressed by AMD3100 (increase in HPC by 159%, CFU-GM by 155%, BFU-E by 185% and CFU-GEMM by 214%) (Figure 22B, C).

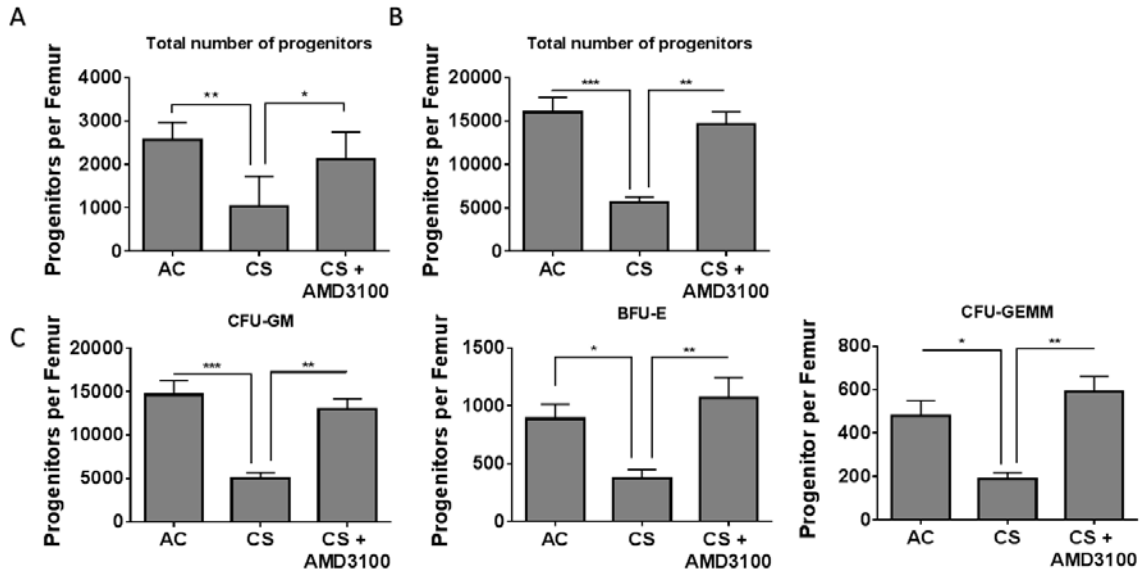


Figure 22. AMD3100 limits CS-induced suppression of BM hematopoietic progenitor cells. C57BL/6 mice were exposed to ambient air or CS for 3 weeks (**A**) or 6 months (**B-C**). **A-B**) Total number of colony forming units. **C**) Total number of colony forming unit-granulocyte, monocyte (CFU-GM), burst forming unit-erythroid (BFU-E) and colony forming unit-granulocyte, erythrocyte, monocyte, and megakaryocyte (CFU-GEMM). Data presented as Mean \pm SEM; * $p < 0.05$, ** $p < 0.01$, *** $p < 0.001$ by ANOVA with Tukey post-hoc.

4.3.2 AMD3100 ameliorates CS-induced lung damage

To analyze whether AMD3100 ameliorates CS-induced emphysematous changes in lungs, we assessed both compliance and inspiratory capacity (maximum volume of air inspired) of lungs of mice exposed to CS for 6 months.

A decline in the inspiratory capacity has been used as a predictor of mortality in COPD patients [284]. Compliance is an indicator of the ability of lung tissue to expand and stretch. Loss of that elastic recoil (shown to be mouse strain dependent [285]), increase in compliance and decrease of resistance is attributed to emphysematous changes [286]. While the same observation of compliance increase in emphysematous lung of both human and mouse, the inspiratory capacity increases in mouse lung with emphysema, which is opposite to the human lung. This is due to the anatomical differences [286].

As seen in emphysema development [287, 288], CS exposure increased compliance and inspiratory capacity of mouse lungs by 17% and 30% respectively. Remarkably, administration of AMD3100 significantly decreased CS-induced increases in both parameters by 14% and 11% respectively (Figure 23A, B).

Analysis of mean linear intercept (MLI) confirmed that AMD3100 suppressed by 11% the emphysematous enlargement of alveoli induced by CS (Figure 23C).

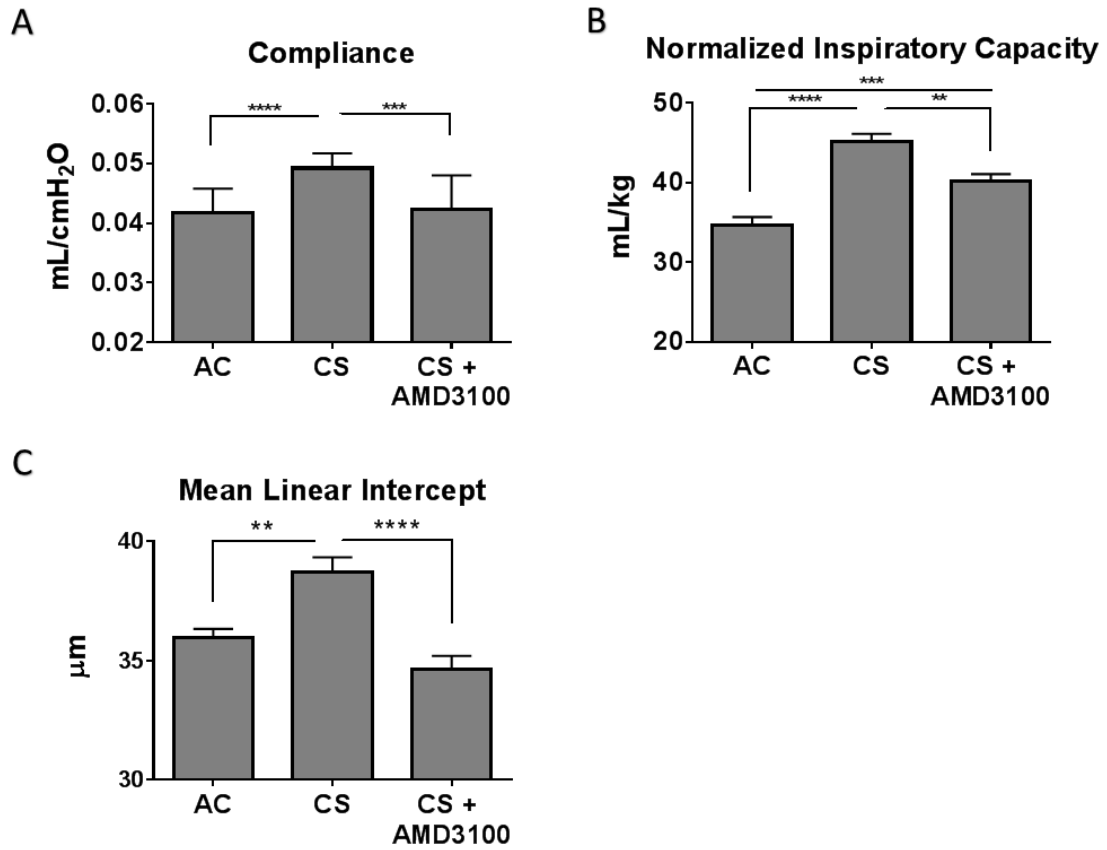


Figure 23. AMD3100 limits CS-induced emphysematous changes in lungs.

C57BL/6 mice were exposed to ambient air or CS for 24 weeks. Lung function (lung compliance, **A**, and inspiratory capacity normalized to mouse weight, **B**) and histological changes (MLI, **C**) were assessed 2 weeks after the last AMD3100 injection. Mean \pm SEM is plotted. * $p < 0.05$ ** $p < 0.01$, *** $p < 0.001$, **** $p < 0.0001$ by ANOVA with Tukey post-hoc.

4.3.2.1 The effect between AMD3100 administration and influx of inflammatory cells to the lung

To analyze whether suppression of emphysematous changes by AMD3100 is associated with a decreased recruitment of inflammatory cells to the lung, we assessed levels of macrophages, lymphocytes, and neutrophils two weeks after the last administration of AMD3100. The data revealed a trend of suppression of the influx of macrophages, lymphocytes, and PMN, however none of the values reached the level of significant difference (Figure 24).

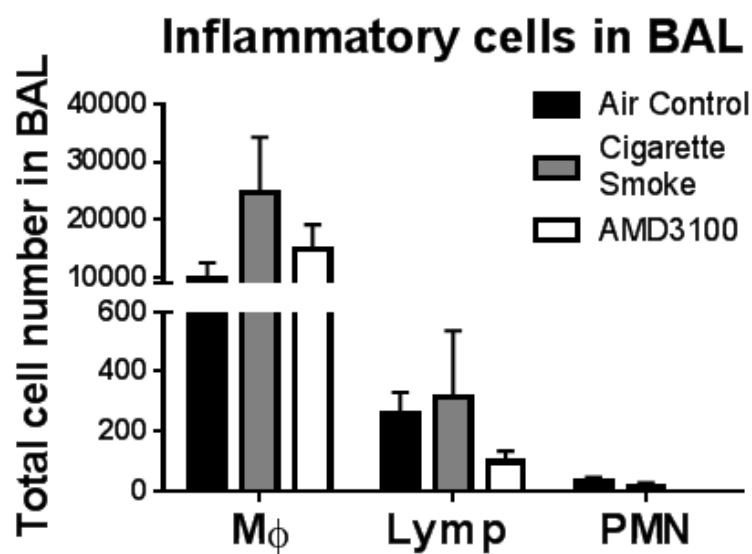


Figure 24. Assessment of the inflammatory cells in BAL (MΦ - macrophages, Lymph - lymphocytes, PMN - polymorphonuclear cells) were assessed 2 weeks after the last AMD3100 injection. Mean \pm SEM is plotted.

4.4 Discussion

Recently, we reported that even short-term CS exposure results in myelosuppression and hence reduction of HPC populations in BM [105]. Interestingly, myelosuppression due to CS happens even prior to detectable lung pathologies, including emphysema development, which, based on pulmonary function tests and lung histology, become apparent around fifth or sixth month of CS exposure. Our laboratory has previously shown that a 3-day CS-exposure resulted in significant decrease in frequency of BFU-E, CFU-GM and CFU-GEMM in BM, whereas a single intravenous administration of human ASC day 2 showed ability to preserve the levels of these cells to levels essentially equivalent to those present in the air control group [105]. Furthermore, the group that received infusion of ASC recovered to a greater extent when compared to the CS-exposed group that was allowed to recover in CS-free environment for seven days, but did not receive cell therapy [105]. In addition to this promising finding demonstrating that ASC therapy ameliorates CS-induced BM damage, our laboratory has also shown that intermittent ASC systemic infusion during the course of CS-exposure lessened the severity of emphysema [45]. Taken together, this data suggests that ASC administration produces a regenerative effect on both BM and lungs in mouse model of emphysema.

The goal of current study was to determine whether intentional mobilization of bone marrow progenitors (CD34 positive cells) in the animals chronically exposed to CS, using the FDA-approved drug AMD3100, would produce the protective effect of the lung function and morphology, which are the primary

characteristics of patients with COPD/emphysema. Since effects of prolonged HPC mobilization on BM pool of cells has never been studied, we analyzed BM HPC levels in mice receiving either brief 5-day long or three intermittent courses (week 1, 12, and 22) of AMD3100 administration. Remarkably, based on the colony assay analyses for three BM lineages, the levels of HPC in AMD3100-treated mice were at the similar level as in the control group (AC) and were independent of treatment regimen: mice receiving a single 5-day administration and mice receiving three five-day administrations.

The mechanism responsible for the protective effect of AMD3100 on HPC in BM is yet to be elucidated. Mobilization of HPC with AMD3100 to peripheral blood has been shown to be short-lived, with peak at one hour post-administration [165]. The number of HPC in the peripheral blood at the time of BM harvest was not assessed in this study, therefore it is unclear whether the intermittent administration of AMD3100 led to extended persistence of BM cells in circulation. The fact that mobilized HPC are mostly in G₀ cell cycle suggests that no proliferation takes place while HPC are in peripheral blood [283].

Independent of the nature of protective mechanism, our findings demonstrate that intermittent administration of AMD3100 is sufficient to preserve HPC levels in BM of mice exposed to CS. The protective effect of AMD3100 on BM cells was observed together with its protective effect on lungs via reduction of the emphysematous changes. This finding suggests that lung rejuvenation may be dependent on the ability of BM to supply sufficient amounts of circulating HPC.

AMD3100 is a known antagonist of CXCR4, a receptor of SDF-1, a chemokine shown to be secreted in tissues subjected to injury, and subsequently attracting inflammatory cells. It has been demonstrated that daily administration of AMD3100 over a short duration results in improvement of symptoms of arthritis in mice, a disease known to have an inflammatory component [277]. The same study also showed that increased expression of SDF-1 at the site of injury contributed to influx of leukocytes, propagating further the inflammatory processes [277]. The overexpression of SDF-1 in tissues has been associated with conditions mediated by inflammatory response, while diseases that are not inflammation-caused (like osteoarthritis) have not been correlated with increased SDF-1 secretion [277, 289]. This ties with the observation that COPD and emphysema are strongly associated with influx of inflammatory cells. Studies have demonstrated that upregulation of SDF-1 is commonly observed in the emphysematous lung tissue [290]. Such increased expression is thought to lead to influx of cells aiding in restoring the damage, and has been beneficial in studies infusing mesenchymal stem cells in order to address lung injury [291]. Whether overexpression of SDF-1 is a truly desirable phenomenon has not reached a consensus yet. Rafii et al. has shown that lung regeneration can be mediated via platelet-derived SDF-1 which promotes neo-alveolization, while SDF-1-deficient platelets were unable to repair the damage [292]. Similarly, ablation of CXCR4 hindered lung damage repair [292]. A study assessing pulmonary hypertension in mice has demonstrated that inhibition of CXCR4/SDF-1 signaling pathway with either AMD3100 or anti-SDF-1 neutralizing antibody improved lung rejuvenation, including alveolization [293].

Makino et al. revealed that pulmonary fibrosis is mediated by CXCR4/SDF-1 signaling mechanism, which is responsible for the accumulation of circulating fibroblasts and lymphocytes in damaged lung parenchyma [294]. The same group postulated that administration of AMD3100 inhibited pulmonary fibrosis and reduced the number of lymphocytes in BAL. It has also been shown that recruitment of macrophages and neutrophils to the lungs could be prevented by AMD3100 [295] or another CXCR4 antagonist 4F-benzoyl-TE14011 [296]. Since inflammatory cells are known to play a critical role in emphysema development [297, 298], whether the observed therapeutic effect of AMD3100 is attributed to its ability to decrease local inflammation requires future investigation.

Taken together, mobilization of HPC may not be the only mechanism mediating lung protection by AMD3100. Inhibitory activity of the drug on CXCR4/SDF-1 axis, potentially reducing the infiltration of the damaged tissue by inflammatory cells and therefore reducing tissue damage may also play a role.

The ability of AMD3100 to limit emphysema progression in mice clearly indicates that AMD3100 may have potential therapeutic value for COPD patients. Although it has been shown that repetitive administration of AMD3100 is associated with various side effects [299, 300], optimization of dose and regiment of treatment may limit the development of side effects while delivering optimal effects to patients with COPD. Based on these findings, AMD3100 may be considered as a candidate for an entirely new indication in treatment and preservation of lung function as a result of exposure to CS.

Chapter 5: Future directions

My studies as described above have addressed several important topics related to the effects of CS on development of pathology and on the potential for therapies based on cellular administration or modulation to treat these pathologies. We have shown that **ASC derived from patients with a history of CS, are compromised in their potential to form dense vascular networks and this effect is due to increased secretion of an inhibitor, the angiostatic factor Activin A.** During our *in vivo* studies we have not assessed the efficacy of administration of ASC from non-CS donors, in mice exposed to CS and subsequently subjected to hindlimb ischemia procedure. While we investigated the therapeutic efficacy of the cells from smokers, we recognize the importance to also assess the physiological environment in patients who smoke, and their response to therapy using cells from healthy donors. Further studies involving Activin A knock-down models are needed to fully elucidate on the mechanism and determine the extent to which Activin A plays a role in limiting vasculogenic potential of ASC from smoking donors.

Our further assessment of CS-induced pathology in a distinct organ system, the kidney, revealed fibrosis formation, capillary rarefaction and iron deposition. While administration of ASC has shown **promise to reverse such renal damage**, it remains important to determine the mechanism of CS-induced fibrosis formation. We hypothesize that this effect is due to EndoMT processes and studies utilizing inducible Tie-2-creER-YFP mouse strain (Tie2 gene is known to drive the

expression of endothelial cells. If eYFP-expressing cells undergo transition into smooth muscle cells, they will continue to express the fluorescent protein) will help address these questions. Incorporating ASC treatment into the study design will allow to determine whether ASC therapy is able to diminish EndMT-associated fibrosis formation.

Finally, our analysis of amelioration of CS-induced myelosuppression and emphysema in mice using AMD3100 showed a very promising finding that an **already approved bone marrow hematopoietic stem and progenitor cell mobilizing agent may offer a promising treatment in patients with compromised bone marrow and lung function**. The mechanism involved in the therapeutic activity of AMD3100 to ameliorate the observed damage still needs to be elucidated. Studies to assess dose response of AMD3100 will be needed to determine the most optimal time points as well as frequency of the drug administration.

While our studies add a significant amount of new information to the general body of knowledge related to the pathological effects of CS, a long-term study involving a large cohort of smokers is still needed to elucidate the relationships among the number of cigarettes smoked in a lifetime, the number of years during which smoking was ongoing, as well as the length of time since smoking cessation and the level of tissue damage and subsequent regeneration.

REFERENCES

1. Stewart, G.G., A history of the medicinal use of tobacco 1492-1860. *Med Hist*, 1967. 11(3): p. 228-68.
2. Musk, A.W. and N.H. de Klerk, History of tobacco and health. *Respirology*, 2003. 8(3): p. 286-90.
3. Doll, R., On the etiology of lung cancer. *J Natl Cancer Inst*, 1950. 11(3): p. 638-40.
4. Alberg, A.J., D.R. Shopland, and K.M. Cummings, The 2014 Surgeon General's report: commemorating the 50th Anniversary of the 1964 Report of the Advisory Committee to the US Surgeon General and updating the evidence on the health consequences of cigarette smoking. *Am J Epidemiol*, 2014. 179(4): p. 403-12.
5. Walton, J.N., et al., *The Oxford medical companion*. 1994, Oxford ; New York: Oxford University Press. xxi, 1038 p.
6. Jamal, A., et al., Current cigarette smoking among adults - United States, 2005-2014. *MMWR Morb Mortal Wkly Rep*, 2015. 64(44): p. 1233-40.
7. Kasza, K.A., et al., Tobacco-Product Use by Adults and Youths in the United States in 2013 and 2014. *N Engl J Med*, 2017. 376(4): p. 342-353.
8. Yauk, C.L., et al., Genetic toxicology and toxicogenomic analysis of three cigarette smoke condensates in vitro reveals few differences among full-flavor, blonde, and light products. *Environ Mol Mutagen*, 2012. 53(4): p. 281-96.
9. DeMarini, D.M., Genotoxicity of tobacco smoke and tobacco smoke condensate: a review. *Mutat Res*, 2004. 567(2-3): p. 447-74.
10. Hecht, S.S., Research opportunities related to establishing standards for tobacco products under the Family Smoking Prevention and Tobacco Control Act. *Nicotine Tob Res*, 2012. 14(1): p. 18-28.
11. Szoltysek-Boldys, I., et al., Influence of inhaled nicotine source on arterial stiffness. *Przegl Lek*, 2014. 71(11): p. 572-5.
12. Li, N., et al., Nicotine Induces Cardiomyocyte Hypertrophy Through TRPC3-Mediated Ca/NFAT Signalling Pathway. *Can J Cardiol*, 2015.
13. Farsalinos, K.E., et al., Acute effects of using an electronic nicotine-delivery device (electronic cigarette) on myocardial function: comparison with the effects of regular cigarettes. *BMC Cardiovasc Disord*, 2014. 14: p. 78.
14. Ferreira, V.M., et al., Chronic Nicotine Exposure Abolishes Maternal Systemic and Renal Adaptations to Pregnancy in Rats. *PLoS One*, 2016. 11(2): p. e0150096.
15. Lee, J. and J.P. Cooke, Nicotine and pathological angiogenesis. *Life Sci*, 2012. 91(21-22): p. 1058-64.
16. Benowitz, N.L., Cigarette smoking and cardiovascular disease: pathophysiology and implications for treatment. *Prog Cardiovasc Dis*, 2003. 46(1): p. 91-111.
17. Heeschen, C., et al., Nicotine stimulates angiogenesis and promotes tumor growth and atherosclerosis. *Nat Med*, 2001. 7(7): p. 833-9.

18. Tsunoda, K., et al., Nicotine-Mediated Ca(2+) -Influx Induces IL-8 Secretion in Oral Squamous Cell Carcinoma Cell. *J Cell Biochem*, 2016. 117(4): p. 1009-15.
19. Lane, D., et al., Up-regulation of vascular endothelial growth factor-C by nicotine in cervical cancer cell lines. *Am J Reprod Immunol*, 2005. 53(3): p. 153-8.
20. Carty, C.S., et al., Nicotine and cotinine stimulate secretion of basic fibroblast growth factor and affect expression of matrix metalloproteinases in cultured human smooth muscle cells. *J Vasc Surg*, 1996. 24(6): p. 927-34; discussion 934-5.
21. Liu, R., et al., Racial Disparity in the Associations of Cotinine with Insulin Secretion: Data from the National Health and Nutrition Examination Survey, 2007-2012. *PLoS One*, 2016. 11(12): p. e0167260.
22. Murphy, S.E., Nicotine Metabolism and Smoking: Ethnic Differences in the Role of P450 2A6. *Chem Res Toxicol*, 2017. 30(1): p. 410-419.
23. Raja, M., et al., Diagnostic Methods for Detection of Cotinine Level in Tobacco Users: A Review. *J Clin Diagn Res*, 2016. 10(3): p. ZE04-6.
24. Motterlini, R. and L.E. Otterbein, The therapeutic potential of carbon monoxide. *Nat Rev Drug Discov*, 2010. 9(9): p. 728-43.
25. Huang, C.C., et al., Hyperbaric oxygen therapy is associated with lower short- and long-term mortality in patients with carbon monoxide poisoning. *Chest*, 2017.
26. Tsai, P.H., et al., Early white matter injuries in patients with acute carbon monoxide intoxication: A tract-specific diffusion kurtosis imaging study and STROBE compliant article. *Medicine (Baltimore)*, 2017. 96(5): p. e5982.
27. Rogers, S., et al., Aryl hydrocarbon receptor (AhR)-dependent regulation of pulmonary miRNA by chronic cigarette smoke exposure. *Sci Rep*, 2017. 7: p. 40539.
28. Gao, Z., et al., TCDD promoted EMT of hFPECs via AhR, which involved the activation of EGFR/ERK signaling. *Toxicol Appl Pharmacol*, 2016. 298: p. 48-55.
29. Shimizu, Y., et al., Benzo[a]pyrene carcinogenicity is lost in mice lacking the aryl hydrocarbon receptor. *Proc Natl Acad Sci U S A*, 2000. 97(2): p. 779-82.
30. Santiago, H.A., et al., Exposure to Secondhand Smoke Impairs Fracture Healing in Rats. *Clin Orthop Relat Res*, 2017. 475(3): p. 894-902.
31. Dunbar, A., W. Gotsis, and W. Frishman, Second-hand tobacco smoke and cardiovascular disease risk: an epidemiological review. *Cardiol Rev*, 2013. 21(2): p. 94-100.
32. Raghuveer, G., et al., Cardiovascular Consequences of Childhood Secondhand Tobacco Smoke Exposure: Prevailing Evidence, Burden, and Racial and Socioeconomic Disparities: A Scientific Statement From the American Heart Association. *Circulation*, 2016. 134(16): p. e336-e359.
33. Al-Sayed, E.M. and K.S. Ibrahim, Second-hand tobacco smoke and children. *Toxicol Ind Health*, 2014. 30(7): p. 635-44.

34. Yankelevitz, D.F., et al., The Association of Secondhand Tobacco Smoke and CT Angiography-Verified Coronary Atherosclerosis. *JACC Cardiovasc Imaging*, 2016.
35. Aydogan, M.S., et al., The effects of secondhand smoke on postoperative pain and fentanyl consumption. *J Anesth*, 2013. 27(4): p. 569-74.
36. Jacob, P., 3rd, et al., Thirdhand Smoke: New Evidence, Challenges, and Future Directions. *Chem Res Toxicol*, 2017. 30(1): p. 270-294.
37. Adhami, N., et al., A Health Threat to Bystanders Living in the Homes of Smokers: How Smoke Toxins Deposited on Surfaces Can Cause Insulin Resistance. *PLoS One*, 2016. 11(3): p. e0149510.
38. Bahl, V., et al., Cytotoxicity of Thirdhand Smoke and Identification of Acrolein as a Volatile Thirdhand Smoke Chemical That Inhibits Cell Proliferation. *Toxicol Sci*, 2016. 150(1): p. 234-46.
39. Due, M.R., et al., Acrolein involvement in sensory and behavioral hypersensitivity following spinal cord injury in the rat. *J Neurochem*, 2014. 128(5): p. 776-86.
40. Al-Arifi, M.N., et al., Impact of cigarette smoke exposure on the expression of cardiac hypertrophic genes, cytochrome P450 enzymes, and oxidative stress markers in rats. *J Toxicol Sci*, 2012. 37(5): p. 1083-90.
41. Kullo, I.J. and T.W. Rooke, CLINICAL PRACTICE. Peripheral Artery Disease. *N Engl J Med*, 2016. 374(9): p. 861-71.
42. MacSweeney, S.T., et al., Smoking and growth rate of small abdominal aortic aneurysms. *Lancet*, 1994. 344(8923): p. 651-2.
43. Ambrose, J.A. and R.S. Barua, The pathophysiology of cigarette smoking and cardiovascular disease: an update. *J Am Coll Cardiol*, 2004. 43(10): p. 1731-7.
44. Glantz, S.A. and W.W. Parmley, Passive smoking and heart disease. Epidemiology, physiology, and biochemistry. *Circulation*, 1991. 83(1): p. 1-12.
45. Schweitzer, K.S., et al., Adipose stem cell treatment in mice attenuates lung and systemic injury induced by cigarette smoking. *Am J Respir Crit Care Med*, 2011. 183(2): p. 215-25.
46. Hilberink, S.R., et al., Smoking cessation in patients with COPD in daily general practice (SMOCC): six months' results. *Prev Med*, 2005. 41(5-6): p. 822-7.
47. Aravamudan, B., et al., Cigarette smoke-induced mitochondrial fragmentation and dysfunction in human airway smooth muscle. *Am J Physiol Lung Cell Mol Physiol*, 2014. 306(9): p. L840-54.
48. Hutchinson, D., et al., Heavy cigarette smoking is strongly associated with rheumatoid arthritis (RA), particularly in patients without a family history of RA. *Ann Rheum Dis*, 2001. 60(3): p. 223-7.
49. Costenbader, K.H., et al., Smoking intensity, duration, and cessation, and the risk of rheumatoid arthritis in women. *Am J Med*, 2006. 119(6): p. 503 e1-9.

50. Manouchehrinia, A., et al., Tobacco smoking and disability progression in multiple sclerosis: United Kingdom cohort study. *Brain*, 2013. 136(Pt 7): p. 2298-304.
51. Li, W., et al., Smoking and risk of incident psoriasis among women and men in the United States: a combined analysis. *Am J Epidemiol*, 2012. 175(5): p. 402-13.
52. Petros, W.P., et al., Effects of tobacco smoking and nicotine on cancer treatment. *Pharmacotherapy*, 2012. 32(10): p. 920-31.
53. Edderkaoui, M., et al., HDAC3 mediates smoking-induced pancreatic cancer. *Oncotarget*, 2016. 7(7): p. 7747-60.
54. Yadav, D. and D.C. Whitcomb, The role of alcohol and smoking in pancreatitis. *Nat Rev Gastroenterol Hepatol*, 2010. 7(3): p. 131-45.
55. Slickers, J.E., et al., Maternal body mass index and lifestyle exposures and the risk of bilateral renal agenesis or hypoplasia: the National Birth Defects Prevention Study. *Am J Epidemiol*, 2008. 168(11): p. 1259-67.
56. Groen In 't Woud, S., et al., Maternal risk factors involved in specific congenital anomalies of the kidney and urinary tract: A case-control study. *Birth Defects Res A Clin Mol Teratol*, 2016.
57. Feng, Y., et al., Maternal lifestyle factors in pregnancy and congenital heart defects in offspring: review of the current evidence. *Ital J Pediatr*, 2014. 40: p. 85.
58. Jenkins, K.J., et al., Noninherited risk factors and congenital cardiovascular defects: current knowledge: a scientific statement from the American Heart Association Council on Cardiovascular Disease in the Young: endorsed by the American Academy of Pediatrics. *Circulation*, 2007. 115(23): p. 2995-3014.
59. Neunteufl, T., et al., Contribution of nicotine to acute endothelial dysfunction in long-term smokers. *J Am Coll Cardiol*, 2002. 39(2): p. 251-6.
60. Ginzel, K.H., et al., Critical review: nicotine for the fetus, the infant and the adolescent? *J Health Psychol*, 2007. 12(2): p. 215-24.
61. Talukder, M.A., et al., Chronic cigarette smoking causes hypertension, increased oxidative stress, impaired NO bioavailability, endothelial dysfunction, and cardiac remodeling in mice. *Am J Physiol Heart Circ Physiol*, 2011. 300(1): p. H388-96.
62. Shah, R.S. and J.W. Cole, Smoking and stroke: the more you smoke the more you stroke. *Expert Rev Cardiovasc Ther*, 2010. 8(7): p. 917-32.
63. Jamal, O., et al., Cigarette smoking worsens systemic inflammation in persons with metabolic syndrome. *Diabetol Metab Syndr*, 2014. 6: p. 79.
64. McEvoy, J.W., et al., Relationship of cigarette smoking with inflammation and subclinical vascular disease: the Multi-Ethnic Study of Atherosclerosis. *Arterioscler Thromb Vasc Biol*, 2015. 35(4): p. 1002-10.
65. Maclay, J.D., et al., Increased platelet activation in patients with stable and acute exacerbation of COPD. *Thorax*, 2011. 66(9): p. 769-74.
66. Corre, F., J. Lellouch, and D. Schwartz, Smoking and leucocyte-counts. Results of an epidemiological survey. *Lancet*, 1971. 2(7725): p. 632-4.

67. Bazzano, L.A., et al., Relationship between cigarette smoking and novel risk factors for cardiovascular disease in the United States. *Ann Intern Med*, 2003. 138(11): p. 891-7.
68. Gill, J.F., S.S. Yu, and I.M. Neuhaus, Tobacco smoking and dermatologic surgery. *J Am Acad Dermatol*, 2013. 68(1): p. 167-72.
69. Butzelaar, L., et al., Currently known risk factors for hypertrophic skin scarring: A review. *J Plast Reconstr Aesthet Surg*, 2016. 69(2): p. 163-9.
70. Towler, J., Cigarette smoking and its effects on wound healing. *J Wound Care*, 2000. 9(3): p. 100-4.
71. Thomsen, S.F. and L.T. Sorensen, Smoking and skin disease. *Skin Therapy Lett*, 2010. 15(6): p. 4-7.
72. Knuutinen, A., et al., Smoking affects collagen synthesis and extracellular matrix turnover in human skin. *Br J Dermatol*, 2002. 146(4): p. 588-94.
73. Turgeon, J., et al., Probucol and antioxidant vitamins rescue ischemia-induced neovascularization in mice exposed to cigarette smoke: potential role of endothelial progenitor cells. *Atherosclerosis*, 2010. 208(2): p. 342-9.
74. Riefkohl, R., et al., Association between cutaneous occlusive vascular disease, cigarette smoking, and skin slough after rhytidectomy. *Plast Reconstr Surg*, 1986. 77(4): p. 592-5.
75. Akoz, T., M. Akan, and S. Yildirim, If you continue to smoke, we may have a problem: smoking's effects on plastic surgery. *Aesthetic Plast Surg*, 2002. 26(6): p. 477-82.
76. Centers for Disease, C. and Prevention, Smoking-attributable mortality, years of potential life lost, and productivity losses--United States, 2000-2004. *MMWR Morb Mortal Wkly Rep*, 2008. 57(45): p. 1226-8.
77. in The Health Consequences of Smoking-50 Years of Progress: A Report of the Surgeon General. 2014: Atlanta (GA).
78. Hare, J.M., et al., Randomized Comparison of Allogeneic Versus Autologous Mesenchymal Stem Cells for Nonischemic Dilated Cardiomyopathy: POSEIDON-DCM Trial. *J Am Coll Cardiol*, 2017. 69(5): p. 526-537.
79. Williams, A.R., et al., Enhanced effect of combining human cardiac stem cells and bone marrow mesenchymal stem cells to reduce infarct size and to restore cardiac function after myocardial infarction. *Circulation*, 2013. 127(2): p. 213-23.
80. Cai, L., et al., Suppression of hepatocyte growth factor production impairs the ability of adipose-derived stem cells to promote ischemic tissue revascularization. *Stem Cells*, 2007. 25(12): p. 3234-43.
81. Wang, H., et al., Transplantation of EPCs overexpressing PDGFR-beta promotes vascular repair in the early phase after vascular injury. *BMC Cardiovasc Disord*, 2016. 16(1): p. 179.
82. Fauzi, A.A., et al., Intraventricular Transplantation of Autologous Bone Marrow Mesenchymal Stem Cells via Ommaya Reservoir in Persistent Vegetative State Patients after Haemorrhagic Stroke: Report of Two Cases & Review of the Literature. *J Stem Cells Regen Med*, 2016. 12(2): p. 100-104.

83. Karantalis, V. and J.M. Hare, Use of mesenchymal stem cells for therapy of cardiac disease. *Circ Res*, 2015. 116(8): p. 1413-30.
84. Kale, S., et al., Bone marrow stem cells contribute to repair of the ischemically injured renal tubule. *J Clin Invest*, 2003. 112(1): p. 42-9.
85. Flex, A., et al., Human cord blood endothelial progenitors promote post-ischemic angiogenesis in immunocompetent mouse model. *Thromb Res*, 2016. 141: p. 106-11.
86. Murray, I.R., et al., Natural history of mesenchymal stem cells, from vessel walls to culture vessels. *Cell Mol Life Sci*, 2014. 71(8): p. 1353-74.
87. Zhang, J.M., et al., Platelet-Derived Growth Factor-BB Protects Mesenchymal Stem Cells (MSCs) Derived From Immune Thrombocytopenia Patients Against Apoptosis and Senescence and Maintains MSC-Mediated Immunosuppression. *Stem Cells Transl Med*, 2016. 5(12): p. 1631-1643.
88. Pires, A.O., et al., Unveiling the Differences of Secretome of Human Bone Marrow Mesenchymal Stem Cells, Adipose Tissue-Derived Stem Cells, and Human Umbilical Cord Perivascular Cells: A Proteomic Analysis. *Stem Cells Dev*, 2016. 25(14): p. 1073-83.
89. Hong, S.J., D.O. Traktuev, and K.L. March, Therapeutic potential of adipose-derived stem cells in vascular growth and tissue repair. *Curr Opin Organ Transplant*, 2010. 15(1): p. 86-91.
90. Rehman, J., et al., Secretion of angiogenic and antiapoptotic factors by human adipose stromal cells. *Circulation*, 2004. 109(10): p. 1292-8.
91. Heo, J.S., et al., Comparison of molecular profiles of human mesenchymal stem cells derived from bone marrow, umbilical cord blood, placenta and adipose tissue. *Int J Mol Med*, 2016. 37(1): p. 115-25.
92. Piltti, K.M., et al., Increasing Human Neural Stem Cell Transplantation Dose Alters Oligodendroglial and Neuronal Differentiation after Spinal Cord Injury. *Stem Cell Reports*, 2017.
93. Collett, J.A., et al., Human adipose stromal cell therapy improves survival and reduces renal inflammation and capillary rarefaction in acute kidney injury. *J Cell Mol Med*, 2017.
94. Daher, S.R., et al., Adipose stromal/stem cells: basic and translational advances: the IFATS collection. *Stem Cells*, 2008. 26(10): p. 2664-5.
95. Gimble, J.M., A.J. Katz, and B.A. Bunnell, Adipose-derived stem cells for regenerative medicine. *Circ Res*, 2007. 100(9): p. 1249-60.
96. Grudzenski, S., et al., The effect of adipose tissue-derived stem cells in a middle cerebral artery occlusion stroke model depends on their engraftment rate. *Stem Cell Res Ther*, 2017. 8(1): p. 96.
97. Duscher, D., et al., Aging disrupts cell subpopulation dynamics and diminishes the function of mesenchymal stem cells. *Sci Rep*, 2014. 4: p. 7144.
98. Ma, N., et al., Adipose-derived stem cells from younger donors, but not aging donors, inspire the host self-healing capability through its secreta. *Exp Biol Med (Maywood)*, 2016.

99. Efimenko, A., et al., Adipose-derived mesenchymal stromal cells from aged patients with coronary artery disease keep mesenchymal stromal cell properties but exhibit characteristics of aging and have impaired angiogenic potential. *Stem Cells Transl Med*, 2014. 3(1): p. 32-41.
100. Perez, L.M., et al., Obese-derived ASCs show impaired migration and angiogenesis properties. *Arch Physiol Biochem*, 2013. 119(5): p. 195-201.
101. Perez, L.M., et al., Altered metabolic and stemness capacity of adipose tissue-derived stem cells from obese mouse and human. *PLoS One*, 2015. 10(4): p. e0123397.
102. El-Ftesi, S., et al., Aging and diabetes impair the neovascular potential of adipose-derived stromal cells. *Plast Reconstr Surg*, 2009. 123(2): p. 475-85.
103. Rennert, R.C., et al., Diabetes impairs the angiogenic potential of adipose-derived stem cells by selectively depleting cellular subpopulations. *Stem Cell Res Ther*, 2014. 5(3): p. 79.
104. Wahl, E.A., et al., Acute stimulation of mesenchymal stem cells with cigarette smoke extract affects their migration, differentiation, and paracrine potential. *Sci Rep*, 2016. 6: p. 22957.
105. Xie, J., et al., Human adipose-derived stem cells ameliorate cigarette smoke-induced murine myelosuppression via secretion of TSG-6. *Stem Cells*, 2015. 33(2): p. 468-78.
106. Kim, H., et al., Diabetic Mesenchymal Stem Cells Are Ineffective for Improving Limb Ischemia Due to Their Impaired Angiogenic Capability. *Cell Transplant*, 2015. 24(8): p. 1571-84.
107. Nakamura, N., et al., High glucose impairs the proliferation and increases the apoptosis of endothelial progenitor cells by suppression of Akt. *J Diabetes Investig*, 2011. 2(4): p. 262-70.
108. Shahid, M.S., W. Lasheen, and K.H. Haider, The modest outcome of clinical trials with bone marrow cells for myocardial repair: is the autologous source of cells the prime culprit? *J Thorac Dis*, 2016. 8(10): p. E1371-E1374.
109. Herreros, M.D., et al., Autologous expanded adipose-derived stem cells for the treatment of complex cryptoglandular perianal fistulas: a phase III randomized clinical trial (FATT 1: fistula Advanced Therapy Trial 1) and long-term evaluation. *Dis Colon Rectum*, 2012. 55(7): p. 762-72.
110. Kokai, L.E., et al., Adipose Stem Cell Function Maintained with Age: An Intra-Subject Study of Long-Term Cryopreserved Cells. *Aesthet Surg J*, 2017. 37(4): p. 454-463.
111. Feisst, V., S. Meidinger, and M.B. Locke, From bench to bedside: use of human adipose-derived stem cells. *Stem Cells Cloning*, 2015. 8: p. 149-62.
112. Zimmerlin, L., et al., Regenerative therapy and cancer: in vitro and in vivo studies of the interaction between adipose-derived stem cells and breast cancer cells from clinical isolates. *Tissue Eng Part A*, 2011. 17(1-2): p. 93-106.
113. Drago, D., et al., The stem cell secretome and its role in brain repair. *Biochimie*, 2013. 95(12): p. 2271-85.

114. Ikegame, Y., et al., Comparison of mesenchymal stem cells from adipose tissue and bone marrow for ischemic stroke therapy. *Cytotherapy*, 2011. 13(6): p. 675-85.
115. Qayyum, A.A., et al., Adipose-derived mesenchymal stromal cells for chronic myocardial ischemia (MyStromalCell Trial): study design. *Regen Med*, 2012. 7(3): p. 421-8.
116. Perin, E.C., et al., Adipose-derived regenerative cells in patients with ischemic cardiomyopathy: The PRECISE Trial. *Am Heart J*, 2014. 168(1): p. 88-95 e2.
117. Madonna, R., et al., Non-invasive in vivo detection of peripheral limb ischemia improvement in the rat after adipose tissue-derived stromal cell transplantation. *Circ J*, 2012. 76(6): p. 1517-25.
118. Fang, B., et al., Favorable response to human adipose tissue-derived mesenchymal stem cells in steroid-refractory acute graft-versus-host disease. *Transplant Proc*, 2007. 39(10): p. 3358-62.
119. Yanez, R., et al., Adipose tissue-derived mesenchymal stem cells have in vivo immunosuppressive properties applicable for the control of the graft-versus-host disease. *Stem Cells*, 2006. 24(11): p. 2582-91.
120. Pers, Y.M., et al., Adipose Mesenchymal Stromal Cell-Based Therapy for Severe Osteoarthritis of the Knee: A Phase I Dose-Escalation Trial. *Stem Cells Transl Med*, 2016. 5(7): p. 847-56.
121. Bura, A., et al., Phase I trial: the use of autologous cultured adipose-derived stroma/stem cells to treat patients with non-revascularizable critical limb ischemia. *Cytotherapy*, 2014. 16(2): p. 245-57.
122. Panes, J., et al., Expanded allogeneic adipose-derived mesenchymal stem cells (Cx601) for complex perianal fistulas in Crohn's disease: a phase 3 randomised, double-blind controlled trial. *Lancet*, 2016. 388(10051): p. 1281-90.
123. Marino, G., et al., Therapy with autologous adipose-derived regenerative cells for the care of chronic ulcer of lower limbs in patients with peripheral arterial disease. *J Surg Res*, 2013. 185(1): p. 36-44.
124. Rubin, J.P., et al., Regulatory Advocacy Update: ASPS Comments in Response to the FDA Draft Guidance Documents on Human Cell and Tissue Products. *Plast Reconstr Surg*, 2017.
125. Bravo, B., et al., Opposite Effects of Mechanical Action of Fluid Flow on Proangiogenic Factor Secretion From Human Adipose-Derived Stem Cells With and Without Oxidative Stress. *J Cell Physiol*, 2017. 232(8): p. 2158-2167.
126. Prochazka, V., et al., Therapeutic Potential of Adipose-Derived Therapeutic Factor Concentrate for Treating Critical Limb Ischemia. *Cell Transplant*, 2016. 25(9): p. 1623-1633.
127. Katagiri, W., et al., Angiogenesis in newly regenerated bone by secretomes of human mesenchymal stem cells. *Maxillofac Plast Reconstr Surg*, 2017. 39(1): p. 8.

128. Baez-Jurado, E., et al., Blockade of Neuroglobin Reduces Protection of Conditioned Medium from Human Mesenchymal Stem Cells in Human Astrocyte Model (T98G) Under a Scratch Assay. *Mol Neurobiol*, 2017.
129. Lu, H., et al., Conditioned media from adipose stromal cells limit lipopolysaccharide-induced lung injury, endothelial hyperpermeability and apoptosis. *J Transl Med*, 2015. 13: p. 67.
130. Anderson, J.D., et al., Comprehensive Proteomic Analysis of Mesenchymal Stem Cell Exosomes Reveals Modulation of Angiogenesis via Nuclear Factor-KappaB Signaling. *Stem Cells*, 2016. 34(3): p. 601-13.
131. Xiang, J., et al., Bone marrow mesenchymal stem cells-conditioned medium enhances vascular remodeling after stroke in type 2 diabetic rats. *Neurosci Lett*, 2017. 644: p. 62-66.
132. Lin, C.H., et al., Molecular Mechanisms Responsible for Neuron-Derived Conditioned Medium (NCM)-Mediated Protection of Ischemic Brain. *PLoS One*, 2016. 11(1): p. e0146692.
133. Danieli, P., et al., Conditioned medium from human amniotic mesenchymal stromal cells limits infarct size and enhances angiogenesis. *Stem Cells Transl Med*, 2015. 4(5): p. 448-58.
134. Gneccchi, M., et al., Paracrine action accounts for marked protection of ischemic heart by Akt-modified mesenchymal stem cells. *Nat Med*, 2005. 11(4): p. 367-8.
135. Timmers, L., et al., Reduction of myocardial infarct size by human mesenchymal stem cell conditioned medium. *Stem Cell Res*, 2007. 1(2): p. 129-37.
136. Cantaluppi, V., et al., Microvesicles derived from endothelial progenitor cells protect the kidney from ischemia-reperfusion injury by microRNA-dependent reprogramming of resident renal cells. *Kidney Int*, 2012. 82(4): p. 412-27.
137. Lee, S., et al., Interplay between CCN1 and Wnt5a in endothelial cells and pericytes determines the angiogenic outcome in a model of ischemic retinopathy. *Sci Rep*, 2017. 7(1): p. 1405.
138. Tachida, Y., et al., Mutual interaction between endothelial cells and mural cells enhances BMP9 signaling in endothelial cells. *Biol Open*, 2017. 6(3): p. 370-380.
139. Merfeld-Clauss, S., et al., Adipose tissue progenitor cells directly interact with endothelial cells to induce vascular network formation. *Tissue Eng Part A*, 2010. 16(9): p. 2953-66.
140. Strassburg, S., et al., Human adipose-derived stem cells enhance the angiogenic potential of endothelial progenitor cells, but not of human umbilical vein endothelial cells. *Tissue Eng Part A*, 2013. 19(1-2): p. 166-74.
141. Traktuev, D.O., et al., Robust functional vascular network formation in vivo by cooperation of adipose progenitor and endothelial cells. *Circ Res*, 2009. 104(12): p. 1410-20.

142. Ingram, D.A., et al., Identification of a novel hierarchy of endothelial progenitor cells using human peripheral and umbilical cord blood. *Blood*, 2004. 104(9): p. 2752-60.
143. Murohara, T., et al., Nitric oxide synthase modulates angiogenesis in response to tissue ischemia. *J Clin Invest*, 1998. 101(11): p. 2567-78.
144. O'Leary, H., X. Ou, and H.E. Broxmeyer, The role of dipeptidyl peptidase 4 in hematopoiesis and transplantation. *Curr Opin Hematol*, 2013. 20(4): p. 314-9.
145. Bajpai, V.K. and S.T. Andreadis, Stem cell sources for vascular tissue engineering and regeneration. *Tissue Eng Part B Rev*, 2012. 18(5): p. 405-25.
146. Christopherson, K.W., 2nd, G. Hangoc, and H.E. Broxmeyer, Cell surface peptidase CD26/dipeptidylpeptidase IV regulates CXCL12/stromal cell-derived factor-1 alpha-mediated chemotaxis of human cord blood CD34+ progenitor cells. *J Immunol*, 2002. 169(12): p. 7000-8.
147. Merfeld-Clauss, S., et al., Adipose Stromal Cell Contact with Endothelial Cells Results in Loss of Complementary Vasculogenic Activity Mediated by Induction of Activin A. *Stem Cells*, 2015. 33(10): p. 3039-51.
148. Merfeld-Clauss, S., et al., Adipose stromal cells differentiate along a smooth muscle lineage pathway upon endothelial cell contact via induction of activin A. *Circ Res*, 2014. 115(9): p. 800-9.
149. Hao, M., R. Wang, and W. Wang, Cell Therapies in Cardiomyopathy: Current Status of Clinical Trials. *Anal Cell Pathol (Amst)*, 2017. 2017: p. 9404057.
150. Meamar, R., et al., The role of stem cell therapy in multiple sclerosis: An overview of the current status of the clinical studies. *Adv Biomed Res*, 2016. 5: p. 46.
151. Wanivenhaus, F., et al., Revision Rate and Risk Factors After Lower Extremity Amputation in Diabetic or Dysvascular Patients. *Orthopedics*, 2016. 39(1): p. e149-54.
152. Hussain, M.A., et al., Efficacy of a Guideline-Recommended Risk-Reduction Program to Improve Cardiovascular and Limb Outcomes in Patients With Peripheral Arterial Disease. *JAMA Surg*, 2016.
153. Otsuka, R., et al., Acute effects of passive smoking on the coronary circulation in healthy young adults. *JAMA*, 2001. 286(4): p. 436-41.
154. Sukmawati, D., et al., The role of Notch signaling in diabetic endothelial progenitor cells dysfunction. *J Diabetes Complications*, 2016. 30(1): p. 12-20.
155. Kang, Y., et al., Unsorted human adipose tissue-derived stem cells promote angiogenesis and myogenesis in murine ischemic hindlimb model. *Microvasc Res*, 2010. 80(3): p. 310-6.
156. Kondo, K., et al., Implantation of adipose-derived regenerative cells enhances ischemia-induced angiogenesis. *Arterioscler Thromb Vasc Biol*, 2009. 29(1): p. 61-6.

157. Mirshahi, F., et al., SDF-1 activity on microvascular endothelial cells: consequences on angiogenesis in in vitro and in vivo models. *Thromb Res*, 2000. 99(6): p. 587-94.
158. Brindle, N.P., P. Saharinen, and K. Alitalo, Signaling and functions of angiopoietin-1 in vascular protection. *Circ Res*, 2006. 98(8): p. 1014-23.
159. An, Y.A., et al., Angiopoietin-2 in white adipose tissue improves metabolic homeostasis through enhanced angiogenesis. *Elife*, 2017. 6.
160. Traktuev, D.O., et al., Urokinase gene transfer augments angiogenesis in ischemic skeletal and myocardial muscle. *Mol Ther*, 2007. 15(11): p. 1939-46.
161. Tang, Y.L., et al., Mobilizing of haematopoietic stem cells to ischemic myocardium by plasmid mediated stromal-cell-derived factor-1alpha (SDF-1alpha) treatment. *Regul Pept*, 2005. 125(1-3): p. 1-8.
162. Askari, A.T., et al., Effect of stromal-cell-derived factor 1 on stem-cell homing and tissue regeneration in ischaemic cardiomyopathy. *Lancet*, 2003. 362(9385): p. 697-703.
163. Ratajczak, M.Z., et al., Expression of functional CXCR4 by muscle satellite cells and secretion of SDF-1 by muscle-derived fibroblasts is associated with the presence of both muscle progenitors in bone marrow and hematopoietic stem/progenitor cells in muscles. *Stem Cells*, 2003. 21(3): p. 363-71.
164. Xu, X., et al., Stromal cell-derived factor-1 enhances wound healing through recruiting bone marrow-derived mesenchymal stem cells to the wound area and promoting neovascularization. *Cells Tissues Organs*, 2013. 197(2): p. 103-13.
165. Broxmeyer, H.E., et al., Rapid mobilization of murine and human hematopoietic stem and progenitor cells with AMD3100, a CXCR4 antagonist. *J Exp Med*, 2005. 201(8): p. 1307-18.
166. Newey, S.E., et al., The hematopoietic chemokine CXCL12 promotes integration of human endothelial colony forming cell-derived cells into immature vessel networks. *Stem Cells Dev*, 2014. 23(22): p. 2730-43.
167. Zhong, J. and S. Rajagopalan, Dipeptidyl Peptidase-4 Regulation of SDF-1/CXCR4 Axis: Implications for Cardiovascular Disease. *Front Immunol*, 2015. 6: p. 477.
168. Ou, X., H.A. O'Leary, and H.E. Broxmeyer, Implications of DPP4 modification of proteins that regulate stem/progenitor and more mature cell types. *Blood*, 2013. 122(2): p. 161-9.
169. Puissant, B., et al., Immunomodulatory effect of human adipose tissue-derived adult stem cells: comparison with bone marrow mesenchymal stem cells. *Br J Haematol*, 2005. 129(1): p. 118-29.
170. Apostolou, E., et al., Activin-A overexpression in the murine lung causes pathology that simulates acute respiratory distress syndrome. *Am J Respir Crit Care Med*, 2012. 185(4): p. 382-91.
171. Verhamme, F.M., et al., Role of activin-A in cigarette smoke-induced inflammation and COPD. *Eur Respir J*, 2014. 43(4): p. 1028-41.

172. Sierra-Filardi, E., et al., Activin A skews macrophage polarization by promoting a proinflammatory phenotype and inhibiting the acquisition of anti-inflammatory macrophage markers. *Blood*, 2011. 117(19): p. 5092-101.
173. Fiore, M.C., Tobacco Control in the Obama Era - Substantial Progress, Remaining Challenges. *N Engl J Med*, 2016. 375(15): p. 1410-1412.
174. Bickerman, H.A. and A.L. Barach, The effect of cigarette smoking on ventilatory function in patients with bronchial asthma and obstructive pulmonary emphysema. *J Lab Clin Med*, 1954. 43(3): p. 455-62.
175. Evans, M.D. and W.A. Pryor, Cigarette smoking, emphysema, and damage to alpha 1-proteinase inhibitor. *Am J Physiol*, 1994. 266(6 Pt 1): p. L593-611.
176. Yang, W., et al., Cigarette smoking extract causes hypermethylation and inactivation of WWOX gene in T-24 human bladder cancer cells. *Neoplasma*, 2012. 59(2): p. 216-23.
177. Nomura, A.M., et al., The association of cigarette smoking with gastric cancer: the multiethnic cohort study. *Cancer Causes Control*, 2012. 23(1): p. 51-8.
178. Unverdorben, M., K. von Holt, and B.R. Winkelmann, Smoking and atherosclerotic cardiovascular disease: part II: role of cigarette smoking in cardiovascular disease development. *Biomark Med*, 2009. 3(5): p. 617-53.
179. Erhardt, L., Cigarette smoking: an undertreated risk factor for cardiovascular disease. *Atherosclerosis*, 2009. 205(1): p. 23-32.
180. Miguez-Burbano, M.J., et al., Ignoring the obvious missing piece of chronic kidney disease in HIV: cigarette smoking. *J Assoc Nurses AIDS Care*, 2010. 21(1): p. 16-24.
181. Jones-Burton, C., et al., Cigarette smoking and incident chronic kidney disease: a systematic review. *Am J Nephrol*, 2007. 27(4): p. 342-51.
182. Jones-Burton, C., et al., Urinary cotinine as an objective measure of cigarette smoking in chronic kidney disease. *Nephrol Dial Transplant*, 2007. 22(7): p. 1950-4.
183. Nagasawa, Y., et al., Cigarette smoking and chronic kidney diseases. *Hypertens Res*, 2012. 35(3): p. 261-5.
184. Hole, B., et al., Treatment of End-stage Kidney Failure without Renal Replacement Therapy. *Semin Dial*, 2016. 29(6): p. 491-506.
185. Briganti, E.M., et al., Smoking is associated with renal impairment and proteinuria in the normal population: the AusDiab kidney study. *Australian Diabetes, Obesity and Lifestyle Study. Am J Kidney Dis*, 2002. 40(4): p. 704-12.
186. Chakkarwar, V.A., Smoking in diabetic nephropathy: sparks in the fuel tank? *World J Diabetes*, 2012. 3(12): p. 186-95.
187. Haroun, M.K., et al., Risk factors for chronic kidney disease: a prospective study of 23,534 men and women in Washington County, Maryland. *J Am Soc Nephrol*, 2003. 14(11): p. 2934-41.
188. Orth, S.R. and E. Ritz, The renal risks of smoking: an update. *Curr Opin Nephrol Hypertens*, 2002. 11(5): p. 483-8.

189. Lin, S.J., et al., Effect of donors' intravenous drug use, cigarette smoking, and alcohol dependence on kidney transplant outcome. *Transplantation*, 2005. 80(4): p. 482-6.
190. Jain, G. and E.A. Jaimes, Nicotine signaling and progression of chronic kidney disease in smokers. *Biochem Pharmacol*, 2013. 86(8): p. 1215-23.
191. Arany, I., et al., A novel U-STAT3-dependent mechanism mediates the deleterious effects of chronic nicotine exposure on renal injury. *Am J Physiol Renal Physiol*, 2012. 302(6): p. F722-9.
192. Orth, S.R. and S.I. Hallan, Smoking: a risk factor for progression of chronic kidney disease and for cardiovascular morbidity and mortality in renal patients--absence of evidence or evidence of absence? *Clin J Am Soc Nephrol*, 2008. 3(1): p. 226-36.
193. Arany, I., et al., Chronic nicotine exposure augments renal oxidative stress and injury through transcriptional activation of p66shc. *Nephrol Dial Transplant*, 2013. 28(6): p. 1417-25.
194. Wright, S.H. and W.H. Dantzler, Molecular and cellular physiology of renal organic cation and anion transport. *Physiol Rev*, 2004. 84(3): p. 987-1049.
195. Messner, B. and D. Bernhard, Smoking and cardiovascular disease: mechanisms of endothelial dysfunction and early atherogenesis. *Arterioscler Thromb Vasc Biol*, 2014. 34(3): p. 509-15.
196. Chin, C.Y., et al., Relation Between Renal Function and Coronary Plaque Morphology (from the Assessment of Dual Antiplatelet Therapy With Drug-Eluting Stents Virtual Histology-Intravascular Ultrasound Substudy). *Am J Cardiol*, 2017. 119(2): p. 217-224.
197. Arany, I., et al., Chronic nicotine exposure exacerbates acute renal ischemic injury. *Am J Physiol Renal Physiol*, 2011. 301(1): p. F125-33.
198. Bhatt, G.C. and R.R. Das, Early versus late initiation of renal replacement therapy in patients with acute kidney injury-a systematic review & meta-analysis of randomized controlled trials. *BMC Nephrol*, 2017. 18(1): p. 78.
199. Levey, A.S. and J. Coresh, Chronic kidney disease. *Lancet*, 2012. 379(9811): p. 165-80.
200. London, G.M., et al., Arteriosclerosis, vascular calcifications and cardiovascular disease in uremia. *Curr Opin Nephrol Hypertens*, 2005. 14(6): p. 525-31.
201. Murugan, R. and J.A. Kellum, Acute kidney injury: what's the prognosis? *Nat Rev Nephrol*, 2011. 7(4): p. 209-17.
202. Horbelt, M., et al., Acute and chronic microvascular alterations in a mouse model of ischemic acute kidney injury. *Am J Physiol Renal Physiol*, 2007. 293(3): p. F688-95.
203. Sutton, T.A., et al., Injury of the renal microvascular endothelium alters barrier function after ischemia. *Am J Physiol Renal Physiol*, 2003. 285(2): p. F191-8.
204. Duffield, J.S., Cellular and molecular mechanisms in kidney fibrosis. *J Clin Invest*, 2014. 124(6): p. 2299-306.
205. Strutz, F.M., EMT and proteinuria as progression factors. *Kidney Int*, 2009. 75(5): p. 475-81.

206. Stefanska, A., B. Peault, and J.J. Mullins, Renal pericytes: multifunctional cells of the kidneys. *Pflugers Arch*, 2013. 465(6): p. 767-73.
207. Lin, S.L., et al., Pericytes and perivascular fibroblasts are the primary source of collagen-producing cells in obstructive fibrosis of the kidney. *Am J Pathol*, 2008. 173(6): p. 1617-27.
208. Lovisa, S., M. Zeisberg, and R. Kalluri, Partial Epithelial-to-Mesenchymal Transition and Other New Mechanisms of Kidney Fibrosis. *Trends Endocrinol Metab*, 2016.
209. LeBleu, V.S., et al., Origin and function of myofibroblasts in kidney fibrosis. *Nat Med*, 2013. 19(8): p. 1047-53.
210. Grgic, I., J.S. Duffield, and B.D. Humphreys, The origin of interstitial myofibroblasts in chronic kidney disease. *Pediatr Nephrol*, 2012. 27(2): p. 183-93.
211. Kriz, W., B. Kaissling, and M. Le Hir, Epithelial-mesenchymal transition (EMT) in kidney fibrosis: fact or fantasy? *J Clin Invest*, 2011. 121(2): p. 468-74.
212. Humphreys, B.D., et al., Fate tracing reveals the pericyte and not epithelial origin of myofibroblasts in kidney fibrosis. *Am J Pathol*, 2010. 176(1): p. 85-97.
213. Piera-Velazquez, S., F.A. Mendoza, and S.A. Jimenez, Endothelial to Mesenchymal Transition (EndoMT) in the Pathogenesis of Human Fibrotic Diseases. *J Clin Med*, 2016. 5(4).
214. Basile, D.P., et al., Impaired endothelial proliferation and mesenchymal transition contribute to vascular rarefaction following acute kidney injury. *Am J Physiol Renal Physiol*, 2011. 300(3): p. F721-33.
215. Wang, Z., et al., Transforming Growth Factor-beta1 Induces Endothelial-to-Mesenchymal Transition via Akt Signaling Pathway in Renal Transplant Recipients with Chronic Allograft Dysfunction. *Ann Transplant*, 2016. 21: p. 775-783.
216. Bickelhaupt, S., et al., Effects of CTGF Blockade on Attenuation and Reversal of Radiation-Induced Pulmonary Fibrosis. *J Natl Cancer Inst*, 2017. 109(8).
217. Panebianco, C., et al., Senescence in hepatic stellate cells as a mechanism of liver fibrosis reversal: a putative synergy between retinoic acid and PPAR-gamma signalings. *Clin Exp Med*, 2016.
218. Du, X.J., et al., Reversal of cardiac fibrosis and related dysfunction by relaxin. *Ann N Y Acad Sci*, 2009. 1160: p. 278-84.
219. Zeisberg, M. and R. Kalluri, Reversal of experimental renal fibrosis by BMP7 provides insights into novel therapeutic strategies for chronic kidney disease. *Pediatr Nephrol*, 2008. 23(9): p. 1395-8.
220. Moens, A.L., et al., Reversal of cardiac hypertrophy and fibrosis from pressure overload by tetrahydrobiopterin: efficacy of recoupling nitric oxide synthase as a therapeutic strategy. *Circulation*, 2008. 117(20): p. 2626-36.
221. Yu, J., et al., Therapeutic Effect and Location of GFP-Labeled Placental Mesenchymal Stem Cells on Hepatic Fibrosis in Rats. *Stem Cells Int*, 2017. 2017: p. 1798260.

222. Qu, Y., et al., Exosomes derived from miR-181-5p-modified adipose-derived mesenchymal stem cells prevent liver fibrosis via autophagy activation. *J Cell Mol Med*, 2017.
223. Nagaishi, K., et al., Mesenchymal stem cell therapy ameliorates diabetic nephropathy via the paracrine effect of renal trophic factors including exosomes. *Sci Rep*, 2016. 6: p. 34842.
224. Ruan, G.P., et al., Induced autologous stem cell transplantation for treatment of rabbit renal interstitial fibrosis. *PLoS One*, 2013. 8(12): p. e83507.
225. Li, L., et al., Mesenchymal stem cell transplantation attenuates cardiac fibrosis associated with isoproterenol-induced global heart failure. *Transpl Int*, 2008. 21(12): p. 1181-9.
226. Charron, A.J., et al., Cablin: a novel protein of the capillary basal lamina. *Am J Physiol*, 1999. 277(5 Pt 2): p. H1985-96.
227. Wang, H., et al., Iron deposition in renal biopsy specimens from patients with kidney diseases. *Am J Kidney Dis*, 2001. 38(5): p. 1038-44.
228. Khalighi, M.A., et al., Intratubular hemoglobin casts in hemolysis-associated acute kidney injury. *Am J Kidney Dis*, 2015. 65(2): p. 337-41.
229. Ballarin, J., et al., Acute renal failure associated to paroxysmal nocturnal haemoglobinuria leads to intratubular haemosiderin accumulation and CD163 expression. *Nephrol Dial Transplant*, 2011. 26(10): p. 3408-11.
230. Chen, H., et al., Effect of short-term cigarette smoke exposure on body weight, appetite and brain neuropeptide Y in mice. *Neuropsychopharmacology*, 2005. 30(4): p. 713-9.
231. Cielen, N., et al., Interaction between Physical Activity and Smoking on Lung, Muscle, and Bone in Mice. *Am J Respir Cell Mol Biol*, 2016. 54(5): p. 674-82.
232. Mangubat, M., et al., Effect of nicotine on body composition in mice. *J Endocrinol*, 2012. 212(3): p. 317-26.
233. Klinkhammer, B.M., et al., Treatment of Renal Fibrosis-Turning Challenges into Opportunities. *Adv Chronic Kidney Dis*, 2017. 24(2): p. 117-129.
234. Shen, Y., et al., c-Myc promotes renal fibrosis by inducing integrin α 5-mediated transforming growth factor- β signaling. *Kidney Int*, 2017.
235. Li, J., et al., Recent Advances in Magnetic Resonance Imaging Assessment of Renal Fibrosis. *Adv Chronic Kidney Dis*, 2017. 24(3): p. 150-153.
236. Loeffler, I. and G. Wolf, Transforming growth factor- β and the progression of renal disease. *Nephrol Dial Transplant*, 2014. 29 Suppl 1: p. i37-i45.
237. Eddy, A.A., Overview of the cellular and molecular basis of kidney fibrosis. *Kidney Int Suppl* (2011), 2014. 4(1): p. 2-8.
238. Farris, A.B. and C.E. Alpers, What is the best way to measure renal fibrosis?: A pathologist's perspective. *Kidney Int Suppl* (2011), 2014. 4(1): p. 9-15.
239. Leonard, E.C., J.L. Friedrich, and D.P. Basile, VEGF-121 preserves renal microvessel structure and ameliorates secondary renal disease following acute kidney injury. *Am J Physiol Renal Physiol*, 2008. 295(6): p. F1648-57.

240. Donizetti-Oliveira, C., et al., Adipose tissue-derived stem cell treatment prevents renal disease progression. *Cell Transplant*, 2012. 21(8): p. 1727-41.
241. Medici, D. and R. Kalluri, Endothelial-mesenchymal transition and its contribution to the emergence of stem cell phenotype. *Semin Cancer Biol*, 2012. 22(5-6): p. 379-84.
242. Zeisberg, E.M., et al., Endothelial-to-mesenchymal transition contributes to cardiac fibrosis. *Nat Med*, 2007. 13(8): p. 952-61.
243. Braga, T.T., J.S. Agudelo, and N.O. Camara, Macrophages During the Fibrotic Process: M2 as Friend and Foe. *Front Immunol*, 2015. 6: p. 602.
244. Hu, M.C., et al., Recombinant alpha-Klotho may be prophylactic and therapeutic for acute to chronic kidney disease progression and uremic cardiomyopathy. *Kidney Int*, 2017. 91(5): p. 1104-1114.
245. Forni, L.G., et al., Renal recovery after acute kidney injury. *Intensive Care Med*, 2017.
246. Collett, J.A., et al., Endothelial colony forming cells ameliorate endothelial dysfunction via secreted factors following ischemia-reperfusion injury. *Am J Physiol Renal Physiol*, 2017: p. ajprenal 00643 2016.
247. Zhou, L., et al., Comparison of human adipose stromal vascular fraction and adipose-derived mesenchymal stem cells for the attenuation of acute renal ischemia/reperfusion injury. *Sci Rep*, 2017. 7: p. 44058.
248. Sheashaa, H., et al., Protective effect of adipose-derived mesenchymal stem cells against acute kidney injury induced by ischemia-reperfusion in Sprague-Dawley rats. *Exp Ther Med*, 2016. 11(5): p. 1573-1580.
249. Roggeri, A., et al., Healthcare costs of the progression of chronic kidney disease and different dialysis techniques estimated through administrative database analysis. *J Nephrol*, 2017. 30(2): p. 263-269.
250. Nankivell, B.J., R.A. Boadle, and D.C. Harris, Iron accumulation in human chronic renal disease. *Am J Kidney Dis*, 1992. 20(6): p. 580-4.
251. Alfrey, A.C., Role of iron and oxygen radicals in the progression of chronic renal failure. *Am J Kidney Dis*, 1994. 23(2): p. 183-7.
252. Guerassimov, A., et al., The development of emphysema in cigarette smoke-exposed mice is strain dependent. *Am J Respir Crit Care Med*, 2004. 170(9): p. 974-80.
253. Rabe, K.F. and H. Watz, Chronic obstructive pulmonary disease. *Lancet*, 2017. 389(10082): p. 1931-1940.
254. Smith, B.M., et al., Pulmonary emphysema subtypes on computed tomography: the MESA COPD study. *Am J Med*, 2014. 127(1): p. 94 e7-23.
255. Yamada, M. and M. Ichinose, Cutting edge of COPD therapy: current pharmacological therapy and future direction. *COPD Research and Practice*, 2015. 1(1): p. 5.
256. Patalano, F., et al., Addressing unmet needs in the treatment of COPD. *Eur Respir Rev*, 2014. 23(133): p. 333-44.
257. Zhen, G., et al., Mesenchymal stem cells transplantation protects against rat pulmonary emphysema. *Front Biosci*, 2008. 13: p. 3415-22.

258. Tibboel, J., et al., Intravenous and intratracheal mesenchymal stromal cell injection in a mouse model of pulmonary emphysema. *COPD*, 2014. 11(3): p. 310-8.
259. de Oliveira, H.G., et al., Combined Bone Marrow-Derived Mesenchymal Stromal Cell Therapy and One-Way Endobronchial Valve Placement in Patients with Pulmonary Emphysema: A Phase I Clinical Trial. *Stem Cells Transl Med*, 2017. 6(3): p. 962-969.
260. Weiss, D.J., Concise review: current status of stem cells and regenerative medicine in lung biology and diseases. *Stem Cells*, 2014. 32(1): p. 16-25.
261. Adachi, Y., et al., Treatment and transfer of emphysema by a new bone marrow transplantation method from normal mice to Tsk mice and vice versa. *Stem Cells*, 2006. 24(9): p. 2071-7.
262. Huertas, A., et al., Bone marrow-derived progenitors are greatly reduced in patients with severe COPD and low-BMI. *Respir Physiol Neurobiol*, 2010. 170(1): p. 23-31.
263. Weinstein, R.S., Glucocorticoid-induced osteoporosis and osteonecrosis. *Endocrinol Metab Clin North Am*, 2012. 41(3): p. 595-611.
264. Rauch, A., et al., Glucocorticoids suppress bone formation by attenuating osteoblast differentiation via the monomeric glucocorticoid receptor. *Cell Metab*, 2010. 11(6): p. 517-31.
265. Liguori, A., et al., Functional impairment of hematopoietic progenitor cells in patients with coronary heart disease. *Eur J Haematol*, 2008. 80(3): p. 258-64.
266. Heeschen, C., et al., Profoundly reduced neovascularization capacity of bone marrow mononuclear cells derived from patients with chronic ischemic heart disease. *Circulation*, 2004. 109(13): p. 1615-22.
267. Kissel, C.K., et al., Selective functional exhaustion of hematopoietic progenitor cells in the bone marrow of patients with postinfarction heart failure. *J Am Coll Cardiol*, 2007. 49(24): p. 2341-9.
268. Janssen, W.J., et al., Circulating hematopoietic progenitor cells are decreased in COPD. *COPD*, 2014. 11(3): p. 277-89.
269. Palange, P., et al., Circulating haemopoietic and endothelial progenitor cells are decreased in COPD. *Eur Respir J*, 2006. 27(3): p. 529-41.
270. Fadini, G.P., et al., Circulating progenitor cells are reduced in patients with severe lung disease. *Stem Cells*, 2006. 24(7): p. 1806-13.
271. Kolb, H.J., Hematopoietic stem cell transplantation and cellular therapy. *HLA*, 2017. 89(5): p. 267-277.
272. Doulatov, S., et al., Hematopoiesis: a human perspective. *Cell Stem Cell*, 2012. 10(2): p. 120-36.
273. Pusic, I. and J.F. DiPersio, Update on clinical experience with AMD3100, an SDF-1/CXCL12-CXCR4 inhibitor, in mobilization of hematopoietic stem and progenitor cells. *Curr Opin Hematol*, 2010. 17(4): p. 319-26.
274. Dar, A., et al., Rapid mobilization of hematopoietic progenitors by AMD3100 and catecholamines is mediated by CXCR4-dependent SDF-1 release from bone marrow stromal cells. *Leukemia*, 2011. 25(8): p. 1286-96.

275. Caocci, G., M. Greco, and G. La Nasa, Bone Marrow Homing and Engraftment Defects of Human Hematopoietic Stem and Progenitor Cells. *Mediterr J Hematol Infect Dis*, 2017. 9(1): p. e2017032.
276. Kim, B.J., et al., Synergistic vasculogenic effects of AMD3100 and stromal-cell-derived factor-1alpha in vasa nervorum of the sciatic nerve of mice with diabetic peripheral neuropathy. *Cell Tissue Res*, 2013. 354(2): p. 395-407.
277. Matthys, P., et al., AMD3100, a potent and specific antagonist of the stromal cell-derived factor-1 chemokine receptor CXCR4, inhibits autoimmune joint inflammation in IFN-gamma receptor-deficient mice. *J Immunol*, 2001. 167(8): p. 4686-92.
278. Nervi, B., D.C. Link, and J.F. DiPersio, Cytokines and hematopoietic stem cell mobilization. *J Cell Biochem*, 2006. 99(3): p. 690-705.
279. Broxmeyer, H.E., et al., Cd45 Cell-Surface Antigens Are Linked to Stimulation of Early Human Myeloid Progenitor Cells by Interleukin-3 (Il-3), Granulocyte Macrophage Colony-Stimulating Factor (Gm-Csf), a Gm-Csf Il-3 Fusion Protein, and Mast-Cell Growth-Factor (a C-Kit Ligand). *Journal of Experimental Medicine*, 1991. 174(2): p. 447-458.
280. Clauss, M., et al., Lung endothelial monocyte-activating protein 2 is a mediator of cigarette smoke-induced emphysema in mice. *J Clin Invest*, 2011. 121(6): p. 2470-9.
281. Glaab, T., et al., Invasive and noninvasive methods for studying pulmonary function in mice. *Respir Res*, 2007. 8: p. 63.
282. Andersen, M.P., et al., Alveolar fractal box dimension inversely correlates with mean linear intercept in mice with elastase-induced emphysema. *Int J Chron Obstruct Pulmon Dis*, 2012. 7: p. 235-43.
283. Bonig, H., et al., Insights into the biology of mobilized hematopoietic stem/progenitor cells through innovative treatment schedules of the CXCR4 antagonist AMD3100. *Exp Hematol*, 2009. 37(3): p. 402-15 e1.
284. Tantucci, C., et al., Inspiratory capacity predicts mortality in patients with chronic obstructive pulmonary disease. *Respir Med*, 2008. 102(4): p. 613-9.
285. Tankersley, C.G., R. Rabold, and W. Mitzner, Differential lung mechanics are genetically determined in inbred murine strains. *J Appl Physiol* (1985), 1999. 86(6): p. 1764-9.
286. Irvin, C.G. and J.H. Bates, Measuring the lung function in the mouse: the challenge of size. *Respir Res*, 2003. 4: p. 4.
287. Heidler, J., et al., Sestrin-2, a repressor of PDGFRbeta signalling, promotes cigarette-smoke-induced pulmonary emphysema in mice and is upregulated in individuals with COPD. *Dis Model Mech*, 2013. 6(6): p. 1378-87.
288. Vanoirbeek, J.A., et al., Noninvasive and invasive pulmonary function in mouse models of obstructive and restrictive respiratory diseases. *Am J Respir Cell Mol Biol*, 2010. 42(1): p. 96-104.
289. Nanki, T., et al., Stromal cell-derived factor-1-CXC chemokine receptor 4 interactions play a central role in CD4+ T cell accumulation in rheumatoid arthritis synovium. *J Immunol*, 2000. 165(11): p. 6590-8.

290. Vuilleminot, B.R., J.F. Rodriguez, and G.W. Hoyle, Lymphoid tissue and emphysema in the lungs of transgenic mice inducibly expressing tumor necrosis factor-alpha. *Am J Respir Cell Mol Biol*, 2004. 30(4): p. 438-48.
291. Zhang, W.G., et al., Regulation of transplanted mesenchymal stem cells by the lung progenitor niche in rats with chronic obstructive pulmonary disease. *Respir Res*, 2014. 15: p. 33.
292. Rafii, S., et al., Platelet-derived SDF-1 primes the pulmonary capillary vascular niche to drive lung alveolar regeneration. *Nat Cell Biol*, 2015. 17(2): p. 123-36.
293. Young, K.C., et al., Inhibition of the SDF-1/CXCR4 axis attenuates neonatal hypoxia-induced pulmonary hypertension. *Circ Res*, 2009. 104(11): p. 1293-301.
294. Makino, H., et al., Antifibrotic effects of CXCR4 antagonist in bleomycin-induced pulmonary fibrosis in mice. *J Med Invest*, 2013. 60(1-2): p. 127-37.
295. Drummond, S., et al., CXCR4 blockade attenuates hyperoxia-induced lung injury in neonatal rats. *Neonatology*, 2015. 107(4): p. 304-11.
296. Yamada, M., et al., The increase in surface CXCR4 expression on lung extravascular neutrophils and its effects on neutrophils during endotoxin-induced lung injury. *Cell Mol Immunol*, 2011. 8(4): p. 305-14.
297. Sharafkhaneh, A., N.A. Hanania, and V. Kim, Pathogenesis of emphysema: from the bench to the bedside. *Proc Am Thorac Soc*, 2008. 5(4): p. 475-7.
298. Tudor, R.M. and I. Petrache, Pathogenesis of chronic obstructive pulmonary disease. *J Clin Invest*, 2012. 122(8): p. 2749-55.
299. Hendrix, C.W., et al., Safety, pharmacokinetics, and antiviral activity of AMD3100, a selective CXCR4 receptor inhibitor, in HIV-1 infection. *J Acquir Immune Defic Syndr*, 2004. 37(2): p. 1253-62.
300. De Clercq, E., The bicyclam AMD3100 story. *Nat Rev Drug Discov*, 2003. 2(7): p. 581-7.

CURRICULUM VITAE

Daria Barwinska

Education:

2011-2017	Indiana University, Indianapolis, IN. Degree: PhD
2005-2009	Anderson University, Anderson, IN. Degree: BA

Additional Trainings:

01/2013-12/2013	Certificate in Business in Life Sciences from Indiana University Kelley School of Business
-----------------	---

Research Positions:

02/2011-07/2011	Microbiologist, Dow AgroSciences, Indianapolis, IN
07/2009-12/2010	Pharmacologist, Eli Lilly & Co, Indianapolis, IN
06/2008-11/2008	Study Director, MicaGenix, Inc., Indianapolis, IN
06/2007-09/2007	Technician, MicaGenix, Inc., Indianapolis, IN

Honors/Awards:

05/2016	Award in Translational Research, Indianapolis VA Medical Center
11/2015	Highest Scoring Abstracts, International Federation for Adipose Therapeutics and Science

05/2015	The Dr. Robert C. Miller Award for Excellence in Vascular Research, Indiana Clinical and Translational Science Institute Award
2013-2015	American Heart Association Pre-Doctoral Award

Memberships:

2014-Present	Member, International Federation for Adipose Therapeutic and Science (IFATS)
2013-Present	American Heart Association (AHA)

Service to my research discipline:

2016	Co-organizer, Symposium on Cellular and Regenerative Therapies, Indianapolis, IN
2015-Present	Member, International Federation for Adipose Therapeutic and Science (IFATS) Website Committee
2012-Present	Organizer, Indiana University Regenerative Medicine Seminar Series, Indianapolis, IN

Peer-Reviewed Publications:

- Xie J, Broxmeyer H, Feng D, Schweitzer K, Yi R, Cook T, Chitteti B, **Barwinska D**, Traktuev D, Van Demark M, Justice M, Ou X, Srour E, Prockop D, Petrache I, March K; *Human adipose-derived stem cells*

ameliorate cigarette smoke-induced murine myelosuppression via TSG-6.

Stem Cells 2015

- Jensen A, Doster D, Hunsberger B, Manning M, Stokes S, **Barwinska D**, March K, Yoder M, Markel T; *Adipose stromal cells increase survival and mesenteric perfusion following intestinal ischemia and reperfusion injury.*

Shock 2016

- Ni K, Mian M, Meador C, Gill A, **Barwinska D**, Cao D, Justice M, Schweitzer K, March K, Petrache I; *Oncostatin M and TNF- α induce alpha-1 antitrypsin production in undifferentiated adipose stromal cells.*

Stem Cells Dev 2017

- **Barwinska D**, Garner J, Davidson D, Eckert G, Cook T, Tholpady S, March k, Park K, Barco C; *Mucosal perfusion preservation by a novel shapeable tissue expander for oral reconstruction.* Plast Reconstr Surg

Glob Open 2017

- **Barwinska D**, Traktuev D, Merfeld-Clauss S, Cook T, Lu H, Petrache I, March K; *Cigarette smoking reduces adipose stromal cell vasculogenic activities and potency to mitigate ischemic conditions.* [submitted]

- **Barwinska D**, Oueini H, Poirier C, Albrecht M, Bogatcheva N, Van Demark M, Justice M, Saliba J, Schweitzer K, Broxmeyer H, March K, Petrache I; *AMD3100 limits cigarette smoke-induced myelosuppression and emphysema development in mice.* [in preparation]